The spatial dimensions of fisheries: improved use of spatial information into fisheries management and information for assessments

Kotaro Ono

A dissertation

submitted in partial fulfillment of the

requirements for the degree of

DOCTOR OF PHILOSOPHY

University of Washington

2014

Reading Committee:

Ray Hilborn

André E. Punt

Owen S. Hamel

Program Authorized to Offer Degree:

School of Aquatic and Fishery Sciences

University of Washington

Abstract

The spatial dimensions of fisheries: improved use of spatial information in fisheries management and information for assessments

Kotaro Ono

Chair of the Supervisory Committee:

Dr. Ray Hilborn

School of Aquatic and Fishery Sciences

Until relatively recently, fisheries resources were managed as single homogeneous units and fisheries management conveniently ignored the presence of spatial heterogeneity in stocks. In nature, species are neither distributed at random nor uniformly, but follow some pattern created by a combination of habitat preference, movement, interspecific species interactions, and fishery exploitation. Ignoring such heterogeneity and managing stocks as single homogeneous units increases the risk of serial depletion and population collapse. It is therefore important to understand and consider the spatial dynamics of a fishery and fish populations to help establish proper management plans which aid the conservation of marine ecosystems. In this dissertation, I developed and tested novel fishery analysis methods which better integrate the spatial structure of fish and fishermen to help improve the quality of information used for fisheries management.

In the first chapter, I developed a multispecies fishery model and examined how the spatial overlap of species could affect the biological and economic performance of commonly used fishery management methods such as the individual quota systems or marine protected areas. In Chapter 2, I examined how the use of spatial closures affected the analysis of fishery catch per unit effort (CPUE) data, which can be used to derive indices of population abundance. From this work, I proposed a new method based on data imputation to reduce bias in the indices of abundance. In Chapter 3, I presented an intuitive but objective way to define spatial strata (using a clustering approach) for analyzing CPUE data, and showed how this method can improve the accuracy of population abundance estimates. Finally, in the last chapter, I applied a novel spatio-temporal statistical model to three large geo-referenced time-series (habitat maps, survey-based fish density estimates and fishery catch data) to study the seasonal dynamics (between Summer and Fall) of a commercially important flatfish species, Pacific Dover sole (*Microstomus pacificus*), off the U.S. West Coast.

The multispecies modeling confirmed that the spatial overlap of species affects both the biological and economic performance of a fishery management system in a complex manner. The presence of a spatial closure increased the amount of bias in the derived index of abundance, however the imputation based method was able to reduce bias for most cases. Furthermore, clustering based area stratification eliminated bias in the derived index of abundance due to selective fishing but was not able to reduce bias when fishing grounds were shifting over time. Finally, the spatio-temporal model applied to Pacific Dover sole revealed that seasonal dynamics (between Summer and Fall) were dominated by movement.

In summary, the inclusion of spatial information in fishery models improved the accuracy of species distribution models, the accuracy of abundance indices used in stock assessment models, and provide insight to managers regarding what to expect in terms of population preservation and fishery profitability by switching management methods. Future studies should keep developing methods to improve the use of spatial information into fisheries stock assessment and management.

TABLE OF CONTENTS

LIST OF FIGURES

LIST OF TABLES

Table Number Page

Acknowledgments

I would like to thank my committee members for the thoughful discussions and comments which helped improve my dissertation and manuscripts. I would like to particulary thank Ray Hilborn for being a great mentor and giving me numerous opportunities to be involved in many projects and for sharing his uncomparable knowledge on fisheries science. A special thanks to Andre Punt for the innumerable comments and revisions on my manuscripts and his lighting fast replies to emails without which I will not have been able to finish as planned.

I am also very grateful for my colleagues at the University of Washington, the University of California Santa Barbara (UCSB), and the Northwest Fisheries Science Center (NWFSC) at NOAA. Particularly, the people at Fishery Resource Analysis and Monitoring Division (FRAM), and Conservation Biology Division (CB) at the NWFSC, the Sustainable Fisheries Group at UCSB, as well as the students in Hilborn lab, Punt lab, Branch lab and Essington labs, both past and present, have been fantastic to spend time discussing about ideas and working on projects together.

For financial support, I thank the NMFS stock assessment grant, NSF/CAMEO grant, the Joint Institute for the Study of the Atmosphere and Ocean (JISAO) under NOAA Cooperative Agreement, and the School of Aquatic and Fishery Sciences for their support.

I would like to sincerely thank my friends in Seattle and in France, who have supported me all these years. Thank you for the innumerable fun board game nights, lunch/brunch/diner events, hiking, crabbing and mushrooming trips, and just being present around us when it mattered.

I am thankful to Charles Simenstad and Guy Fontenelle without whom I would have not been able to come to the U.S. in the first place.

Finally, I sincerely thank my family without whom life would be much harder and less exciting. In particular, I am thankful for my parents, my parents-in-law and my brother- and sister-in-law who were always present at times that really mattered. And of course, I am deeply grateful for the love and support of my wife, Marine Brieuc, without whom, I will probably not be what I am right now and, without whom, I cannot have such an amazing life.

Introduction

Until relatively recently, fisheries resources were managed as single homogeneous units and fisheries management conveniently ignored the presence of spatial heterogeneity in stocks. However, it has been long known that many factors could potentially affect the distribution of fish over time and space in marine ecosystems (Whittaker et al. 1973). For instance, fish may have a specific habitat preference that can vary with life stage and season. Species mobility can also vary with ontogeny and scale, and as species interact with their prey and predators. Finally, fishers apply differential pressure to stocks depending on their knowledge, tradition, and regulations ruling the fishery (Salas and Gaetner 2004, Van Putten et al. 2011).

Ultimately, fishing is governed by the fishing opportunity, and if two species cannot be caught separately nor caught at the ideal ratio, there is no other choice than to overfish or underfish one or the other. Worm et al. (2009) noted that if the objective of a fishery is to maximize the ecosystem-wide catch, 25% of the stocks within an ecosystem will be on average "collapsed", i.e. at less than 10% of their unfished biomass. On the other hand, if overfishing is prohibited, as in the U.S. under the Magnuson-Stevens Act (MSA; NOAA 1996), the fishery might lose a substantial amount of yield because productive stocks will be underexploited (Hilborn et al. 2012). A variety of multi-species management methods have therefore been implemented around the world to reduce the conflict between loss of potential yield and overfishing unproductive stocks. Among these are incentive-based management (Branch et al 2009), spatial management (Gaines et al. 2010), and changes to fishing gear (Hicks and McClanahan 2012). However, the outcome of these management methods may change depending on the spatial overlap of

exploited species. It is therefore important to explore to what extent changes in the spatial overlap of species can impact the outcome of a fishery management measures.

Among the management methods mentioned above, marine closures and marine protected areas are currently being implemented worldwide (http://ocean.nationalgeographic.com/ocean/take-action/marine-protected-areas/) and are becoming a more common management tool (Lester et al. 2009, Gaines et al. 2010, Fox et al. 2012). However, spatial closures can lead to problems in assessing the status of populations. For example, Field et al. (2006) indicated that the presence of area closures can bias stock assessment results, in unpredictable directions.

In many countries, stock assessments are now mandatory and provide the basis for fisheries management. Fishery-independent survey data are often the data of choice for stock assessments, but these data are expensive and sometimes exist only for a short time period, if at all. On the other hand, fishery-dependent data, especially the catch per day fished or catch per tow (catch per unit effort, CPUE), are easier to collect and are also commonly available over extended time periods. Therefore, CPUE data have been widely used in the literature to provide an index of stock abundance through CPUE index standardization (Hilborn and Walters 1992; Maunder et al. 2004). It is thus important to examine the effect of spatial closures on CPUE indices and develop solutions to reduce bias in the derived indices of abundance.

In addition to the impact of spatial closures on CPUE standardization, many factors can potentially affect raw CPUE values over time and space (Maunder et al. 2006). For example, vessel targeting behavior, temporal changes in species' distribution, and technological changes are recognized as factors that can influence CPUE trends. Thus, it is important to account for variables that can influence CPUE in regression models and "standardize" CPUE data (reviewed

by Maunder and Punt 2004). Additionally, area strata are often included as an independent variable in CPUE standardization. In theory, each area stratum should be as homogenous, in terms of its specific density, as possible to be biologically meaningful (Bishop 2006). However, this is seldom the case, and instead many analysts use grid cells created in an ad hoc manner (e.g. regional boundaries) as strata in CPUE standardizations (Nakano 1998). The use of ad-hoc strata can potentially lead to "Simpson's paradox" (Simpson 1951): a trend that appears in different subgroups of areas that disappears when these subgroups are aggregated, and the reverse trend appears instead. Simpson's paradox can potentially result in a biased index of abundance, which can then lead to erroneous fisheries management advice. It is therefore important to develop and evaluate alternative area stratification methods that objectively define spatial strata and reduce the potential biases created by ad hoc area stratification.

In addition to fishery CPUE data, some countries also conduct surveys to collect large scale bio-physical information on living marine resources and their habitats. Survey data facilitates the examination of species spatial distributions and the influence of fishing on those distributions. Improved understanding of species distributions can help guide conservation actions for example, by setting targeted spatial closures. By combining three large scale spatio-temporal data sources (detailed benthic habitat data from the continental shelf and slope off the U.S. West Coast, fish density estimates from an extensive fishery-independent research survey, and commercial fishing catch data) with a novel spatio-temporal modeling technique, it is possible to examine the seasonal dynamics of commercially important marine species and look at the fine-scale effect of fishing on the populations.

Objectives

This study is divided into four chapters that develop and test methods to better integrate the spatial structure of fish and fisheries to help improve fisheries management advice.

Chap. 1: Evaluate the effect of species spatial overlap on the biological and economic performance of a multi-species fishery managed under different management methods (namely a total allowable catch regulated limited entry fishery, an individual quota system and spatial management).

Chap. 2: Develop a standardization method for fishery CPUE data, and compare its accuracy with other conventional methods given a variety of spatial closures.

Chap. 3: Develop an objective method to define spatial strata in CPUE analysis and examine how it affects the accuracy of the derived index of abundance compared to an ad hoc area stratification.

Chap. 4: Apply a novel spatio-temporal model to Pacific Dover sole (*Microstomus pacificus*) studying the seasonal dynamics of the species and the population response to fishing.

Chapter 1 - How does species association affect mixed stock fisheries management? A comparative analysis of the effect of marine protected areas, discard bans, and individual fishing quotas.

Abstract

We developed a spatially-explicit bio-economic model of a mixed-stock fishery with an unproductive and a productive stock to examine how the spatial overlap between species affects the outcome of a fishery under alternative management methods. We considered a competitive total allowable catch (TAC) system, with and without a ban on discards, and an individual vessel quota (IVQ) fishery managed either to maximum sustainable yield (MSY) or maximum economic yield (MEY). We also evaluated the utility of marine protected areas (MPAs) designed to protect the unproductive species for each management scenario. Banning discarding (whether under a TAC or IVQ) created the biggest increase in profit regardless of species overlap as it moves the target species biomass toward Bmey. MPAs reduced the profit in most cases and were not always successful at conserving the unproductive stock above a target size. The IVQ system under MEY produced the most profit among all scenarios while preserving the populations above some target values in most cases, but an IVQ managed to MSY produced lower profits than a competitive TAC with a discard ban at some levels of species overlap.

Introduction

Because many species share the same habitat (or fishing ground) and selectivity of most fishing gear is imperfect, many if not most fisheries around the world are multispecies fisheries. This type of fishery is problematic in situations where low productivity stocks are mixed and caught

together with high productivity stocks. Indeed, several authors have pointed out that in such situations, there is a risk of substantially overfishing or underfishing some of the stocks (Hilborn et al. 2004; Worm et al. 2009; Hilborn et al. 2012). Worm et al. (2009), for example, determined that when ecosystem-wide catch is maximized, several stocks within the ecosystem are depleted. On the other hand, if overfishing is prohibited as in the U.S. by the Magnuson-Stevens Fishery Conservation and Management Act (U.S, Public Law 104-297), yields from many multispecies fisheries are likely to be lost as productive stocks are underexploited to avoid overfishing weaker stocks (Hilborn et al. 2012).

In order to manage these mixed stock fisheries, different management methods have been proposed and tried in different jurisdictions. Among these are individual vessel quotas (IVQs) and spatial management using marine protected areas (MPAs). IVQs have been shown to have many positive effects on the fishery by decreasing total discard rates (Branch 2006, 2009; Branch et al. 2006b), improving economic efficiency by eliminating overcapitalization (Branch 2009), or stabilizing catch over time (Essington 2010). IVQs have also been criticized on equity grounds for concentrating profit in the hands of a few (see Branch 2009 for review). Similarly, MPAs or spatial closures have received a lot of attention as a tool to protect species diversity, vulnerable population biomass (e.g. overfished species' biomass), and habitat, or to increase catch and/or biomass (Halpern 2003; Lester et al. 2011). However, the utility of an MPA depends on the species characteristics, size, and location of the MPAs (Botsford et al. 2003; Sale et al. 2005) and on how the MPA impacts effort outside the closed areas (Holland 2000; Smith and Wilen 2003).

Designing an effective management system requires understanding human (vessel) behavior under the management system (Salas and Gaetner 2004; Fulton et al. 2011; Smith and Wilen 2003) as well as the ability to enforce rules (Branch 2009). Fishers have often been viewed in the literature as individual foragers trying to maximize their utility or profit, which depends on the species distribution, price, gear efficiency, and a variety of cost factors (Gordon 1953; Hilborn and Kennedy 1992). They change their behavior in response to the economic and management incentives which can lead to different fishery outcomes. For example, if fisheries are managed through a simple total allowable catch (TAC) or individual trip limits with no discarding control, vessels have no incentive to alter their catch composition to match their mix of species to the TAC, if doing so would decrease their profit (Poos et al. 2010). They are therefore likely to discard species for which the catch limit is reached so long as they can profit from the other species. On the other hand, under an IVQ system with enforcement of no-discard rules, fishers would have to adjust their fishing location, gear, or both in order to meet their quotas for different stocks (Branch and Hilborn 2008, Lomeli and Wakefield 2013). Although factors such as regulation, tradition, and competition can influence fisher's behavior (Branch et al. 2006a, Salas et al. 2004, van Putten et al. 2011), vessel distribution and the species composition of catch depends critically on the species distribution and overlap on the grounds. Species distributions and co-occurrence often depend on habitat and ecological requirements that correlate with depth, latitude, substrate and temperature. Consequently, fishing patterns may be strongly influenced by the biotic and abiotic characteristics of the fisheries (Poos et al. 2010).

In this study, we use a bioeconomic model to explore how variation in species association can affect the performance of a multispecies fishery (both ecological (depletion level) and economic (net profit)) under different management regimes. The bioeconomic model is based on a two-

species fishery where high and low productivity species are caught together to varying degrees. A few studies have compared performance of MPAs for mixed-stock fisheries under alternative management approaches (Holland 2003) or managing mixed-stock fisheries with IVQs (Holland and Herrera 2006; Poos et al. 2010; Toft et al. 2011). This study makes additional contributions by exploring how the effectiveness of discard bans, IVQs, and MPAs varies with the degree of overlap between fish stocks of differing productivity. We also show how the TACs associated with MEY change with the degree of stock mixing and a variety of other biological and economic factors. We test two major types of management systems: a TAC-regulated-limited entry fishery (where there is a competition among vessels for the limited TAC), and a TAC-regulated fishery where the TAC is divided up among fishers (i.e. an IVQ system). We also evaluate the influence of a discard ban for the TAC-regulated fishery and the consequence of implementing a spatial closure (or MPA) designed to protect the weaker stock.

Material and method

Model description

The bioeconomic model includes two species distributed over a linear array of 100 cells (n_a =100). The species biological parameters are set so that the weak stock (unproductive stock) has an exploitation rate producing MSY (F_{MSY}) that is respectively a quarter, a third (base case) or a half of the stronger stock (productive stock) while having the same virgin biomass (Table 1.1). We set the price of the weak stock at a quarter, three-quarters (base case) or equal to the price of the strong stock to illustrate the case of a fishery with a valuable productive targeted species and a less productive bycatch species of equal or lower value (Table 1.1). We assume that each species distribution is influenced by its habitat preference defined by a habitat suitability index

(*HSI*) which controls the spatial distribution of recruitment and movement (Gruss et al. 2011). *HSI* has been often used in the literature to determine preferred habitat for terrestrial animals or freshwater species such as salmon (Guay et al. 2000), and is represented in this study by a discrete Gaussian distribution across the linear habitat. This index ranges from [0; 1] where 0 indicates unsuitable habitat and 1 the most preferred habitat. We create an array of different level of species overlap (species association) by changing the species *HSI* distributions (Fig. 1.1). The species overlap (*A*) is calculated as the product of the species distribution divided by the product when species are completely overlapping in distribution (eq 1.1):

$$A = \frac{\sum_{a=1}^{100} f(a)g(a)}{\sum_{a=1}^{100} f(a)f(a)} \tag{1.1}$$

Where *f* and *g* are the probability density functions corresponding to the distribution of the strong and the weak species respectively and each spans between [1; 100].

In this study, the population dynamics of both species follows an annual sequence of events: growth and recruitment at the beginning, followed by fishing, and lastly, movement.

Biological component of the model: growth and recruitment

Growth and recruitment are modeled annually using the Deriso-Schnute delay difference model (Schnute 1985) (eq 1.2):

$$\begin{aligned} B'_{s,a,y} &= (1+\rho_s)B_{s,a,y}s_s(1-\mu_{s,a,y}) \\ &\quad -\rho_s s_s(1-u_{s,a,y})\left(s_s(1-u_{s,a,y-1})B_{s,a,y-1,} - \rho_s R_{s,a,y-L-2,}w_{s,L-1}\right) + R_{s,a,y-L-1}w_{s,L} \end{aligned} \tag{1.2}$$

where $B'_{s,a,y}$ is the biomass of the species *s*, in area *a*, during the year *y*, after fishing, growth, recruitment, and before movement. $B_{s,a,y}$ is the biomass of the species *s*, in area *a*, at the start of

the year y, before fishing. ρ_s is the Brody growth coefficient for the species s (from the weight at age relationship). $w_{s,L}$ is the weight at recruitment age L for the species s. $w_{s,L-1}$ is the pre-recruitment weight. $R_{s,a,y-L-1}$ is the lagged recruitment. s_s is the natural survival rate for species s, assumed to be constant over time and space, and $u_{s,a,y}$ is the harvest rate for species s, in the area a.

We assume in this study that the recruits come from a common pool of larvae and settle to each area as a normalized function of the habitat quality ($HSI_{s,a}$) (eq 1.3)

$$R_{s,a,y+L+1} = \frac{4R_s^0 h_s \sum_{a=1}^{n_a} B_{s,a,y}}{B_s^0(1-h_s) + \sum_{a=1}^{n_a} B_{s,a,y}(5h_s - 1)} \frac{\exp(-\beta(1-HSI_{s,a})^2)}{\sum_{a=1}^{n_a} \exp(-\beta(1-HSI_{s,a})^2)} \quad (1.3)$$

The first term in equation 3 determines the overall number of recruits, where R^0_s is the total virgin recruitment of the species s over the whole area, $B_{0,s}$ is the total virgin biomass of the species s over the whole area, h_s is the steepness (the fraction of R^0_s obtained at spawning stock of 0.2 $B_{0,s}$) of the Beverton and Holt stock-recruitment relationship for the species s, and $B_{s,y,a}$ is the biomass of the species s, in area a, at the beginning of the year y, before fishing. The second term in equation 3 determines the spatial distribution of recruits. A concentration factor β determines the degree to which recruitment is concentrated in preferred habitat. The larger β is, the more concentrated is the distribution of recruitment toward habitat with a higher *HSI* (Fig. 1.2). This might represent a situation where larvae have a large dispersal range but the strength of local hydrodynamics together with individual swimming ability jointly determine the degree to which larvae settle in the preferred habitat. A similar impact might result from lower post settlement mortality in areas with preferred habitat. While the spatial distribution of recruitment

and (as we describe below) fish movement are a function of *HSI*, we assume that growth and natural mortality rates are spatially homogenous. A rationale for this is that areas with higher *HSI* have higher carrying capacity and can sustain (attract) a larger fish capacity (due to more abundant food and habitat), but that positive impacts of more abundant food and habitat are offset by increased fish density equilibrating growth rate and survival rates across areas. This is consistent with an ideal free distribution assumption.

The catch component of the model: the fleet dynamics

Ten identical vessels harvest the populations under the specified harvest limits and with their behavior depending on the management system. We assume each vessel has a perfect knowledge of the expected catch in each site and that they are not forward looking. Vessels, fishing consecutively, maximize expected profit on each trip by choosing to fish in the site with the highest expected profit, net of quota costs in the case of IVQs (eq 1.4).

$$(1.4) \qquad \pi_{a,t} = \sum_{s=1}^{2} (B_{s,a,t,y} q_s - D_{s,a,t})(p_s - p'_{s,y}) - Q_t$$

where $\pi_{a,t}$ is the expected profit from fishing area a on fishing trip t, $B_{s,a,t,y}$ is the biomass of the species s present in area a, during the period t of year y, q_s is the catchability coefficient for species s, $D_{s,a,t}$ are the discards of species s, p_s is the ex-vessel fish price of species s, $p'_{s,y}$ is the quota price for species s in year y, and Q_t is the cost per trip. The quota price is zero for all scenarios except the IVQ scenarios in which it varies annually as described in the management scenarios below. The landed price of fish is assumed to be constant. Fish are assumed to be discarded once the TAC for that species has been reached in the scenarios where discarding is not banned. The catchability coefficient and the cost per trip were adjusted in this simulation so

that it resulted in effort levels of 250-750 individual trips, and vessels were able to catch the whole quota when species were spatially segregated.

The biomass for each species in each location is updated after each trip:

$$B_{s,a,t+1,y} = B_{s,a,t,y} - C_{s,a,t,y} \quad (1.5)$$

Where $C_{s,a,t,y}$ is the catch of species s in area a on trip t, during year y, and is equal to

$$C_{s,a,t,y} = e_{a,t} B_{s,a,t,y} q_s \quad (1.6)$$

where $e_{a,t}$ equals 1 for the area chosen by the vessel on trip t and zero in all other areas. Depending on the management scenario, vessels continue fishing until either one or both TACs are reached or until expected profit is no longer positive in any location. The total exploitation rate ($u_{s,a,y}$) for species s in the area a, during year y is the total catch in that area divided by the biomass at the start of the year y, $B_{s,a,y}$,

$$u_{s,a,y} = \frac{\sum_t C_{s,a,t,y}}{B_{s,a,y}} \quad (1.7)$$

Note that while the vessels in the IVQ scenario consider the quota price when deciding where to fish, the expenditures on quota represent transfers between quota owners and thus do not enter into the calculation of the total annual profit generated by the fishery which is simply the total landed catch multiplied by the ex-vessel fish price less harvest costs.

$$Fleet\,\pi = \sum_{t=1}^{T} \sum_{s=1}^{2} p_s (C_{s,t} - D_{s,t}) - Q_t \quad (1.8)$$

Note that $C_{s,t}$ and $D_{s,t}$ in equation 1.8 are the catch and discards from trip t summed across areas which, since only one area is fished per trip, is equal to the catch and discards in the area chosen.

Adults movement

After growth, recruitment, and harvest, each species disperses according to a diffusive movement model described in equations 1.9 and 1.10 below. The movement between any two cells depends on their *HSI* and the distance between the two areas.

$$\alpha_{a,i} \equiv \frac{HSI_{s,a} \exp(-\gamma d_{a,i})}{\sum_{a=1}^{n_a} HSI_{s,a} \exp(-\gamma d_{a,i})} \quad (1.9)$$

where $\alpha_{a,i}$ is the probability that fish moves from area *a* to *i*. We assumed that fish movement probability follows an exponential decaying function with the distance $d_{a,i}$ between the cell of origin *a* to the adjacent cell *i* adjusted by the habitat attractiveness (Cowen et al. 2007) where the parameter γ controls the slope of the exponential decay. The larger the value (γ>1), the closer the fishes stay to the cell of origin *a* (sedentary) and the less dependent they become on the habitat quality. In contrast, as γ becomes smaller (γ<1) the fish become more mobile and the impact of *HSI* on fish movement increases.

The biomass after movement of a species *s* in a cell *a* is the net difference between immigration and emigration (eq 1.10) where $B'_{s,a,y}$ is the biomass of the species *s*, in area *a*, during the year *y* after fishing, growth and recruitment, and before movement (eq 1.2). This population corresponds to the population at the beginning of the following year.

$$B_{s,a,y+1} = \sum_{i=1}^{n_a} B'_{s,a,y} \alpha_{i,a} - \sum_{i=1}^{n_a} B'_{s,a,y} \alpha_{a,i} \quad (1.10)$$

Management scenarios

We assume in this study that the managers have perfect knowledge of the biology and economics of the fishery and they set the catch limit according to the harvest control rule illustrated in Fig 3 or, in the IVQ MEY scenario, to achieve maximum annual profit.

Each simulation begins with both species in equilibrium at 50% of their carrying capacity which is obtained by running the model for 150 years without harvest then dividing the population by 2. The model is then run for another 70 years with the so-called "40-10" rule as used in the U.S. West coast (except for the IVQ MEY scenario as detailed below). Under this control rule, when the biomass is above 40% of virgin biomass ($0.4B_0$), the quota is set to the catch corresponding to F_{MSY}; when the biomass falls between $0.4B_0$ and the threshold stock size of $0.1B_0$, the TAC is reduced linearly from the catch corresponding to F_{MSY} to zero; and the fishery is closed when biomass drops below $0.1B_0$ (Fig. 1.3). Although it is possible to determine the exact F_{MSY}, we used the exploitation rate that leads to $0.4B_0$ (depletion level of 40% of with respect to the virgin biomass) as a proxy for F_{MSY} as it corresponds to the cut-off points of the 40-10 rule. In this study, we combine this harvest control rule with 6 different management scenarios affecting the regulations.

The first management scenario, referred hereafter as the "TAC with discard", is a limited-entry fishery with total allowable catch for each species that is fished competitively by the ten vessel fleets. In this scenario, vessels discard the species for which the TAC has been reached and keep fishing until it is no longer profitable or until both TACs are taken. Fishers are assumed to maximize revenue on each trip without consideration of the species mix, expecting that any effort they make to reduce catch of the weak stock will reduce their overall share of catch before

the fishery is closed that year. This race-for-fish (where individual boats race to get as much as the total allowable catch as possible) might also lead to increases in costs as vessels try to increase their share of the catch by increasing the power and speed of their vessels; however, we do not attempt to explicitly model these potential cost increases.

The second scenario mimics a limited-entry fishery with an MPA (referred to as "TAC with MPA" hereafter) and is structured the same as the TAC with discard scenario except some areas are closed in order to protect the less productive stock (Fig. 1.1). There are a number of factors that could change the effectiveness of an MPA at conserving the weak stock. Among others, the size, spacing, duration of MPAs, and the dispersal distance of the species are important factors (Sale et al. 2005). In this study, we set up a single MPA but of different sizes covering respectively between 15% and 30% of the range of one species for the total duration of the simulation. The center of the MPA is purposely set to the mode of the distribution of the weaker stock (hence to the best suitable habitat) to maximize protection of the weaker species (following Rodwell et al. 2003).

The third TAC scenario, "TAC MSY", is identical to the first except that discard is not allowed. All vessels thus stop fishing when the TAC for either species is reached.

We then simulate an IVQ managed fishery where the participants receive an equal share of the total TAC (no quota trading is simulated in this study since vessels are homogeneous and catch is deterministic). Under the scenario referred to as "IVQ MSY", vessels adjust the fishing location over the season (year) in order to maximize their profit taking into consideration the TACs of both species which are set at F_{MSY}. In practice this means vessels avoid areas where they may catch too much of the constraining species in order to be able to take the TAC of the productive

species. Such behavior has indeed been documented in IVQ fisheries (Branch and Hilborn 2008). In this study, the optimal level of avoidance is incentivized by subtracting the cost of quota for the unproductive species from the expected profit (see eq. 1.4). Increasing the quota value makes fishing in areas with high expected catch of the weak stock less attractive and diverts effort to areas with lower concentrations of the weak stock.

Following Holland and Schnier (2006), the quota price is adjusted each year to the level that optimizes avoidance of the weak stock in the sense that it results in maximum fleet wide profit (summed over all vessels) for that year. This does not necessarily ensure both TACs are completely taken because avoiding catch of the weak stock is costly when the stocks overlap, which creates a trade-off between higher avoidance that allows higher total catches and less avoidance which reduces costs. Once the quota value that leads to maximum profit for the year is calculated, it is used to determine the fishing effort distribution within a year. Quota price is constant within a year but can vary between years as TACs and the overlap of species vary. As noted earlier, quota costs are not counted in the actual calculation of profit when comparing management scenarios since they are not a true cost, just a transfer of profit from the fisherman to the quota owner (which may be one and the same).

Another variant of the IVQ scenario implemented in this study is the "IVQ with MPA" scenario which mimics an IVQ fishery where an MPA is imposed to protect the weak stock as described above. The last IVQ scenario is "IVQ MEY". This scenario differs from all the other scenarios as the control rule is no longer the "40-10" rule. The harvest rates that determine the TACs for each species are set, for the whole simulation time, at the levels that maximize the fishery-wide total profit. Hence, for each level of species overlap, a new set of F_{MEY} are determined: a combination

of grid search and numerical optimization is used to determine the set of F values that maximizes the equilibrium fishery-wide profit. When both species are spatially segregated, the species F_{MEY} that maximizes fishery-wide profit is the species-specific F_{MEY}.

Performance metrics to compare scenarios

We compare the performance between scenarios based on biological and economic criteria. The biological criterion we use is the population depletion level, DL_s, for both the weak and strong stocks in the final year of the simulation (year 75).

$$DL_s = \frac{\sum_a B_{s,a,75}}{B_{0,s}} \quad (11)$$

Under the 40-10 management rule, we would expect the populations for both species to reach 40% of B_0 by year 75 (at equilibrium) if catch for each species was equal to the respective TAC. Any end year depletion level above $B_{40\%}$ ($DL_s > B_{40\%}$) would be an indication of underexploitation (lost yield) and any level below ($DL_s < B_{40\%}$) would indicate overexploitation.

The primary economic criterion that we examine is the average of annual profit (equation 8) over the last 25years of simulation. The average was taken instead of a single year value (the end year profit for example) because of the change in fishing patterns over time. Due to the change in population distribution (as a consequence of fishing and fish movement), the effort distribution might change between years (i.e. profitable grounds could be different) and can lead to variation in profit year to year. The average profit over the last 25 years provides a performance metric that is not sensitive to annual variation. We track annual gross revenues and total costs so that we can distinguish how each impacts profit.

We also compare how spatial distribution of effort and biomass, and total annual effort (number of trips) differ between management scenarios and across ranges of habitat overlap to see how vessels changed their fishing pattern in response to the management settings.

Sensitivity tests

To test the sensitivity of our results (both biological and economic metrics) to key parameters, we rerun the above six managements scenarios but by changing the following parameters: (1) the price of the weak stock compared to the strong stock (half, three quarter, or one); (2) the difference in species productivity, μ (the productive species is twice, three times or four times more productive); (3) the cost factor (the base case or half that); (4) the MPA size (15% and 30% protection) and its location (centered on the unproductive stock, between stocks and centered on the productive stock); (5) the larval diffusion rate (low β=16 and high β=4 diffusion); and (6) the adult movement range (low γ=5 and high γ=1 movement). We then examine sensitivity of the ending year depletion levels (for both species) and the average (last 25years of simulation) profit to different habitat overlap levels, as each of these key parameters was varied.

Results

Change in profitability and depletion in the TAC fisheries (with and without discard)

The "TAC with discard" scenario generally resulted in low profitability for all levels of species overlap (Fig. 1.4, a). Furthermore, it showed an increasing overexploitation of the unproductive stock with increasing habitat overlap, moving from a depletion level of 40% at low overlap level to about 5% with high overlap (Fig. 1.4, g). As overlap of the species increases (Fig. 1.5, a-d), effort becomes more concentrated in areas where the species overlap (Fig. 1.6, a-d) causing the

catch of the weak species to reach the TAC before the TAC of the strong stock is caught. However, since discarding is allowed in this scenario, the unproductive stock is discarded while trying to catch the remaining TAC of the productive stock, allowing total catch of the weak stock to continue to increase with species overlap. This decreased the equilibrium landings of the unproductive species leading to a declining trend in the revenue curve with increased species overlap (Fig. 1.4, a). In contrast, the cost decreased first then stabilized after a certain level of spatial overlap (Fig. 1.4, a) because no extra effort was needed to land both species TACs (Fig. 1.4, a). When combining both curves, the profit curve follows a dome shape with respect to the habitat overlap (Fig. 1.4, a).

Suppressing the discarding behavior from the "TAC with discard" fishery, the "TAC MSY" scenario resulted in profitability up to three times higher than the "TAC with discard" case (Fig. 1.4, b) and both populations were preserved above the $B_{40\%}$ target level for all levels of species overlap (Fig. 1.4, h). The equilibrium distributions of the species and the relative spatial distribution of effort is similar to the "TAC with discard" scenario (Fig. 1.5, e-h, and 1.6, e-h). However, in the "TAC MSY" scenario, overall fishing effort continued to decline as habitat overlap increased (Fig. 1.4, n). The average effort over the last 25 years of simulation changed from mid-600 to 200 (~70% change) for "TAC MSY" over the range of habitat overlap simulated, as opposed to mid-600 to 500 (~25% change) for the "TAC with discard". Although the constraint of the weak stock led to decreasing yields of the strong stock (increasing amount of forgone yield) with increasing habitat overlap, profit increased since effort and costs declined (Fig. 1.4, b,n).

Change in profitability and depletion in the IVQ fisheries

The "IVQ MSY" scenario resulted in increasing profit with habitat overlap similar to the "TAC MSY" scenarios (Fig. 1.4, c), but showed a somewhat different depletion pattern for both species (Fig. 1.4, i). Both species were fished at the F_{MSY} level until a mid to high level of overlap (Fig. 1.4, i) as opposed to the "TAC MSY" case where the strong stock quickly became underexploited with any overlap (Fig. 1.4, h). Under the IVQ, it was only at a high level of species overlap that the strong stock was underexploited (Fig. 1.4, i). With moderate levels of overlap, the fleet operating under the "IVQ MSY" scenario was able to avoid the weak stock, which in turn, enabled them to fish down the stronger stock to a lower biomass (Fig. 1.4, i). In equilibrium, the relative spatial distributions of the species and of effort for the "TAC MSY" and "IVQ MSY" scenarios are similar but overall effort levels are higher under "IVQ MSY". Although revenues remain slightly higher under the "IVQ MSY" scenario with low to moderate species overlap, profits are lower than the "TAC MSY" as a consequence of higher effort and higher costs (Fig. 1.4, c *vs.* 1.4, b) with up to 30% decrease for the base case setting.

However, when TACs in the IVQ scenarios were set to achieve fishery-wide MEY criteria, the "IVQ MEY" scenario led to higher profit than the "TAC MSY" case, especially at low to moderate levels of species overlap (Fig. 1.4, d *vs* 1.4, b) with up to 200% increase in profit for the base case setting. At low species overlap, catch and effort of the strong stock was kept much lower in "IVQ MEY" scenario than either the "TAC MSY" or "IVQ MSY" scenarios. The biomass of the strong stock was consequently higher which reduced the effort and cost necessary to take the TAC and increased profit.

The effect of MPA on the profit and depletion

All of the scenarios with MPAs led to lower profit than scenarios without MPAs (Fig. 1.4, e,f *vs* 1.4, a-d). The MPA scenarios resulted in higher effort levels compared to the other strategies as vessels were excluded from the most profitable areas with higher fish concentrations (Fig. 1.4, q,r, 1.5, q-x, and 1.6, q-x). The average effort over the last 25 years fluctuated between 400 to over 600. The greater the overlap between the weak and strong stock, the more the strong stock was protected by the MPA and the less of its biomass was available for fishing (Fig 1.5t, x, and Fig. 1.6, t,x). This increased cost and reduced profit. However, the increase in fishing effort was not monotonic over different levels of habitat overlap but showed a slight sinusoidal trend (Fig. 1.4, q, r). The fishing effort first decreased as more unproductive stock became jointly harvestable with the productive species (Fig. 1.5, q-x and 1.6, q-x). However, as the overlap increased, more and more of the productive species biomass built up in the MPA requiring more effort to harvest the quota for that species outside the MPAs (Fig. 1.5, q-x and 1.6, q-x). As the overlap became extreme, the effort again decreased because only grounds with medium to low abundance for both species could be fished (Fig. 1.5, q-x and 1.6, q-x). Furthermore, under the base case scenario settings, both the "IVQ MPA" and the "TAC with MPA" led to similar biological results since the MPA was able to keep both stocks from falling below the $B_{40\%}$ target (Fig. 1.4, k,l). Additionally, the use of MPA led to increasing levels of forgone yield for the weak stock as the level of overlap decreased and an opposite trend for the strong stock (Fig. 1.4, k,l). Indeed, at low level of distribution overlap between the weak and strong stock, the only harvestable ground for the weak stock did not have enough of both species to be profitable thus the weak stock was underexploited (Fig. 1.5, q,u and 1.6, q,u).

Sensitivity tests to various model parameters[1]

To conserve space, we present here only one figure for the sensitivity analysis (Fig. 1.7) and the rest are summarized in table format (Table 1.2, a,b). Similar figures for each sensitivity analysis are provided in the supplementary material.

By increasing the weak stock price, the total profit of the fishery increased for all management methods (Fig. 1.7, a-f). The MPA scenarios consistently had the lowest profit among all scenarios and for all levels of species overlap (up to 4 times lower than the IVQ MEY at high level of habitat overlap), but they were not very sensitive to the change in the weak stock price (as most of the weak stock population was protected under the MPA) (Fig. 1.7, e-f). In contrast, the "TAC MSY" scenario showed largest increases in profit with a change in the weak stock price, especially at low to mid level of species overlaps for which the increase was up to 200% (Fig. 1.7, b). When the two stocks were spatially segregated and the weak stock price was low, there was little targeting of the weak stock since revenue was insufficient to cover the cost of fishing leading to high biomass for the weak stock at low overlap levels (Fig. 1.7, h). But as the weak stock price increased, targeting of the weak stock increased as it became profitable on its own. At the same time this led to an increasing underuse of the strong stock quota with increasing species overlap (Fig. 1.7, m). In the "IVQ" scenarios, profit increased with higher weak stock price and a higher proportion of the quota for both species was used (Fig. 1.7, c,i,o).

[1] Figures showing detailed results of the sensitivity analysis are included in the supplementary material. These figures show sensitivity of profit and depletion of weak and strong stocks to the difference in productivity between the two stocks (Fig. A1.1), fishing cost (Fig. A1.2), size of MPA (Fig. A1.3), location of MPA (Fig. A1.4), adult movement range parameter (Fig. A1.5), and spatial concentration of recruitment (Fig. A1.6).

The "IVQ MEY" had the highest profit among all scenarios but at low weak stock price, the fishery MEY solely depended on the strong stock quota thus led to the deliberate overexploitation (biomass falling below the $0.4B_0$ target level) of the weak stock with high species overlap (Fig. 1.7, d,j,p).

Increased productivity of the strong stock (and thus increasing differences in productivity of the two stocks) increased the total profit made by all fisheries as it increased the TAC for the stronger stock (Table 1.2). However, the change in profit level was not equal across the level of habitat overlap. Under the "TAC with discard" scenario the increase in productivity of the strong stock led to a higher profit at low to mid level of habitat overlap but to a slight decrease in profit at higher overlap levels (Table 1.2, a). The increase in the strong stock TAC was profitable for the fishery at first because more fish were caught without compromising the weak stock population. As the overlap increased, discarding increasingly reduced the weak stock biomass and slightly decreased the equilibrium profit level. Eliminating the discarding behavior removed this tendency and profit kept increasing with increasing species overlap (Table 1.2, a).

Reducing the cost of fishing did not change the equilibrium depletion level of the weak and strong stocks for the "TAC with discard", "TAC MSY" and the "IVQ MSY" scenarios but increased the total level of profit for all scenarios (Table 1.2, a). In addition, at lower cost, the profits of the scenarios without MPAs were much closer to each other than with higher costs. This is because at reduced cost, both species F_{MEY} were much closer to their F_{MSY}, especially at low to mid level of species overlap (Fig. 1.8, f). For mid to high level of species overlap, the F_{MEY} for the weak stock became higher than F_{MSY} causing the weak stock biomass to fall below its $0.4B_0$ target level for the "IVQ MEY" case.

Increasing species movement rates (lower γ) generally decreased the fishery-wide profit and did not influence much the depletion level of the stocks for all scenarios except the ones with MPA (Table 1.2, a). Profits were decreased because fish were more evenly distributed which reduced the ability of the fleet to concentrate effort in high density areas and therefore decreased the average catch per unit effort and increased costs. With very low movement rate, a smaller (15%) MPA was enough to keep the weaker stock above the target level ($B_{40\%}$), but as movement rate increased, it became harder to protect the weaker species and a bigger MPA was necessary to maintain the population above the 40% target level which drove down profit. This is due to the spillover and fishing-the-line effects (Walters et al. 2007; Kellner et al. 2007).

Lowering the spatial concentration of recruitment toward areas with high *HSI* (i.e. assuming a lower β) impacted the shape of the biomass distribution (wider distribution with a lower β) for both populations (Fig. 1.2). This changed the fleet distribution and the subsequent fishery performance. With lower concentration of recruitment, profit is lower for all scenarios (Table 1.2, a). Similar to increasing the adult movement rate, decreasing concentration of recruitment leads to a more evenly distributed fish stock and lower average CPUE. The lower concentration of recruitment also led to higher biomass levels (less depletion) for both weak and strong stocks, especially with low to moderate species overlap (Table 1.2, a). With lower concentration of recruitment catch of the strong stock was limited by profitability rather than the TAC.

As mentioned earlier, the MPA cases led to the lowest profitability but their relative efficiency (both ecological and economic) was very sensitive to the size, location and movement rate of the fish. By doubling the reserve size (from 15% to 30%), both the weak stock and the strong stock became more and more underexploited (at a level above 80% of B_0) and fishery profitability

decreased (Table 1.2, b). Better biological and economic performance was generally obtained when setting the MPA at the modal distribution of the weaker stock, except when the 2 species distributions were completely apart or completely overlapping (Table 1.2, b). With a 50% level of species overlap, profit was the same whether the MPA was centered on the weak or the strong stock, but the stock on which the MPA was centered was less depleted.

Discussion

Total allowable catch or individual quota?

In this study we have shown that, for a multispecies fishery managed with a competitive TAC, the risk of depleting the unproductive stock can increase as the overlap of the species increases if discarding is allowed. This is a consequence of discarding the unproductive species (when its catch has reached its TAC) while continuing to harvest the productive species until its TAC is taken. In addition, this behavior leads to a lower equilibrium catch of the unproductive stock, and hence to reduced profit. If catches of the unproductive stock are limited by a discard ban, catch of the productive stock may be constrained, but this does not necessarily reduce profit. By prohibiting discarding, profitability in the "TAC MSY" scenario actually increases with the degree of species overlap while still preserving both species above the target population level. This is partly because increasing species overlap reduces costs by allowing joint targeting. In addition, the increased overlap reduces the catch of the productive stock since the TAC of the unproductive stock constrains it. Consequently biomass of the productive stock increases and costs per unit of catch decline, leading to an increase in profit. In effect, the constraint of the unproductive stock's TAC moves the fishery for the productive stock away from MSY and

toward MEY (Fig. 1.8). Although catch and revenue at MEY are lower than MSY the drop in revenue is more than made up for by a reduction in cost.

With the base price and cost assumptions, our "IVQ MSY" scenario led to a similar trend of increasing profitability with increased species overlap but with generally lower profit than the TAC fishery with a discard ban. In the "IVQ MSY" fishery, the distribution of effort adjusts to maximize profit each year. The reason for this lower equilibrium profit is related to the relationship between F_{MEY} and F_{MSY}. Under the base case assumptions, F_{MEY} is well below F_{MSY} (Fig. 1.8, a), and, under the "TAC MSY" scenario, fishing is forced to stop before all the quota for the strong stock is used due to the weak stock quota constraint. Thus, the realized effort (and harvest rate) is lower than F_{MSY}, and closer to F_{MEY} (Fig. 1.4, o,p, 1.7, a). In contrast, under the "IVQ MSY" scenario, effort is shifted away from the areas with high catch rates of the unproductive stock. This result had been seen in empirical studies – e.g., by comparing quota use in the BC groundfish trawl fishery to the UW West coast groundfish trawl fishery when the former was under IVQs while the latter was not (Branch and Hilborn 2008). Avoidance of the unproductive stocks allows higher catches of the productive stock and higher revenues in the short term, but maintains catches closer to MSY than occur under the "TAC MSY" scenario. Consequently the biomass of the productive stock remains lower and harvest costs are higher.

Although the "TAC MSY" scenario led to a higher profit level than the "IVQ MSY" or "TAC with discard", it was much lower than the "IVQ MEY" scenario except at very high species overlap. The "IVQ MEY" scenario was much more profitable than all the other scenarios, especially at low to mid level of overlap, because of the large difference in the values of F_{MEY} and F_{MSY} in the base case setting (Fig. 1.8, a and see Clark 1990). However, when the fishing

cost was reduced, the F_{MEY} levels became much closer to the F_{MSY} values which decreased the difference in profit between the scenarios for all levels of species overlap (Fig. 1.8, b). The "IVQ MEY" scenario did lead to situations where the weak stock biomass fell below the target size of $0.4B_0$., but this happened only at high level of species overlap and when the weak stock price became so low that it did not contribute much to the total profit or when the cost of fishing was reduced (Fig. 1.8, b,f).

The economic benefits of the IVQ are arguably underestimated in this study as we made the assumptions that the price of fish was fixed. In reality, prices change throughout the year, depending on the supply and demand of the market and the quality of the product among other things. Prices in IVQ fisheries have often increased as a consequence of increasing quality and avoidance of market gluts (Herrmann 1996). IVQs also add some flexibility for fishers to choose their fishing period (Scheld et al. 2012) which may enable them to land fish when demand and prices are higher or when catch rates are higher thereby reducing harvest costs. Additionally a cooperative game between fishers under the IVQ program could lead to more efficient outcome (Costello and Deacon 2007). It should also be noted that under competitive TACs (e.g., the "TAC with discard" and the "TAC MSY" scenarios) there are many ways for profit to be dissipated that we did not model in this study. These include increased costs and reduced prices that are often the consequence of a race for fish that ensues when fishers compete with each other for their share of the TAC (see Branch et al. 2006a for review). Thus although our results suggested profits could be higher under the "TAC MSY" scenario than under the "IVQ MSY" scenario at low to moderate levels of species overlap, this advantage could be eroded completely by cost increases associated with a race-for-fish.

Ensuring compliance with a discard ban in a TAC based fishery would also require substantial monitoring effort which would be costly. Real time observer or CCTV-systems would likely be required. Similar monitoring would also be required to prohibit discarding in IVQ fisheries, but these additional costs are offset by the higher expected profitability operating under and IVQ system. Full observer coverage was implemented in the BC trawl fishery (Branch 2009) and the U.S. West coast trawl fishery when IVQs were implemented (PFMC and NMFS 2010). These monitoring costs are covered by industry in BC and will be in the U.S. though they are partially covered by the government the first few years.

To summarize, our simulation study showed clear gains from eliminating the discarding that occurred under the "TAC with discard" scenario. This also helped keep both populations above a specified target level. Although the TAC fishery with a discard ban was found to provide a higher profit than the "IVQ MSY" scenario for some levels of species overlap, the difference was reduced when species overlap was higher. The performance of the "TAC MSY" scenario also hinges on the assumption that costs do not increase or prices fall due to a race-for-fish, both of which would reduce profitability relative to an IVQ.

Effect of MPA on population size and profitability

This study, like many other studies on MPAs showed that spatial closures could potentially be used to conserve an unproductive stock but that the efficiency was contingent upon the characteristics of the catch species. Similar to the results of Walters et al. (2007), even a limited dispersal (larval or adult) compromised the effectiveness of an MPA to protect species within the reserve and the species abundance was reduced all the way to the center of the MPA due to the edge effect. Moreover, MPAs generally reduced the potential profitability of the fishery whether

used in a TAC based fishery or in an IVQ fishery. However, like Sanchirico and Wilen (1999), we found a few situations in which the use of an MPA was more profitable than the "TAC with discard" without an MPA. This occurred only in our sensitivity analysis when species had a high movement rate and high overlap. However, MPAs did not provide a higher profit level when used together with an IVQ system. The MPA model we used in this study was however quite simple and conclusions might differ if one considered other factors discussed in the literature such as networks of MPA, compensatory process, or maternal effect (Botsford et al. 2003; Berkeley 2006; Gaines et al. 2010).

Model limitations and potential extensions

In this study, we examined the behavior and outcomes of a mixed stock fishery under a few typical management systems using a simple bioeconomic model of two species parameterized based on two rockfish species of the U.S. West coast: the canary rockfish (*Sebastes pinniger*) and the yellowtail rockfish (*Sebastes flavidus*). While this simple model is useful to understand more directly how key parameters and assumptions impact the relative performance of different management approaches for a multispecies fishery with overlapping species of varying productivity, we acknowledge that it lacks realism. In addition to including only two species, the model makes a number of simplifying assumptions including deterministic population dynamics and perfect information for both managers and fishers. Most multispecies fisheries (such as a groundfish trawl fishery) involve more than two species and temporal variation in population dynamics and uncertainty for managers and fishers are nearly always present in fisheries. Furthermore, there are a number of factors that we do not include in our model that can influence the behavior of fish or fishers [e.g., density-dependent fish movement (Thorson et al. 2012);

schooling behavior (Thorson et al. 2012); habit/tradition (Holland and Sutinen 2000); risk preference (Holland 2008) or price response to the market (Herrmann 2006) to name a few].

Relaxing our simplifying assumptions would likely alter the absolute results of our simulations and could alter the relative performance of alternative management approaches we model. For example, in a fishery with more species, it may become increasingly difficult to control the mix of species in catch which would tend to reduce the difference between the "TAC MSY", "IVQ MSY" and "IVQ MEY" scenarios. Similarly, factors that limit the ability of or effort by fishers to avoid catch of the weaker stock would impact relative results.

Adding stochasticity and uncertainty might impact the findings of the model as well. Random variation in recruitment or growth would be expected to create variation in outcomes from year to year, but we would expect to see similar average results as the deterministic model. We expect that stochastic variation in habitat preference (recruitment distribution or adult movement) would have a similar effect as a higher diffusion rate which we did explore. However, uncertainty about the biological system that results in improper setting of TACs and/or MPAs could clearly impact the absolute performance and quite possibly, the relative performance of alternative management approaches. For example MPAs have been suggested as a hedge against uncertainty that might lead to TACs being set too high (Lauck et al. 1998). Strict adherence to TACs for the unproductive stock could also be costly if they were set too low due to underestimates of abundance or productivity (Holland and Herrera 2006). It would therefore be useful to evaluate how these management approaches perform in the face of uncertainty.

We did try introducing random noise to expected catch rates to explore how vessel-level uncertainty in catch rates across location affects the model. The biological and economic results

of these simulations were very similar to the deterministic case. There was a slight change in the absolute catch and profit level, but the relative performance of the management scenarios was not substantively different. However it might be useful to consider other forms of uncertainty or behavioral responses to uncertainty (e.g. risk aversion) that might lead to more systematic differences in targeting behavior which could alter the relative effectiveness of particular management approaches (e.g., by changing how fishers respond to a closure or the incentives crated by IVQs).

Our analysis focused on the economic and biological performance of the multispecies fishery but there are other performance criteria that might be considered. These include for example, food security, boat safety, biodiversity protection and other social or ecosystem services that might be provided by an MPA for example (see Branch 2009 or Gaines et al. 2010 for review). We also consider only equilibrium outcomes, so don't account for the opportunity costs of forgone yields that might be required build stocks to levels associated with MEY.

This study takes a first step at analyzing the bio-economic performance of a multispecies fishery under several typical management methods and shows the importance of considering the species distribution overlap. A natural extension of the study is to build a more realistic model of population dynamics and vessel dynamics in order to conduct a management strategy evaluation of alternative management approaches for specific fisheries. Such work could potentially take advantage of the several simulation platforms that have been developed over the past decades such as the ISIS-fish (Pelletier and Mahévas 2005) or Atlantis (Kaplan et al. 2011).

Table 1.1. Simulation parameters for the base case scenarios

Parameters	Weak stock	Strong stock
Growth and recruitment parameters		
Intercept of the Brody growth equation (α)	0.6	0.6
Slope of the Brody growth equation (ρ)	0.95	0.95
Pre-recruitment weight (w_{k-1})	0.7	0.7
Recruitment weight (w_k)	0.85	0.85
Natural mortality (m)	0.13	0.21
Virgin recruitment (R_0)	4.01	7.79
Steepness (h)	0.4	0.6
Management parameter		
F_{MSY}	0.06	0.18
Movement/diffusion parameters		
Fish movement concentration parameter (γ)	16	16
Recruitment diffusion parameter (β)	5	5
Fishing parameters		
Fish price	0.75	1
Cost per trip (Q_a)	6000	6000

Table 1.2a. Summary table of the sensitivity analysis of profit and depletion of weak and strong stocks to an increase in productivity difference, size of MPA, adult movement range, and a decrease in fishing cost and spatial concentration of recruitment. An increase is indicated with (+), a decrease with (-). The intensity of changes is expressed by repeating the respective sign multiple times e.g. (+++) >50% increase, (++) between 10-50%, (+) between 2-10%, (·) below 2%.

	Difference in productivity						*Cost of fishing*						*Adult movement*						*Larval diffusion*					
	1	2	3	4	5	6	1	2	3	4	5	6	1	2	3	4	5	6	1	2	3	4	5	6
Change in profit																								
[0-25%[habitat overlap	++	++	++	++	++	++	+++	+++	+++	+++	+++	+++	--	--	--	--	--	--	---	---	---	---	---	---
[25-75%] habitat overlap	-	++	++	++	++	++	+++	+++	+++	++	+++	+++	--	--	--	--	+	++	---	---	---	--	---	---
]75-100%] habitat overlap	--	++	+	++	++	++	+++	++	++	++	+++	+++	-	-	--	-	+++	+++	-	--	--	--	--	--
Change in the weak stock depletion																								
[0-25%[habitat overlap	-	-	·	+	·	·	-	-	·	--	--	--	+	+	+	·	--	--	+++	+++	+++	++	++	++
[25-75%] habitat overlap	-	·	·	+	-	-	·	·	·	--	--	--	-	-	-	+	--	--	++	++	++	++	+	+
]75-100%] habitat overlap	--	·	-	-	-	-	·	·	-	--	--	--	-	-	-	--	---	--	+++	·	·	++	·	·
Change in the strong stock depletion																								
[0-25%[habitat overlap	·	·	·	+	·	·	·	·	·	--	·	·	+	+	+	·	+	+	+++	+++	+++	++	+++	+++
[25-75%] habitat overlap	+	++	·	+	+	+	·	·	·	--	-	-	·	-	·	·	-	-	++	++	++	++	++	++
]75-100%] habitat overlap	+	++	-	++	+	+	·	·	--	--	--	--	+	·	+	-	--	-	+++	·	++	++	++	++

Scenario number description:

1. TAC with discard
2. TAC MSY
3. IVQ MSY
4. IVQ MEY
5. TAC with MPA
6. IVQ with MPA

Table 1.2b. Summary table of the sensitivity analysis of profit and depletion of weak and strong stocks to an increase in productivity difference, size of MPA, adult movement range, and a decrease in fishing cost and spatial concentration of recruitment. An increase is indicated with (+), a decrease with (-). The intensity of changes is expressed by repeating the respective sign multiple times e.g. (+++) >50% increase, (++) between 10-50%, (+) between 2-10%, (·) below 2%.

	MPA size		*MPA on the strong stock*		*MPA between the two stocks*	
	5	6	5	6	5	6
Change in profit						
[0-25%[habitat overlap	--	--	---	---	+++	+++
[25-75%] habitat overlap	--	--	-	--	+++	+++
]75-100%] habitat overlap	---	---	--	--	+	+
Change in the weak stock depletion						
[0-25%[habitat overlap	++	++	--	--	--	--
[25-75%] habitat overlap	+++	+++	--	--	--	--
]75-100%] habitat overlap	+++	+++	-	-	-	-
Change in the strong stock depletion						
[0-25%[habitat overlap	·	·	+++	+++	--	--
[25-75%] habitat overlap	++	++	+++	+++	-	-
]75-100%] habitat overlap	++	++	+	+	·	·

Scenario number description:

4. TAC with discard
5. TAC MSY
1. IVQ MSY
4. IVQ MEY
5. TAC with MPA
6. IVQ with MPA

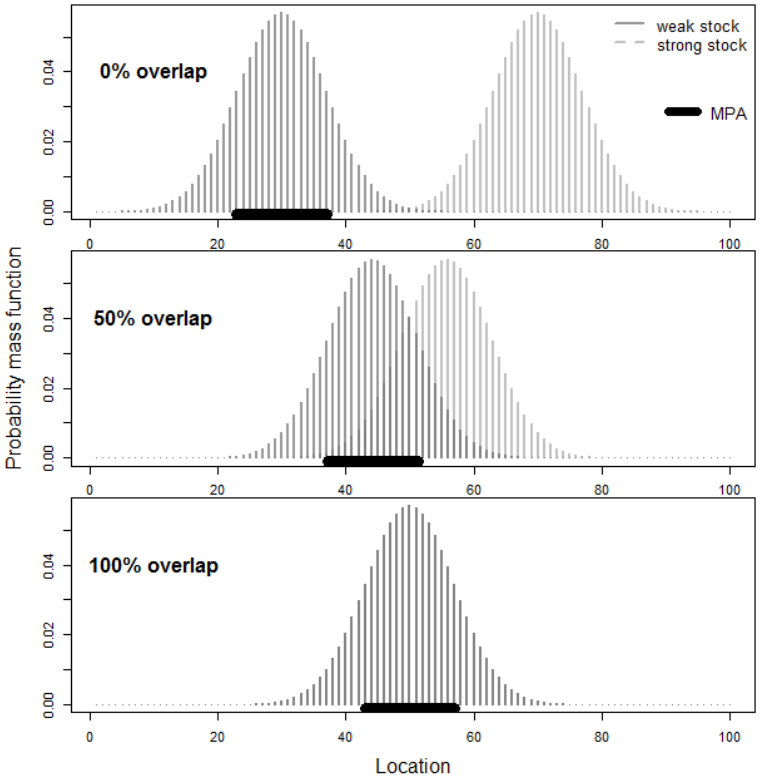

Figure 1.1: Calculation of the species overlap

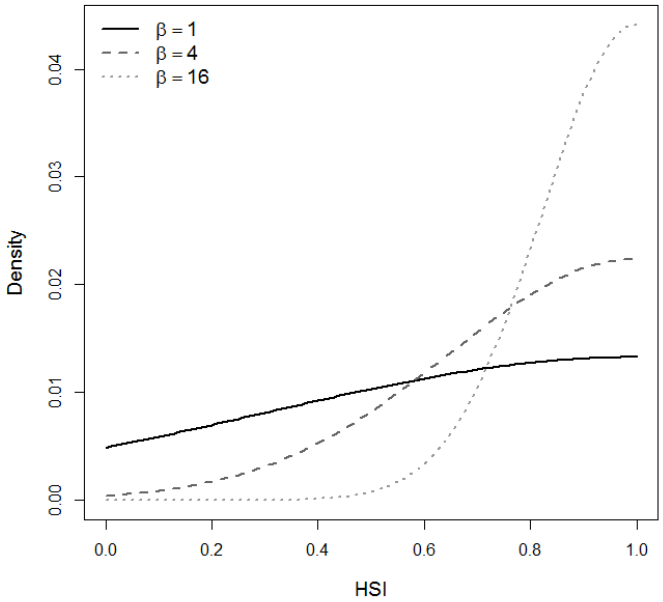

Figure 1.2: Effect of the concentration factor β on the proportion of recruits to each habitat quality (*HSI*)

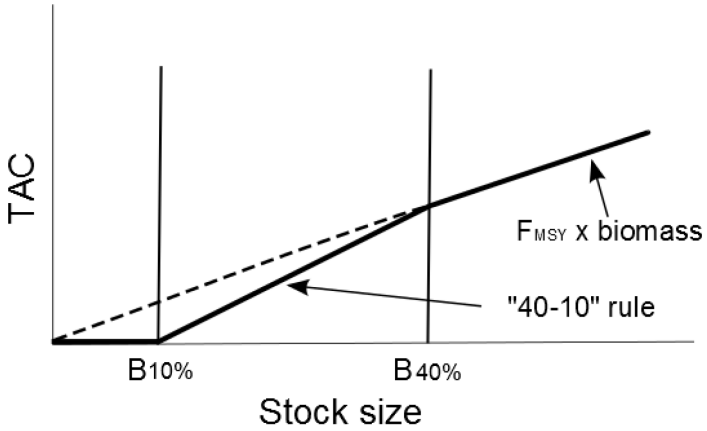

Figure 1.3: Catch limit under the "40-10" rule

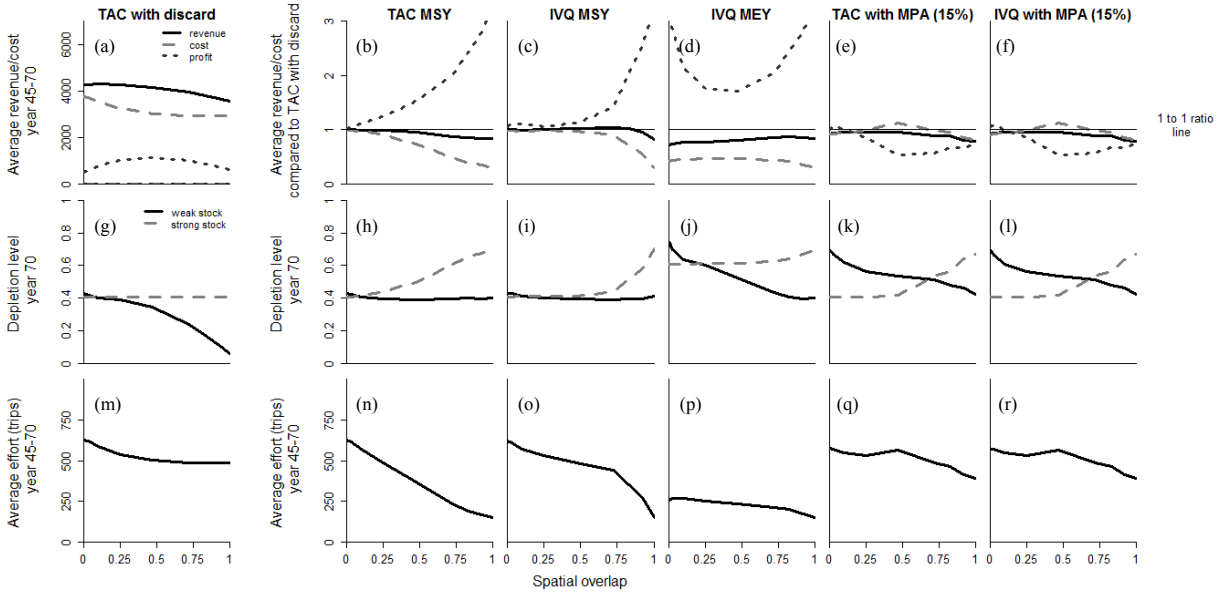

Figure 1.4: Economic (revenue, cost, profit) (panels a-f), ecologic (biomass depletion relative to the virgin biomass) (panels g-l) and fishing (effort) (panels m-r) performance indicators of the six management scenarios (TAC with discard, TAC MSY, IVQ MSY, IVQ MEY, TAC with MPA, IVQ with MPA) at different level of spatial overlap between the unproductive and productive species. The panel on the left shows the result for the TAC with discard scenario while the panels on the right is relative to the TAC with discard scenario (for the economic performance indicator only).

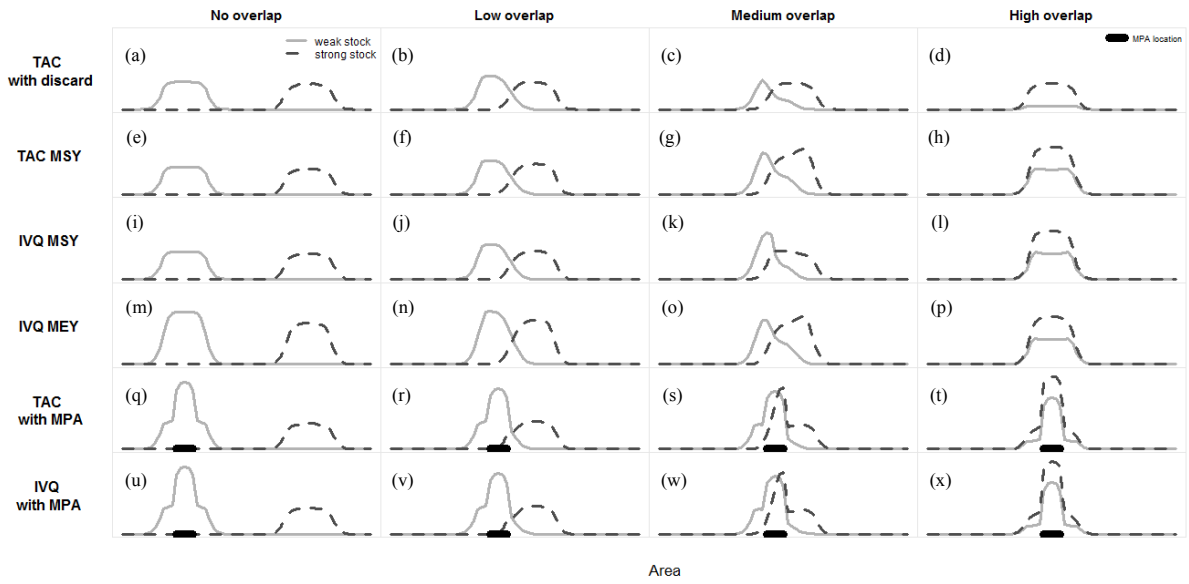

Figure 1.5: Equilibrium population distribution (year 70 of simulation) of the weak stock (solid line) and strong stock (dash line) for different level of spatial overlap (no (0% overlap) (panels a, e, i, m, q, u), low (33% overlap) (panels b, f, j, n, r, y), mid (66% overlap) (panels c, g, k, o, s, w), high overlap (100% overlap) (panels d, h, l, p, t, x)) and for the base case management scenarios.

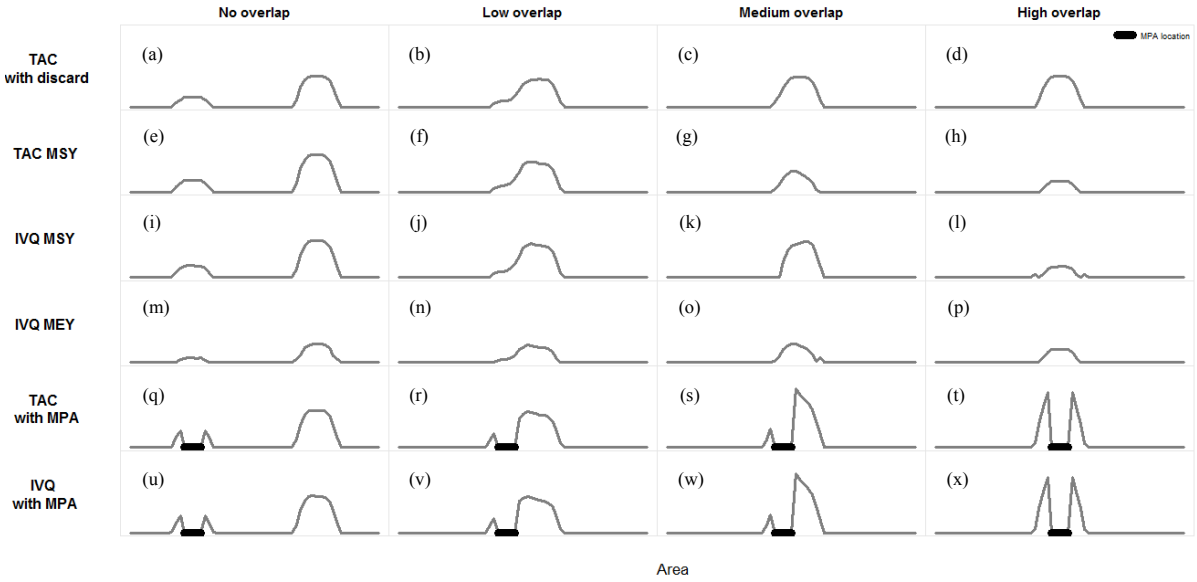

Figure 1.6: Equilibrium effort distribution (year 70 of simulation) for different level of spatial overlap (no (0% overlap) (panels a, e, i, m, q, u), low (33% overlap) (panels b, f, j, n, r, y), mid (66% overlap) (panels c, g, k, o, s, w), high overlap (100% overlap) (panels d, h, l, p, t, x)) and for the base case management scenarios.

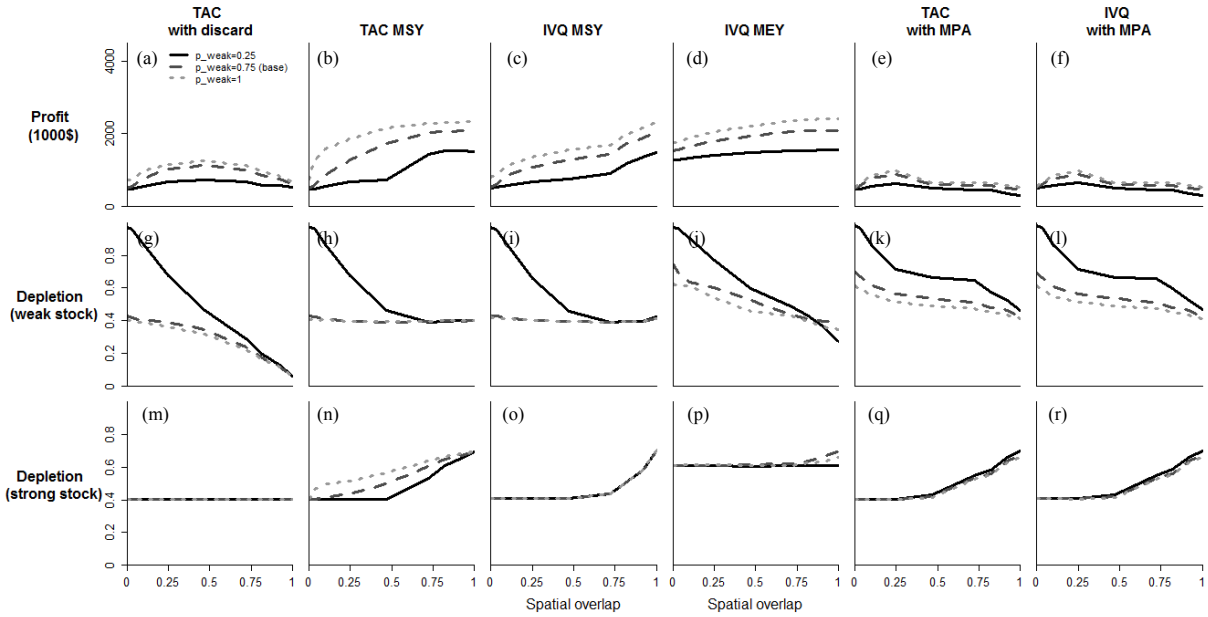

Figure 1.7: Sensitivity analysis of the economic (profit) and ecologic (depletion level) performance indicators to the weak stock price (compared to the fixed strong stock price of 1).

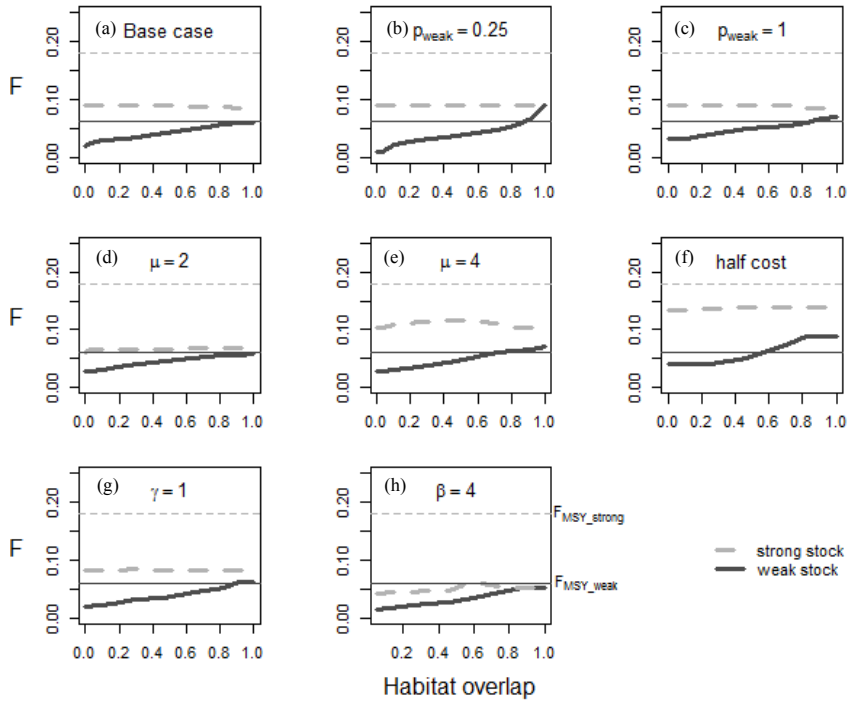

Figure 1.8: The harvest rate (F) for each species and for each habitat overlap level that leads to the fishery-wide MEY. Results are from the base case and the 7 other sensitivity tests.

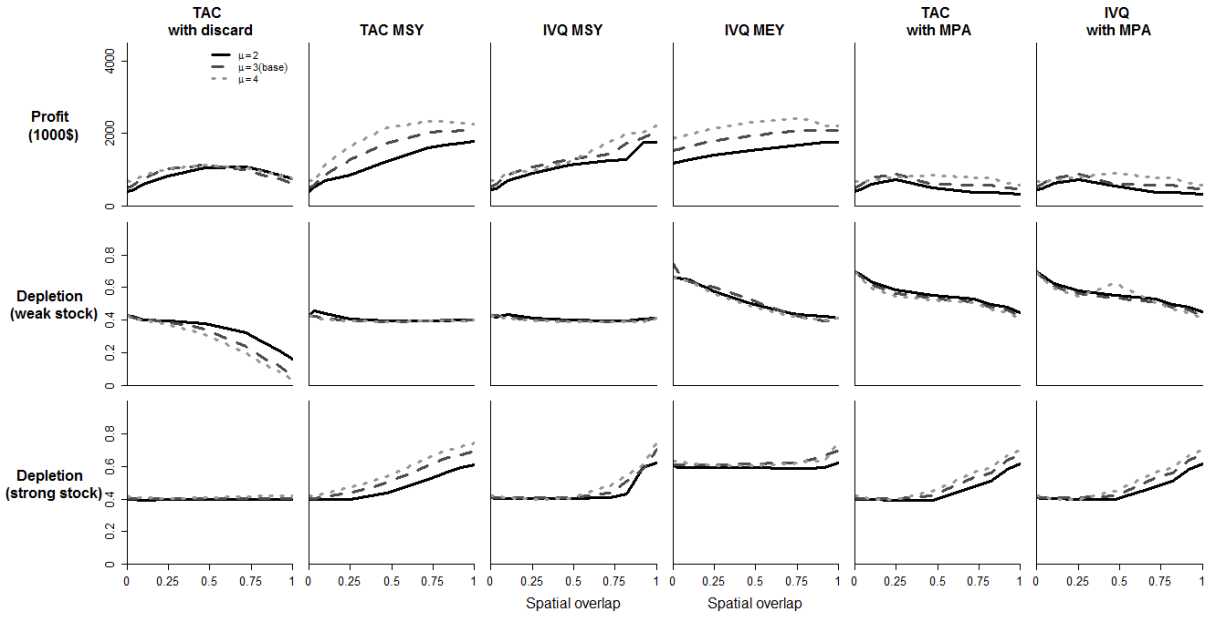

Figure A1.1: Sensitivity analysis of the economic (profit) and ecologic (depletion level) performance indicators to the difference in productivity between the two stocks, μ (ratio of the strong stock F_{MSY} over the weak stock F_{MSY}).

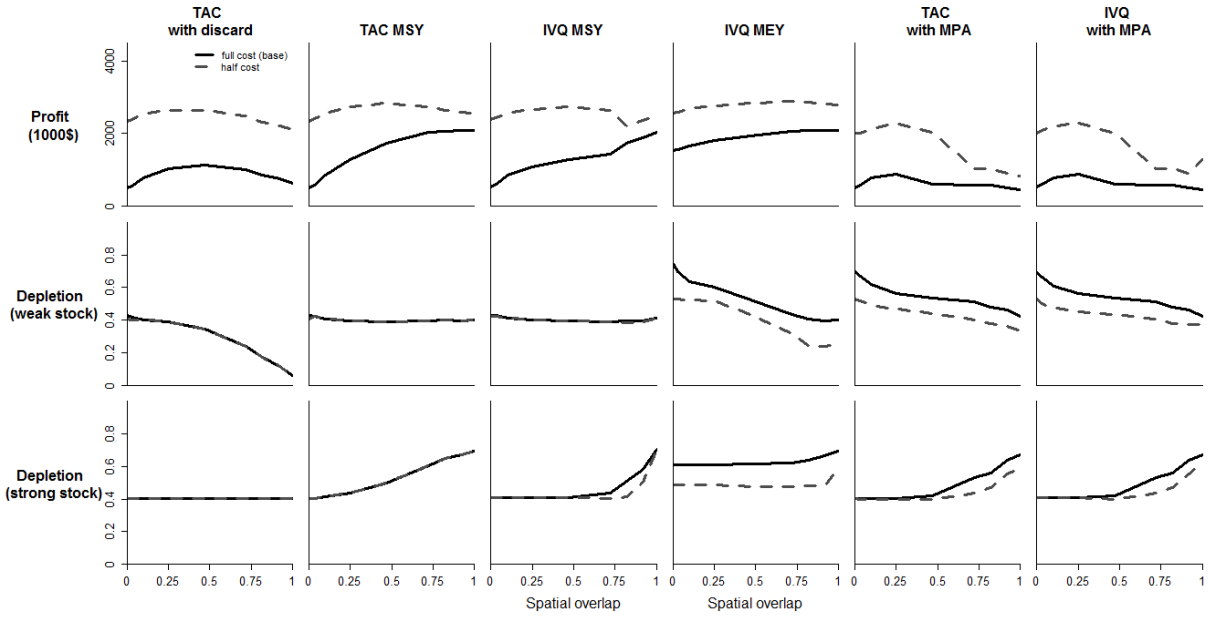

Figure A1.2: Sensitivity analysis of the economic (profit) and ecologic (depletion level) performance indicators to cost.

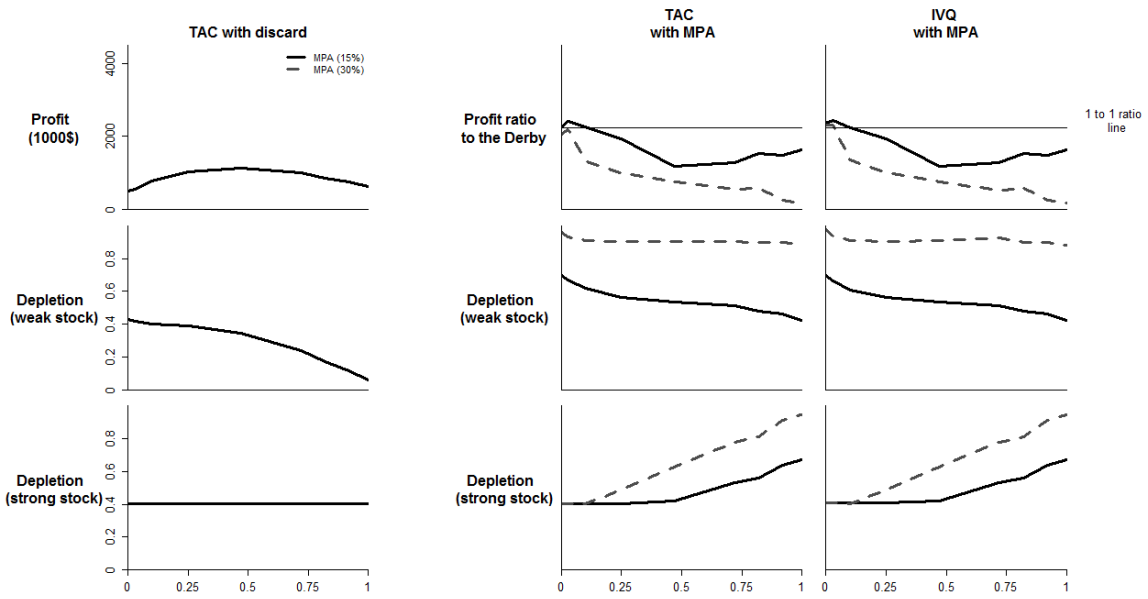

Figure A1.3: Sensitivity analysis of the economic (profit) and ecologic (depletion level) performance indicators to the MPA size. The panel on the left shows the result for the TAC with discard scenario while the panels on the right is relative to the TAC with discard scenario (for the economic performance indicator only).

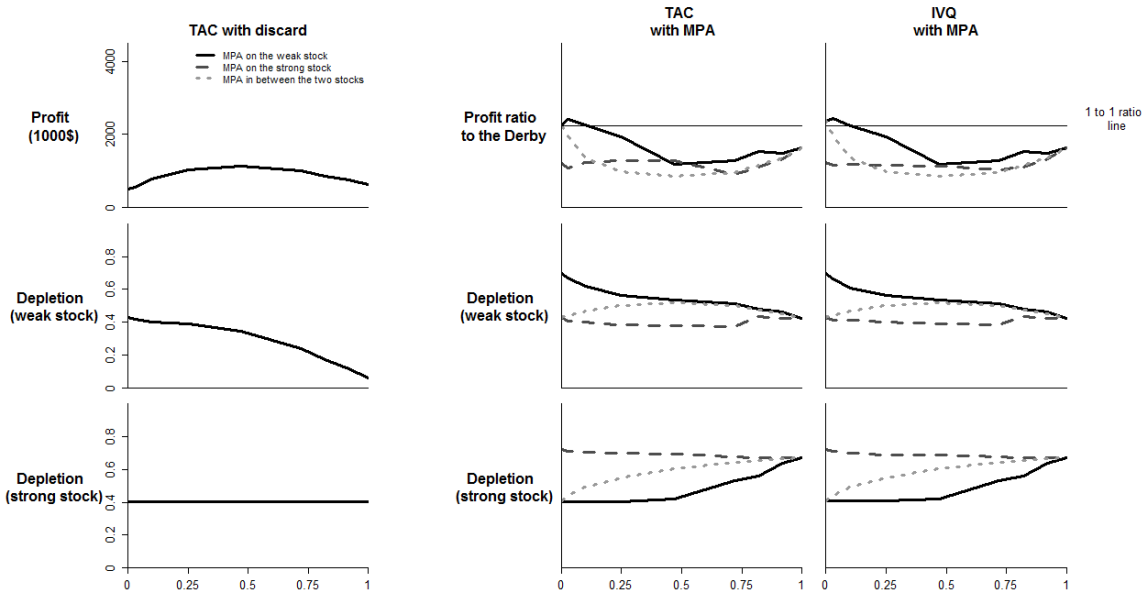

Figure A1.4: Sensitivity analysis of the economic (profit) and ecologic (depletion level) performance indicators to the MPA location. The panel on the left shows the result for the TAC with discard scenario while the panels on the right is relative to the TAC with discard scenario (for the economic performance indicator only).

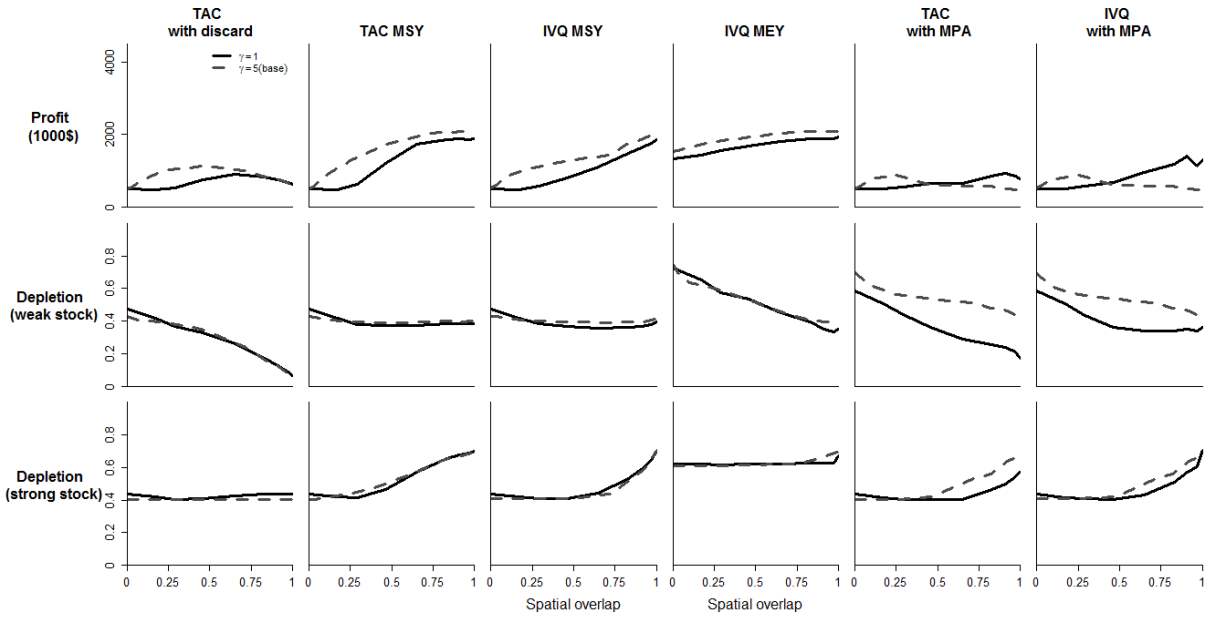

Figure A1.5: Sensitivity test of the economic (profit) and ecologic (depletion level) performance indicators to the adult movement range parameter (γ). Results are from the 5 management systems and for different level of spatial overlap between the unproductive and productive species

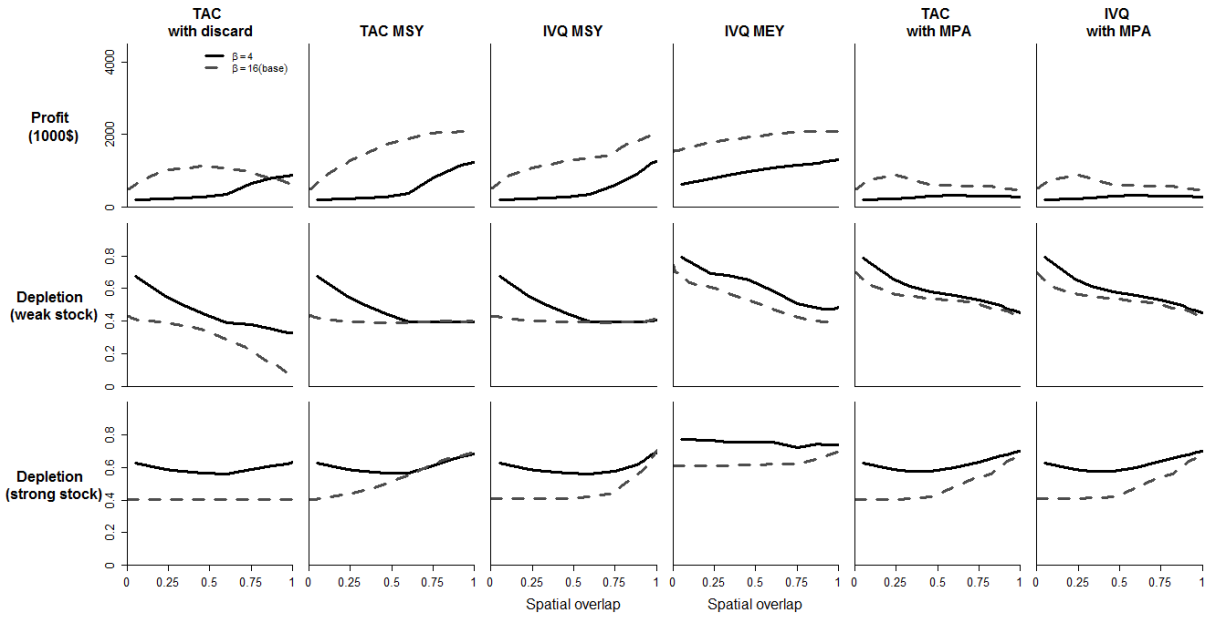

Figure A1.6: Sensitivity test of the economic (profit) and ecologic (depletion level) performance indicators to the spatial concentration of recruitment (β). Results are from the 6 management systems and for different level of spatial overlap between the unproductive and productive species.

Chapter 2 - How do marine closures affect the analysis of catch and effort data?

Abstract

Fisheries managers increasingly use marine closures as a tool to conserve ecosystems, biodiversity, and fish abundance. Despite the suggested benefits of closed areas, the lack of or limited data collection within them leads to issues in assessing the status of populations. We investigated how spatial closures impacted the reliability of the indices of abundance obtained from standardization approaches applied to catch per unit effort data. The presence of closed areas generally introduced a bias in the derived index of abundance, and the magnitude of bias increased as the portion of the population in closed areas increased. The bias was generally positive for the pre-closure period and negative post-closure, leading to a conservative estimate of the ratio of current to virgin biomass for the final years of the study period. An imputation model proposed in this study produced the least biased and most precise indices of abundance for most levels of species protection. It also provided one of the most accurate estimate of final year depletion. The collection of ancillary data was only helpful to reduce bias in the estimate of final year depletion when area closures protected a large portion of the population or when closures were implemented early in the time series. However, the precision of the estimates of final year depletion decreased as a larger portion of population was protected by the closures.

Introduction

The analysis of commercial or recreational catch per unit effort (CPUE) data has a long history in fishery science because CPUE has often been the only data source available to reflect changes in population size (Hilborn and Walters 1992, Bordalo-Machado 2006). These data are easier

and cheaper to collect than survey data, and have been used as an index of abundance in many fishery assessments (Polacheck et al. 1993, Maunder 2001, Campbell 2004, Maunder and Punt 2004). However, it has also been long recognized that fishery-dependent data are not straightforward to use. Fishery CPUE data are not only influenced by changes in fish abundance, but also by many other factors such as choices of fishing location or technological changes (Beverton and Holt 1957, Maunder et al. 2006). Consequently, CPUE data have often been "standardized" before being used as an index of abundance in assessments. "Standardization" consists of attempting to remove the effects of biotic and abiotic variables that can affect the raw CPUE so that the resulting index only reflects changes in abundance over time. Common standardization methods include the use of mixed and fixed effects versions of generalized linear or additive models (Maunder and Punt 2004). CPUE standardization also involves selecting an error distribution for the data (e.g., modeling zero-inflation (Maunder and Punt 2004) or over-dispersion (Thorson et al. 2012)), as well as conducting model selection using standard tools such as information criteria, including AIC (Burnham and Anderson 2002).

Recently, management methods have evolved to respond to societal objectives such as sustainability, profitability and minimization of the environmental impacts of fishing. For example, the U.S. West coast groundfish fishery has recently transitioned from a trip limit system to an individual quota system to increase stewardship and create individual economic stability (PFMC and NMFS 2010). Spatial closures have also been placed in many coastal regions to protect essential fish habitat and marine ecosystems (e.g. the Marine Life Protection Act (MLPA) related closures in California or the extensive marine reserves in Australia), biodiversity (Halpern and Warner 2002, Lester et al. 2009), or overfished species (Lester et al. 2009). Many species share the same habitat, and overfished species often co-occur with

important and abundant commercial species. This is the case on the west coast of the U.S where the depleted darkblotched rockfish (*Sebastes crameri*) co-occurs with the abundant shortspine thornyhead (*Sebastolobus alascanus*) and the depleted canary rockfish (*Sebastes pinniger*) co-occurs with the abundant yellowtail rockfish (*Sebastes flavidus*) (Williams and Ralston 2002). In this situation, spatial closures not only protect overfished species from being harvested, but also eliminate valuable fishing grounds. Closed areas therefore displace fishing effort, potentially changing the relationship between CPUE and fish abundance (Kellner et al. 2007).

Another complication associated with area closures is that they often preclude data collection inside the closure using common survey gears, such as bottom trawls. This has sometimes led researchers to filter out pre-closure period data coming from closed areas, and using only the data from areas that have been fished consistently (e.g. Haltuch et al. 2013), even though the validity of this approach is unknown. More recently, there has been an increasing effort to monitor population size and biodiversity inside marine reserves to track changes in population abundance over time. These surveys often include the use of remotely operated underwater vehicles (Clarke et al. 2009), divers (Edgard and Smith 2009), video cameras (Irigoyen et al. 2013), or non-destructive fishing gears such as traps or hook and line (Clements et al. 2012). The existence of such ancillary data could potentially provide information on the population size within the closures and help construct a better index of total abundance.

We used a simulation-estimation framework to determine how spatial closures affect the performance of various CPUE standardization methods and how sensitive the performances of these standardization methods are to the characteristics of the closed areas (patchiness, size and time when implemented), to the mobility of the target species, as well as to the presence of

ancillary indices for the closed areas. The analyses are based on a generic situation which is characteristic of many actual managed systems, but are not tailored to any one system.

Materials and methods

General approach

The effect of spatial closures on the performance of CPUE standardization methods is examined as follows: 1) develop an operating model consisting of a spatially-explicit population dynamics model coupled with a stochastic vessel dynamics model; 2) simulate CPUE data; 3) apply various CPUE standardization methods to the generated data; 4) repeat steps 2 and 3 many times to capture the variability of the results; and 5) compare the derived indices of abundance with the true abundance trajectories, and hence quantify error rates and the relationship between bias, CPUE standardization method, the nature of the closed areas and assumptions about fleet behavior.

The operating model

A spatially-explicit model (20 x 20 areas; n_a=400) of a single fish stock, coupled with vessel dynamics model is used to generate the CPUE data (Fig. 2.1 and 2.2). The model works as follows. (1) Generate a map of depth distribution and determine the initial fish distribution, (2) For each year of an arbitrarily chosen 30-year projection (n_y=30) period: (2.1) distribute the fishing effort to each area given the population distribution at the start of the year, and calculate the catch in each area, (2.2) adjust the population abundance for catch and growth in each area, and (2.3) redistribute fish spatially based on movement probabilities. This generates catch and effort data on the 20 x 20 grid which are then used for CPUE standardization.

Population dynamics

The underlying population dynamics are governed by a deterministic logistic model with a yearly time step, referred to as a Schaefer model in fisheries (Schaefer 1954), and modified to accommodate movement dynamics (Carruthers et al. 2011b) controlled by habitat (depth) preference and mobility. The population biomass $B_{a,t}$ in area a at time t evolves through time as a function of the catch $C_{a,t}$ in area a during year t, the intrinsic rate of growth of the stock r, the "regional" carrying capacity of area a K_a (Carruthers et al. 2011b), the biomass of animals emigrating $EM_{a,t}$, and the biomass of animals immigrating $IM_{a,t}$:

$$B_{a,t+1} = B_{a,t} + rB_{a,t}(1-\frac{B_{a,t}}{K_a}) - C_{a,t} - EM_{a,t} + IM_{a,t} \quad (2.1)$$

The movement between areas during year t is calculated as follows. The probability M_{ab} of moving from area a to area b is a function of the Euclidian distance d_{ab}=||a-b|| between the centers of gravity of the two areas and the relative preference of the habitat in area b compared to that in the rest of the areas. Fish migration is represented by an exponential decay function that depends on the distance d_{ab} and rate λ (Moilanen and Nieminen 2002, Ono et al. 2013) and fish depth preference follows a lognormal distribution with parameters (μ, σ) where z_x is the depth of area x (Ono et al. 2013) (Fig. 2.1c, Table 2.1).

$$M_{\mathrm{ab}} = \frac{e^{-\lambda d_{ab}} \frac{1}{z_b} e^{-\frac{(\ln z_b - \mu)}{2\sigma^2}}}{\sum_{x=1}^{n_a} e^{-\lambda d_{ax}} \frac{1}{z_x} e^{-\frac{(\ln z_x - \mu)}{2\sigma^2}}} \quad (2.2)$$

Depth (the unique habitat variable in this study) is simulated from a multivariate normal distribution with a mean that changes linearly with respect to the y-coordinate of the areas and an

exponential decay covariance function that depends on distance *d* between areas (eq 2.3). The linear increase in depth with the y-coordinate mimics a coastline (represented by the x-coordinate) that slowly increases in depth with the distance from coast.

$$(2.3) \quad Z \sim MVN(\underline{\mu}, \boldsymbol{\Sigma}); \quad \mu_b = \alpha y_b; \quad \Sigma_{a,b} = \tau^2 \exp(-\xi d_{ab})$$

where Z is the depth variable (Fig. 2.1, upper panels), y_b is the y-coordinate of area *b*, α is the trend parameter for depth (also determines the patchiness of depth distribution), τ^2 is the variance parameter, and ξ controls the rate at which the spatial correlation declines with distance (Table 1). The simulated depth is then standardized so that it spans a specific range (Table 2.1).

The biomass of emigrants from area *a* ($EM_{a,t}$) and that of immigrants to area *a* ($IM_{a,t}$) at time *t* is calculated as:

$$(2.4) \quad EM_{a,t} = \sum_{b \neq a} M_{ab} B_{a,t} \;;\; IM_{a,t} = \sum_{b \neq a} M_{ba} B_{b,t}$$

The biomass in each area at the start of the simulation is assumed to be K_a. K_a is obtained by determining the stationary distribution of the population over areas *d* that satisfies the conditions:

$$(2.5) \quad \begin{aligned} B_{a,t=1} &= Kd \\ d &= Md \end{aligned}$$

where *K* is the total (across populations) carrying capacity, *d* is the positive eigenvector of the movement probability matrix *M* corresponding to the first eigenvalue (Carruthers et al. 2011b).

Fleet dynamics

The total amount of nominal effort across all areas and all vessels during year *t, E_t,* is generated from a lognormal distribution with mean given by a logistic function of time and a CV of 0.2, where $\overline{E_T}$ is the final year effort, i.e.:

$$(2.6) \quad E_{.,t} = \lfloor \log N(\frac{\overline{E_T}}{1+\exp(-0.1t)}, CV = 0.2) \rfloor$$

These integer effort levels are then distributed randomly among twenty vessels (n_v=20). Each vessel has its own catchability coefficient q_v generated from a lognormal distribution with parameters ($\bar{q} = 0.1$, CV_q=0.2). The differences in q_v among vessels reflects differences in vessel characteristics or skipper skill among vessels. The q_v are time-invariant, but are equal to 0 in the closed areas i.e. $q_{a,v} = 0\big|_{a \in closure}$. Area closure is implemented by closing certain depth zones to fishing, as is often done in the West coast of the United States (Table 2.1).

Vessel *v* distributes its effort during year *t*, $E_{,t,v}$, to each fishing ground *a* with a probability $p_{a,t,v}$ that depends on the mean expected catch in each area. This approach is a stochastic version of the so-called "gravity model" (Caddy, 1975). It is assumed that vessels have perfect information about the biomass in each fishing ground, but their catch rate is variable by grid cell.

$$(2.7) \quad p_{a,t,v} = \frac{B_{a,t}\left(1-e^{-q_{a,v}}\right)}{\sum_{x=1}^{n_a} B_{x,t}\left(1-e^{-q_{x,v}}\right)}$$

The amount of effort (fishing trips) for vessel *v* in area *a* during year *t*, $E_{a,t,v}$, follows a multinomial distribution with probability $p_{a,t,v}$:

(2.8) $E_{a,t,v} \sim Multinomial(E_{.,t,v}, p_{a,t,v})$

One consequence of this effort allocation algorithm is that many areas will be unfished throughout the time series and fishing areas will change over time. Specifically, the number of high CPUE areas will decrease over time due to fishing, which increases the number of fished areas over time.

Randomness in the catch was introduced by sampling the realized catchability for trip e by vessel v, $q'_{v,e}$, from a Tweedie distribution with a mean $\mu=q_v$ and values for p and Φ of 1.2 and 0.1 respectively. The Tweedie distribution belongs to the exponential family, and has mean μ and variance $\Phi\mu^p$. It is a continuous distribution with an added mass at 0 when $1<p_v<2$. This distribution is therefore a good candidate to simulate zero-inflated CPUE data, as it is often observed in practice (Maunder and Punt 2004). In this study, the proportion of zero catches was between 15-20%. The total catch $C_{a,t}$ in area a and time t is determined as follows:

(2.9) $$C_{a,t} = B_{a,t}\left(1 - e^{-\sum_{v=1}^{n_v}\sum_{e=1}^{E_{a,t,v}} q'_{v,e}}\right)$$

$C_{a,t}$ is redistributed among vessels and fishing events to generate catch per unit effort for the e^{th} trip by vessel v, in area a, during year t, $C_{a,t,v,e}$, used for the CPUE standardization, as follows:

(2.10) $$C_{a,t,v,e} = C_{a,t}\frac{q'_{v,e}}{\sum_{v=1}^{n_v}\sum_{e=1}^{E_{a,t,v}} q'_{v,e}}$$

The well-known Baranov catch equation arises from the combination of equations 9 and 10.

Standardizing the CPUE data

General approach

CPUE standardization was performed using the generated catch and effort data, in addition to spatial information (depth) and vessel identification number. Since the generated data contain many zero catches, a delta model (also called hurdle model) (Maunder and Punt 2004) was used to analyze the data. In this analysis, the presence/absence of fish was modeled using a binomial model, and the positive catch data using a lognormal distribution. Model selection using AICc was used to select between lognormal, normal and gamma distributions for the positive catches; the gamma model was usually the best (>95% of simulations), followed by the lognormal then the normal, but gamma model often (>25% of simulations) failed to converge. Therefore, the lognormal model was chosen to model the positive catch data for all analyses for consistency. The statistical analyses were performed using the generalized linear modeling (glm) framework in the programming language R (R Core Team 2013). The final standardization model is:

$$(2.11)\quad \mathrm{p}(\mathrm{CPUE}_{\mathrm{a,t,v}} > 0) = \frac{e^{\mu' + \gamma_t' + \beta' depth_a + \kappa' depth_a^2 + \delta_v'}}{1 + e^{\mu' + \gamma_t' + \beta' depth_a + \kappa' depth_a^2 + \delta_v'}}$$

$$(2.12)\quad \mathrm{E}(\mathrm{CPUE}_{\mathrm{a,t,v}} \mid \mathrm{CPUE}_{\mathrm{a,t,v}} > 0) = e^{\mu + \gamma_t + \beta\ depth_a + \kappa\ depth_a^2 + \delta_v}$$

where μ (and μ') is the mean, γ_t (and γ_t') the year effect, β and κ (and β' and κ') the habitat covariate effects (effect of depth and depth^2), and δ_v (and δ_v') the vessel effect. The results of the delta model are used to create an index for year t, $\widehat{I_t'}$, that is the sum of the predicted catch (predicted probability of catch multiplied by the expected catch) for each area for an arbitrary

vessel 1 (Maunder and Punt (2004) suggest using the vessel that is the most representative of the fishery, but in this simulation any vessel is equally likely):

$$(2.13)\quad \widehat{I}'_t = \sum_{a=1}^{n_a} p(CPUE_{a,t,v=1} > 0) E(CPUE_{a,t,v=1} \mid CPUE_{a,t,v=1} > 0)$$

The final index of abundance $\widehat{I}_t$ is obtained by dividing $\widehat{I}'_t$ by its geometric mean (Francis 1999).

Competing models to standardize CPUE data when spatial closures are present

Indices of abundance are computed for a few commonly used CPUE standardization approaches:

(1) The Raw CPUE model ("Raw") is just the total catch divided by the total effort.

(2) The Habitat model ("Habitat") includes the depth of the catch (and its quadratic term) as habitat covariates in the glm (eq 2.11-2.12).

(3) The "Continuous fishing" model is structurally the same as the "Habitat" model, except that the data are restricted to the areas that have been fished continuously for the whole time series, i.e., the data analyzed exclude catch and effort information from the closed areas even for the period before the closure is implemented.

(4) The "Closure explicit" model applies the habitat model separately to the pre-closure $[1, t_{closure}\text{-}1]$ and post-spatial closure $[t_{closure}, n_y]$ periods. The index derived from each model is then combined (eq 2.14) and standardized by its geometric mean.

$$(2.14)\quad \widehat{\mathrm{I}}' = (\widehat{I}'^{\,pre}_{1}, \ldots, \widehat{I}'^{\,pre}_{t_{closure}-1}, \widehat{I}'^{\,post}_{t_{closure}}, \ldots, \widehat{I}'^{\,post}_{n_y})$$

(5) The "Closure imputed" model is the same as "Closure explicit" model except that the predicted catch in the closed areas during the post-closure period is extrapolated from the

pre-closure period using Equation 15. This extrapolation is based on the assumption that the fish biomass in the closed area is constant, i.e.

$$\text{For } t \in [t_{closure}, n_y], \quad \hat{I}'^{post}_{t} = \sum_{a \notin closure} p(CPUE_{a,t,v=1} > 0) E(CPUE_{a,t,v=1} \mid CPUE_{a,t,v=1} > 0) + \sum_{a \in closure} p(CPUE_{a,t_{closure}-1,v=1} > 0) E(CPUE_{a,t_{closure}-1,v=1} \mid CPUE_{a,t_{closure}-1,v=1} > 0) \tag{2.15}$$

CPUE standardization models with ancillary data

In certain occasions, there may be data on population size trends inside the closed area. The abundance index derived from the ancillary data can then be used to predict the CPUE values for the closed area. However, the scale of the ancillary data might not match that of the predicted CPUE from the standardization model. The abundance index based on the ancillary data is therefore extrapolated as needed and standardized to be consistent with the predicted CPUE from the closed area in the last year of pre-closure period.

$$\text{For } t \in [t_{closure}, n_y], \quad \hat{I}'^{ancillary}_{t,\text{stand}} = \frac{\hat{I}'^{ancillary}_{t}}{\hat{I}'^{ancillary}_{t_{closure}-1}} \sum_{a \in closure} p(CPUE_{a,t_{closure}-1,v=1} > 0) E(CPUE_{a,t_{closure}-1,v=1} \mid CPUE_{a,t_{closure}-1,v=1} > 0) \tag{2.16}$$

$$\text{For } t \in [t_{closure}, n_y], \quad \hat{I}'^{post}_{t} = \sum_{a \notin closure} p(CPUE_{a,t,v=1} > 0) E(CPUE_{a,t,v=1} \mid CPUE_{a,t,v=1} > 0) + \hat{I}'^{ancillary}_{t,\text{stand}} \tag{2.17}$$

Five scenarios are simulated to examine the sensitivity of the above "Closure imputed" method (Table 2.2):

The ancillary data are collected every year after a closure is implemented and the derived index is proportional to the actual biomass ("Continuous ancillary").

The ancillary index is proportional to actual biomass, but is collected infrequently. Any missing values in the index are replaced by the predicted values based on a loess spline (if data points>4) or linear model (if data points ≤4) fit to the ancillary index time series ("Discontinuous ancillary").

Same as for "Continuous ancillary", but the ancillary index is noisier ("Noisy ancillary").

An ancillary index is available every year, but is not proportional to the biomass: it is hyperstable (changes slower than the actual biomass) ("Hyperstable ancillary").

An ancillary index is available every year, but is not proportional to the biomass: it is hyperdepleted (changes more rapidly than the actual biomass) ("Hyperdepleted ancillary").

Simulation scenarios

Several scenarios are used to examine the effects of spatial closures on the CPUE standardization methods (Tables 2.1 and 2.3). These scenarios are based on a factorial design using the following cases:

The amount of target species habitat that is protected by the spatial closure. Model performance is evaluated when the area closure protects only poor quality habitat ("Poor", 0-50m), medium quality habitat ("Medium", 25-75m), or good habitat ("Good", 50-100m) (Fig. 2.1c). The habitat quality in this study is directly associated with higher population abundance as fish are attracted to good habitat (Eq 2.2). The "Poor", "Medium" and "Good" cases protect about 5%, 20% and 40% of the population, respectively.

When the closed area is implemented: a) 5 years ("Early"), b) 15 years ("Base") or c) 25 years ("Late") from the start of the model projection period.

Sensitivity analysis

A set of sensitivity tests is conducted to investigate the effects of various assumptions on the results (Tables 2.1 and 2.3). All sensitivity analyses were performed for "Base case" settings, except for the variable tested. The term "Base case" refers to a case with "Medium species protection", "Base closure", "Base patchiness", "Base CV for vessel catchability", "Base number of vessels", "Base movement", "Base level of zero inflation", and "Base depletion level". The patchiness of the depth distribution, therefore, the patchiness of spatial closures. Performance is evaluated for "Base" (α=5) and "High" (α=0) patchiness (Fig. 2.1a,b). The CV of vessel catchability coefficients. Sensitivity is explored to when vessels have three levels of relative fishing efficiency: "Low" (CV_q=0.1), "Base" (CV_q=0.2) and "High" (CV_q=0.4). The number of vessels participating in the fishery: n_v=10 ("Low"), 20 ("Base"), and 40 ("High"). The mobility of the species. Some species are more or less mobile than others. Therefore, the sensitivity of the results is examined for cases where animals are sedentary ("No movement", $M_{a,b} = 0\big|_{b \neq a}$) and where they perform habitat-dependent movement ("Base"); The variance inflation factor p of the Tweedie distribution which determines the frequency of zeroes in the data: "Low" (p=0.05), "Base" (p=0.1), and "High" (p=0.2); The ratio of the final year biomass to the virgin biomass (controlled through the value of the ending year effort $\overline{E_T}$); and cases with a "Base" level of population depletion ($\overline{E_T} = 250$) (Fig. 2.2) and a "High" level of depletion $\overline{E_T} = 350$ are examined.

Performance evaluation

We evaluated the performance of the various CPUE standardization approaches using two metrics: 1) the relative error (RE) in the derived index of abundance ($\widehat{I}_t$) (2.18) over time, and 2) the RE of the final year depletion estimate (B_{30}/B_1), which is often a quantity of management interest (eq 2.19). The true biomass was rescaled (B_t') by its geometric mean over years to match the scale of the derived indices of abundance and to be able to evaluate model performance.

$$(2.18) \quad RE_t = \frac{(\widehat{I}_t - B_t^{'})}{B_t^{'}}$$

$$(2.19) \quad RE_{depletion} = \frac{(\widehat{I_{30}}/\widehat{I}_1 - B_{30}^{'}/B_1^{'})}{B_{30}^{'}/B_1^{'}}$$

For both metrics, the median relative error (MRE) provides information about bias and the variance in RE quantifies the precision. A "Control" case in which data are generated when there are no area closures is used to identify the effect of area closures.

Results

Effect of spatial closures on CPUE standardization

The effect of proportion of species protected

In general, bias increased and precision decreased for all CPUE standardization methods as the spatial closure protected a larger portion of the target population (Fig. 2.3, b-f vs. h-l vs. n-r). The derived indices of abundance for the "Control" were positive biased at the start of the time series (12%) and negatively biased at the end (-6%), and this trend in bias increased with the amount of spatial closure for "Raw", "Habitat" and "Continuous fishing" (Fig. 2.3, b-d, h-j, n-p and Table 2.4, a,b,c). "Raw", "Habitat" and "Continuous fishing" displayed a positive bias of

about 15% at the start of the time series and a -5% bias at the end of the time series when species protection was “poor” (Table 2.4, b). With a “good” protection, the bias changed to 54%, 34%, and 21% at the start and -38%, -28%, and -27% at the end, for “Raw”, Habitat” and “Continuous fishing” respectively (Table 2.4, c).

The direction of bias pre- or post-closure depended on the amount of protection for “Closure explicit” and “Closure imputed”. Specifically, bias decreased from 4% to below -5% before closure and stayed around 5% after closure with a low level of protection (“Poor protection”) (Fig. 2.3, e,f and Table 2.4, b). For mid-level of protection (“Medium protection”), bias was mostly negative before closure and positive after closure for “Closure explicit” and “Closure imputed” (Fig. 2.3, k,l). However, bias was higher for “Closure explicit” than for “Closure imputed” and its bias decreased from -0.01% to below -12% before closure and from 20% to 1% after closure (Fig. 2.3, k, and Table 2.4, a). The situation reversed at high level of species protection (“Good protection”) and bias was mostly positive before closure and decreased from positive to negative after closure (Fig. 2.3, q,r). The difference in bias between “Closure explicit” and “Closure imputed” grew again and bias ranged with [10%; 25%] pre-closure, and decreased from 16% to -25%, for “Closure explicit” (Fig. 2.3, q and Table 2.4, c). Bias was between [0%; 11%] before closure and decreased from 11% to -10% after closure for “Closure imputed” (Fig. 2.3, r and Table 2.4, c).

“Closure imputed” generally led to the least biased (lowest MRE) and most precise indices of abundance (lowest variation in RE). This was especially the case at high levels of species protection where the bias for “Closure imputed” varied over time between [-10%; 11%] while it varied between [-25%; 24%] for the second least biased method (“Closure explicit”) and

between [-38%; 54%] for the worst method ("Raw") (Fig. 2.3, r vs. 3n-q and Table 2.4, c). The precision of "Closure imputed" varied between [0.002; 0.012] while it varied between [0.004; 0.013] for the second best method ("Habitat") and between [0.004; 0.035] for the worst method ("Closure explicit") (Fig. 2.3, r vs. 3n-q and Table 2.4, c). As a consequence, "Closure imputed" also produced amongst the least biased estimates of final year depletion (along with "Closure explicit") for various levels of species protection and timing of area closure (7 out of the 9 cases) (Fig. 2.4). It provided close to unbiased estimates of final year depletion for poor to medium protection (except for early closure (Fig. 2.4, a,b)) whereas the other methods, except the "Closure explicit", were negatively biased by [-30%; -10%] (Fig. 2.4, a,b,d,e,g,h). "Closure imputed" was negatively biased by [-25%; 5%] with "Good protection" while the other methods had a much higher bias [-60%; 30%] (Fig. 2.4, c,f,i).

The "Raw" model provided the most biased indices of abundance, and its bias grew as the closed area protected a larger portion of the population (Fig. 2.3, b,h,n, Table 2.4, a,b,c). "Raw" had also the most biased estimates of final year depletion (Fig. 2.4).

The effect of timing of closure

The timing of closure mainly shifted the timing of the biases (Fig. 2.5): all models had the original temporal pattern of bias except for "Closure imputed", which had higher bias during the final years when closures were implemented early (Fig. 2.5, f and Table 2.4, d,e,f). The bias in the estimate of final year depletion was not sensitive to the timing of area closure except for the "Closure imputed" model (Fig. 2.4).

The effect of ancillary data

The use of ancillary data reduced bias in the estimate of final year depletion when either a large portion of the population was in the closed area ("Good protection") or when area closure was implemented early in the time series but not both at the same time (Fig. 2.6, a,b,f,i). For example, bias in the final year depletion decreased from -20% ("Closure imputed") to -10% for "Noisy ancillary", to close to unbiased for "Continuous ancillary" and "Discontinuous ancillary", and stayed at -20% for "Hyperstable ancillary" and "Hyperdepleted ancillary" (Fig. 2.6, f,i) when protection was "good" and the closures were implemented at the middle or late in the time series, Similarly, bias in the final year depletion decreased from 25% for "Closure imputed" to 5% for "Continuous ancillary", 10% for "Discontinuous ancillary" and "Noisy ancillary", and stayed at 25% for "Hyperstable ancillary" and "Hyperdepleted ancillary" when protection was "medium" and the closures were implemented early in the time series (Fig. 2.6, b). The influence of ancillary data was much reduced when protection was "poor" and the closures were implemented early in the time series (Fig. 2.6, a vs. b). For the rest of scenarios, the inclusion of ancillary data did not improve or slightly increased the bias in the estimates of final year depletion (Fig. 2.6, c,d,e,g,h). Additionally, the precision of the derived index of abundance decreased compared to "Closure imputed" when a higher portion of the population was in the closed area for "Continuous ancillary", "Discontinuous ancillary" and "Noisy ancillary": the level of precision was similar to blind imputation ("Closure imputed") at "poor" level of protection (Fig. 2.6, a,d,g), but there was up to 2-fold, 3-fold, and 5-fold increase in variance for "Continuous ancillary", "Discontinuous ancillary", and "Noisy ancillary" respectively, when protection was 'good' (Fig. 2.6, c).

The effect of closed area patchiness

More patchiness in distribution did not change the trend in bias over time, but decreased the absolute value of bias (Table 2.4, a vs. j). While as many as 16 out of 42 MRE values in Table 2.4a were above 10% (in absolute value), only one MRE value was above 10% in Table 2.4j.

The effect of species mobility

No fish movement between areas accentuated the bias throughout the time series, and increased the variability of the errors (Table 2.4, a vs. k). Without movement, the absolute bias was higher than 10% 21 out of 42 cases (Table 2.4, k) compared to 16 for the base case (Table 2.4, a). Among these 21 values, 12 were higher than 20% (in an absolute value) while only three had that much bias for the base case. Moreover, the variance in RE was greater or equal to that for the base case 30 out of 42 times for the scenario without fish movement (Table 2.4, k vs. a).

The effect of depletion level

A more depleted population accentuated the bias in the derived index of abundance for "Raw", "Habitat" and "Continuous fishing", but did not affect their precision (Table 2.4, r vs. a). Bias decreased from 22% to -17%, 19% to -13%, and 20% to -14% for "Raw", "Habitat" and "Continuous fishing" respectively for the base case (Table 2.4, a) while it decreased from 28% to -22%, 20% to -19%, and 21% to -19% respectively for the "High depletion" scenario (Table 2.4, r).

Sensitivity analysis to the number of vessels, CV of vessel catchability, amount of zero inflation

The extent of bias was largely independent of the number of vessels, the amount of zero inflation in the data and the between-vessel variation in catchability (Table 2.4, a vs. l,m,n,o,p,q).

Discussion

The presence of closed areas introduced a temporal pattern of bias in the derived index of abundance, and the magnitude of bias increased as the portion of population in the closed area increased. The bias was generally positive for the pre-closure period and negative post-closure. This trend in bias has important management implications as it leads to an overly pessimistic estimate of recent biomass. The estimate of final year depletion was generally negatively biased for most CPUE standardization methods (except for the "Closure explicit" and "Closure imputed") and the bias increased as the proportion of population in the closed area became larger. The estimate of final year abundance was about 50% lower than the actual value for some standardization methods, such as "Raw". In the U.S., such an overly conservative estimate can potentially misclassify a population as over-fished and necessitate a rebuilding plan (Rosenberg et al. 2006). This emphasizes the risk of using the raw catch per unit effort data as an index of population abundance, as highlighted by Myers and Worm (2003) and Polacheck (2006). The "Control" case also showed a trend in bias which was exacerbated with a closed area. This is due to the simulated fishing behavior where effort is preferably targeted towards areas with the highest abundance (Hilborn and Walters 1992, Walters 2003). In fact, the bias in the abundance indices disappeared when fishing effort was randomly distributed spatially (Fig. 2.A.1, "Control random").

The results for "Closure explicit", the CPUE standardization method that applied the regression separately to the pre- and post-closure periods, were surprising; the trend in bias in the derived index of abundance changed according to the fraction of population within the area closure. This was probably due to the trade-off between the inherent bias of the derived index of abundance and the amount of biomass protected. This index has a tendency to respectively over- and

underestimate the population size at the start and end of a time series. Since "Closure explicit" standardized the CPUE data twice (once for the pre-closure and once for the post-closure period), the bias shifted twice in the time series. However, the post-closure CPUE standardization has a tendency to misestimate the effect of depth, as areas with highest abundance become less available for analysis as the amount of area closure increases.

The indices of abundance for "Closure imputed" were generally more precise and less biased than those produced by "Closure explicit" by imputing data for the closure post-closure using a pre-closure estimate, and "Closure imputed" was often the best method. The use of "Closure imputed" could therefore alleviate the potential management issue mentioned above. The only exception was when the closure was early and protection was "poor" to "medium". In this case, the estimates of final year depletion were more biased for "Closure imputed" than "Closure explicit". The reduction in bias over time for the post-closure period worsened the estimate of final year depletion due to bias in the pre-closure period. The performance of "Closure imputed" was not sensitive to the assumptions made in this study, including the magnitude of the CV in vessel catchability, the number of vessels participating in the fishery, the extent of zero inflation in the catch data and the population depletion (Table 2.4). However, even "Closure imputed" could not eliminate the bias when the area closure protected a large fraction of the population or when the closures occurred early in the time series.

The use of ancillary data was not always able to reduce bias in the estimates of abundance and final year depletion. It was only able to do so when a large portion of the population was protected by the area closures or when closures were implemented early in the time series. In such case, any type of ancillary data (among the ones investigated) was able to reduce or not

change the of bias in the final year depletion (but at the cost of lower precision), especially at a higher level of protection. Aside from these cases, the use of ancillary data generally led to a similar or worse level of bias in the estimates of final year depletion.

Collectively, these findings suggest that the data imputation approach is a good option to take when standardizing CPUE for fishery-dependent or -independent data when closed areas exist. This study emphasizes the importance of data imputation for missing observations (Beverton and Holt 1957, Walters 2003). This is all the more important as indices of abundance are sometimes the major source of information to evaluate the stock status (Hilborn and Walters 1992; Maunder and Punt 2013).

The post-closure imputation method proposed in this study does not only apply to fishery-dependent or -independent data in the presence of closed areas. Any actions (management related, vessel dynamics and others) that displaces effort away from an area can potentially create a similar effect as an area closure. Forty-one species in U.S. were declared to be overfished as of 2012 with severe catch constraints imposed on them (NOAA, 2013). One of the consequences of these constraints is that they displace fishing effort away from regions with abundant overfished species and creates a situation similar to a closed area (Holland and Jannot 2012).

As in any study, the results of this study are based on several assumptions. For instance, there is no major mismatch between the operating model and the CPUE standardization models. In reality, the variables affecting the changes in CPUE are unknown and many of them might not be measurable or hard to measure (Maunder et al. 2006). Moreover, it is widely recognized that fishery-dependent CPUE data could be not proportional to biomass: the so-called hyperdepletion or hyperstability that we have partially examined in this study (Hilborn and Walters 1992, Harley

et al. 2001). All of these effects could potentially change the outcome of the study and further investigation is needed. Finally, it is also common to stratify the study area into smaller zones and treat them as factors in the CPUE standardization model (Maunder and Punt 2004) and how this is done can impact the performance of CPUE standardization methods.

Marine closures and marine protected areas are now being implemented worldwide (http://ocean.nationalgeographic.com/ocean/take-action/marine-protected-areas/) and becoming a common tool for management (Lester et al. 2009, Gaines et al. 2010, Fox et al. 2012). Although there are many claimed benefits with the MPAs (Lester et al. 2009) there are still some limitations that cannot be forgotten which could complicate stock assessments. For example, Field et al. (2006) indicated that the presence of area closures can bias assessments and that the direction of bias remained unpredictable. In many countries, stock assessments are now mandatory and provide the basis for fishery management. It is therefore important to develop solutions for the negative impacts of closed areas on stock assessments as well those of non-heterogeneity in spatial distribution of fishing effort more generally (Punt and Methot 2004, McGilliard and Hilborn 2010, Wilson et al. 2010, Babcock and MacCall 2011). Finally, we also need to keep developing new methods to deal with area closure in assessment models as marine reserves might continue expanding around the globe.

The imputation method proposed in this study could be a good alternative to some traditional CPUE standardization approaches and can help providing an index of abundance that is less biased in general.

Table 2.1: Table of model specification

Parameters	Values
Depth distribution (exponential covariance function)	
Variance (τ^2)	200
Range (ξ)	10
Trend/patchiness (α)	Base (5), High (0)
Standardized depth range	[0-300]
Closed area set-up	
Depth zone under closure	Poor (0-50), Medium (25-75), Good (50-100)
Timing of implementation of the closed area	Early (year 5), Base (year 15), Late (year 25)
Population parameters	
Sum of area carrying capacity (K)*	100000
Intrinsic rate of growth (r)*	0.15 yr^{-1}
Fish mobility	No, Yes
Movement/diffusion parameters	
Mean depth preference (μ)	Base (120), No movement (NA)
Variance of depth preference in log scale (σ^2)	0.25
Fleet dynamics parameters	
Number of vessels (n_v)	Low (10), Base (20), High (40)
Mean catchability ($\overline{q}$)	0.1
Coefficient of variation of the catchability (CV_q)	Low (0.1), Base (0.2), High (0.4)
Catch zero inflation parameter (ϕ)	Low (0.05), Base (0.1), High (0.2)
Ending year fishing effort ($\overline{E_T}$)	Base (250), High (350)

*: this value is an average based on 22 West Coast groundfish species

Table 2.2: Model specification for scenarios with ancillary data

Scenario name	Scenario description	Equations for the index
Continuous ancillary	Ancillary index is collected every year during closure and is proportional to biomass	$\widehat{I}_t^{ancillary} = B_t e^{\varepsilon_t - \frac{0.15^2}{2}}$ with $\varepsilon_t \sim N(0, 0.15^*)$
Discontinuous ancillary	Ancillary index is collected every 4 years during closure and is proportional to biomass	$\widehat{I}_t^{ancillary} = B_t e^{\varepsilon_t - \frac{0.15^2}{2}}$ with $\varepsilon_t \sim N(0, 0.15)$
Noisy ancillary	As for 'continuous ancillary', except the index is noisier.	$\widehat{I}_t^{ancillary} = B_t e^{\varepsilon_t - \frac{0.3^2}{2}}$ with $\varepsilon_t \sim N(0, 0.3)$
Hyperstable ancillary	As for 'continuous ancillary', except the index exhibits hyperstability	$\widehat{I}_t^{ancillary} = B_t^{0.5} e^{\varepsilon_t - \frac{0.15^2}{2}}$ with $\varepsilon_t \sim N(0, 0.15)$
Hyperdepleted ancillary	As for 'continuous ancillary', except the index exhibits hyperdepletion	$\widehat{I}_t^{ancillary} = B_t^{1.5} e^{\varepsilon_t - \frac{0.15^2}{2}}$ with $\varepsilon_t \sim N(0, 0.15)$

* value based on the coefficient of variation estimate from Figure 3 of Irigoyen et al. 2013 or Figure 4 of Clements et al. 2012

Table 2.3: Scenario descriptions. A dash indicates the base level.

ID	Effort	Zero inflation	Vessel numbers	Vessel q CV	Fish movement	Habitat Patchiness	Time of closure	Species protection
a	Base	Base	Base	Base	Base	Base	Base	Medium
b	-	-	-	-	-	-	-	Poor
c	-	-	-	-	-	-	-	Good
d	-	-	-	-	-	-	Early	Medium
e	-	-	-	-	-	-	Early	Poor
f	-	-	-	-	-	-	Early	Good
g	-	-	-	-	-	-	Late	Medium
h	-	-	-	-	-	-	Late	Poor
i	-	-	-	-	-	-	Late	Good
j	-	-	-	-	-	High	-	Medium
k	-	-	-	-	No	-	-	Medium
l	-	-	-	Low	-	-	-	Medium
m	-	-	-	High	-	-	-	Medium
n	-	-	Low	-	-	-	-	Medium
o	-	-	High	-	-	-	-	Medium
p	-	Low	-	-	-	-	-	Medium
q	-	High	-	-	-	-	-	Medium
r	High	-	-	-	-	-	-	Medium

Table 2.4: Bias (MRE) and precision (variance of RE estimates) of the derived indices of abundance by scenario. Shading intensity indicates the level of bias: no shading [-0.1; 0.1], light shading [-0.2; -0.1] or [0.1; 0.2], and darker shading <-0.2 or >0.2.

ID	Model	Time of closure						
		1	5	10	15	20	25	30
a	Control	0.12 (0.009)	0.06 (0.007)	0.03 (0.005)	-0.02 (0.003)	-0.03 (0.003)	-0.04 (0.003)	-0.06 (0.004)
	Raw	0.22 (0.012)	0.12 (0.009)	0.08 (0.006)	0.02 (0.006)	-0.08 (0.003)	-0.13 (0.004)	-0.17 (0.004)
	Habitat	0.19 (0.010)	0.10 (0.009)	0.07 (0.005)	0.04 (0.006)	-0.07 (0.003)	-0.11 (0.004)	-0.13 (0.004)
	Continuous fishing	0.20 (0.012)	0.09 (0.010)	0.08 (0.005)	0.03 (0.006)	-0.07 (0.003)	-0.12 (0.004)	-0.14 (0.004)
	Closure explicit	-0.01 (0.010)	-0.07 (0.014)	-0.12 (0.010)	0.20 (0.018)	0.11 (0.011)	0.06 (0.011)	0.01 (0.006)
	Closure imputed	0.01 (0.008)	-0.05 (0.012)	-0.09 (0.008)	0.10 (0.007)	0.07 (0.006)	0.05 (0.006)	0.05 (0.004)
b	Control	0.12 (0.009)	0.06 (0.007)	0.03 (0.005)	-0.02 (0.003)	-0.03 (0.003)	-0.04 (0.003)	-0.06 (0.004)
	Raw	0.16 (0.01)	0.07 (0.007)	0.02 (0.004)	-0.01 (0.004)	-0.03 (0.004)	-0.06 (0.003)	-0.06 (0.003)
	Habitat	0.13 (0.011)	0.07 (0.007)	0.02 (0.004)	-0.01 (0.003)	-0.03 (0.005)	-0.05 (0.004)	-0.04 (0.005)
	Continuous fishing	0.14 (0.011)	0.07 (0.007)	0.02 (0.004)	-0.01 (0.003)	-0.03 (0.005)	-0.05 (0.004)	-0.04 (0.005)
	Closure explicit	0.04 (0.009)	-0.03 (0.014)	-0.06 (0.008)	0.06 (0.008)	0.05 (0.011)	0.04 (0.009)	0.04 (0.009)
	Closure imputed	0.04 (0.008)	-0.02 (0.013)	-0.05 (0.008)	0.04 (0.007)	0.04 (0.01)	0.05 (0.008)	0.05 (0.008)
c	Control	0.12 (0.009)	0.06 (0.007)	0.03 (0.005)	-0.02 (0.003)	-0.03 (0.003)	-0.04 (0.003)	-0.06 (0.004)
	Raw	0.54 (0.017)	0.42 (0.018)	0.37 (0.014)	0.01 (0.005)	-0.23 (0.004)	-0.32 (0.003)	-0.38 (0.005)
	Habitat	0.34 (0.013)	0.25 (0.012)	0.21 (0.009)	0.10 (0.005)	-0.11 (0.005)	-0.26 (0.004)	-0.28 (0.005)
	Continuous fishing	0.21 (0.035)	0.21 (0.015)	0.20 (0.016)	0.13 (0.006)	-0.09 (0.005)	-0.24 (0.004)	-0.27 (0.005)
	Closure explicit	0.24 (0.013)	0.19 (0.024)	0.17 (0.017)	0.16 (0.011)	-0.09 (0.009)	-0.23 (0.006)	-0.25 (0.007)
	Closure imputed	0.11 (0.007)	0.05 (0.012)	0.02 (0.007)	0.11 (0.004)	-0.01 (0.003)	-0.08 (0.002)	-0.10 (0.002)
d	Control	0.12 (0.009)	0.06 (0.007)	0.03 (0.005)	-0.02 (0.003)	-0.03 (0.003)	-0.04 (0.003)	-0.06 (0.004)
	Raw	0.26 (0.014)	0.17 (0.01)	0.06 (0.004)	-0.03 (0.002)	-0.06 (0.005)	-0.09 (0.003)	-0.13 (0.004)
	Habitat	0.21 (0.012)	0.14 (0.009)	0.03 (0.005)	-0.04 (0.004)	-0.07 (0.004)	-0.06 (0.004)	-0.10 (0.005)
	Continuous fishing	0.24 (0.015)	0.14 (0.008)	0.03 (0.005)	-0.04 (0.004)	-0.07 (0.004)	-0.07 (0.004)	-0.10 (0.005)
	Closure explicit	-0.11 (0.027)	0.20 (0.012)	0.09 (0.006)	0.02 (0.005)	-0.02 (0.005)	-0.02 (0.004)	-0.05 (0.004)
	Closure imputed	-0.14 (0.016)	0.02 (0.006)	0.01 (0.004)	0.00 (0.002)	0.03 (0.002)	0.06 (0.002)	0.08 (0.003)
e	Control	0.12 (0.009)	0.06 (0.007)	0.03 (0.005)	-0.02 (0.003)	-0.03 (0.003)	-0.04 (0.003)	-0.06 (0.004)
	Raw	0.16 (0.01)	0.10 (0.006)	0.03 (0.004)	-0.01 (0.004)	-0.04 (0.002)	-0.06 (0.002)	-0.08 (0.004)
	Habitat	0.12 (0.011)	0.07 (0.005)	0.03 (0.005)	-0.01 (0.003)	-0.03 (0.003)	-0.05 (0.003)	-0.04 (0.004)
	Continuous fishing	0.13 (0.011)	0.07 (0.005)	0.03 (0.005)	-0.02 (0.003)	-0.03 (0.003)	-0.05 (0.003)	-0.04 (0.004)
	Closure explicit	-0.05 (0.028)	0.09 (0.006)	0.06 (0.005)	0.00 (0.004)	-0.01 (0.004)	-0.03 (0.004)	-0.02 (0.004)
	Closure imputed	-0.06 (0.024)	0.04 (0.006)	0.02 (0.004)	0.00 (0.003)	0.01 (0.003)	0.01 (0.003)	0.03 (0.003)
f	Control	0.12 (0.009)	0.06 (0.007)	0.03 (0.005)	-0.02 (0.003)	-0.03 (0.003)	-0.04 (0.003)	-0.06 (0.004)
	Raw	0.93 (0.05)	0.34 (0.015)	0.04 (0.004)	-0.10 (0.003)	-0.18 (0.004)	-0.22 (0.004)	-0.23 (0.004)
	Habitat	0.56 (0.023)	0.34 (0.015)	0.06 (0.006)	-0.06 (0.004)	-0.14 (0.003)	-0.18 (0.003)	-0.20 (0.005)
	Continuous fishing	0.40 (0.044)	0.35 (0.015)	0.07 (0.005)	-0.05 (0.004)	-0.13 (0.003)	-0.18 (0.003)	-0.20 (0.005)
	Closure explicit	0.39 (0.083)	0.36 (0.014)	0.07 (0.005)	-0.05 (0.005)	-0.13 (0.005)	-0.17 (0.003)	-0.20 (0.006)
	Closure imputed	-0.01 (0.012)	0.04 (0.004)	-0.01 (0.001)	-0.01 (0.001)	0.00 (0.001)	0.01 (0.001)	0.03 (0.002)
g	Control	0.12 (0.009)	0.06 (0.007)	0.03 (0.005)	-0.02 (0.003)	-0.03 (0.003)	-0.04 (0.003)	-0.06 (0.004)
	Raw	0.18 (0.01)	0.09 (0.008)	0.03 (0.004)	0.00 (0.004)	-0.04 (0.002)	-0.06 (0.003)	-0.14 (0.004)
	Habitat	0.15 (0.011)	0.07 (0.007)	0.03 (0.004)	0.02 (0.004)	-0.04 (0.003)	-0.05 (0.004)	-0.12 (0.004)
	Continuous fishing	0.16 (0.012)	0.06 (0.008)	0.04 (0.005)	0.02 (0.005)	-0.03 (0.004)	-0.05 (0.004)	-0.13 (0.004)
	Closure explicit	0.08 (0.008)	-0.05 (0.007)	-0.09 (0.004)	0.10 (0.004)	0.07 (0.004)	0.05 (0.025)	0.05 (0.025)
	Closure imputed	0.1 (0.008)	0.02 (0.007)	-0.02 (0.004)	-0.02 (0.004)	-0.08 (0.003)	0.12 (0.015)	0.07 (0.015)
h	Control	0.12 (0.009)	0.06 (0.007)	0.03 (0.005)	-0.02 (0.003)	-0.03 (0.003)	-0.04 (0.003)	-0.06 (0.004)
	Raw	0.16 (0.01)	0.07 (0.007)	0.01 (0.004)	-0.02 (0.003)	-0.06 (0.002)	-0.06 (0.002)	-0.08 (0.002)
	Habitat	0.14 (0.011)	0.06 (0.007)	0.02 (0.004)	0.01 (0.003)	-0.05 (0.003)	-0.05 (0.003)	-0.05 (0.003)
	Continuous fishing	0.14 (0.011)	0.07 (0.007)	0.01 (0.004)	0.01 (0.004)	-0.05 (0.003)	-0.05 (0.003)	-0.05 (0.003)
	Closure explicit	0.10 (0.01)	0.02 (0.008)	-0.02 (0.004)	-0.02 (0.004)	-0.07 (0.003)	0.09 (0.015)	0.10 (0.015)
	Closure imputed	0.10 (0.01)	0.03 (0.008)	-0.01 (0.004)	-0.01 (0.004)	-0.07 (0.003)	0.07 (0.012)	0.08 (0.012)

i	Control	0.12 (0.009)	0.06 (0.007)	0.03 (0.005)	-0.02 (0.003)	-0.03 (0.003)	-0.04 (0.003)	-0.06 (0.004)
	Raw	0.26 (0.011)	0.16 (0.008)	0.10 (0.005)	0.07 (0.005)	0.02 (0.003)	-0.21 (0.003)	-0.39 (0.005)
	Habitat	0.18 (0.011)	0.09 (0.008)	0.06 (0.004)	0.05 (0.004)	-0.02 (0.003)	-0.04 (0.004)	-0.26 (0.005)
	Continuous fishing	0.07 (0.023)	0.06 (0.011)	0.06 (0.011)	0.03 (0.011)	0.00 (0.007)	-0.03 (0.004)	-0.24 (0.005)
	Closure explicit	0.16 (0.01)	0.07 (0.01)	0.05 (0.005)	0.03 (0.005)	-0.02 (0.004)	0.02 (0.027)	-0.25 (0.016)
	Closure imputed	0.12 (0.01)	0.05 (0.008)	0.01 (0.004)	0.00 (0.004)	-0.05 (0.004)	0.07 (0.013)	-0.09 (0.006)
j	Control	0.04 (0.007)	0.03 (0.003)	-0.01 (0.006)	0.01 (0.004)	-0.01 (0.003)	-0.03 (0.004)	-0.03 (0.003)
	Raw	0.12 (0.008)	0.05 (0.004)	0.03 (0.004)	-0.01 (0.004)	-0.06 (0.003)	-0.06 (0.004)	-0.08 (0.004)
	Habitat	0.09 (0.006)	0.02 (0.005)	0.02 (0.005)	0.01 (0.007)	-0.04 (0.004)	-0.04 (0.004)	-0.05 (0.005)
	Continuous fishing	0.09 (0.006)	0.04 (0.006)	0.03 (0.005)	0.01 (0.007)	-0.04 (0.004)	-0.05 (0.004)	-0.05 (0.005)
	Closure explicit	0.00 (0.006)	-0.07 (0.008)	-0.07 (0.005)	0.09 (0.012)	0.05 (0.006)	0.04 (0.005)	0.02 (0.009)
	Closure imputed	-0.01 (0.005)	-0.06 (0.008)	-0.06 (0.006)	0.04 (0.009)	0.03 (0.004)	0.05 (0.003)	0.04 (0.007)
k	Control	0.12 (0.010)	0.08 (0.006)	0.05 (0.005)	-0.01 (0.002)	-0.05 (0.003)	-0.06 (0.003)	-0.07 (0.004)
	Raw	0.32 (0.020)	0.23 (0.015)	0.18 (0.009)	0.07 (0.010)	-0.09 (0.003)	-0.21 (0.007)	-0.29 (0.010)
	Habitat	0.26 (0.016)	0.20 (0.015)	0.16 (0.011)	0.09 (0.009)	-0.09 (0.003)	-0.19 (0.006)	-0.28 (0.010)
	Continuous fishing	0.27 (0.019)	0.22 (0.017)	0.14 (0.013)	0.09 (0.009)	-0.09 (0.003)	-0.20 (0.006)	-0.28 (0.010)
	Closure explicit	0.10 (0.015)	0.04 (0.013)	0.03 (0.013)	0.23 (0.017)	0.04 (0.006)	-0.10 (0.010)	-0.19 (0.014)
	Closure imputed	0.05 (0.010)	0.03 (0.008)	-0.01 (0.007)	0.13 (0.008)	0.02 (0.003)	-0.04 (0.004)	-0.09 (0.004)
l	Control	0.13 (0.008)	0.07 (0.005)	0.04 (0.004)	0.00 (0.003)	-0.03 (0.002)	-0.05 (0.002)	-0.06 (0.002)
	Raw	0.21 (0.010)	0.15 (0.007)	0.07 (0.004)	0.03 (0.005)	-0.08 (0.003)	-0.13 (0.005)	-0.15 (0.004)
	Habitat	0.15 (0.010)	0.11 (0.007)	0.06 (0.004)	0.03 (0.003)	-0.06 (0.005)	-0.12 (0.005)	-0.12 (0.004)
	Continuous fishing	0.17 (0.012)	0.11 (0.008)	0.07 (0.005)	0.03 (0.003)	-0.06 (0.005)	-0.12 (0.006)	-0.12 (0.004)
	Closure explicit	-0.04 (0.008)	-0.06 (0.007)	-0.10 (0.006)	0.20 (0.014)	0.08 (0.011)	0.03 (0.008)	0.02 (0.008)
	Closure imputed	0.00 (0.007)	-0.03 (0.007)	-0.07 (0.005)	0.09 (0.005)	0.04 (0.005)	0.04 (0.005)	0.05 (0.004)
m	Control	0.10 (0.009)	0.06 (0.006)	0.00 (0.004)	-0.01 (0.004)	-0.01 (0.005)	-0.05 (0.004)	-0.03 (0.005)
	Raw	0.23 (0.017)	0.12 (0.006)	0.08 (0.005)	0.03 (0.005)	-0.09 (0.003)	-0.13 (0.003)	-0.18 (0.005)
	Habitat	0.19 (0.019)	0.10 (0.006)	0.09 (0.011)	0.03 (0.006)	-0.06 (0.006)	-0.13 (0.005)	-0.15 (0.007)
	Continuous fishing	0.19 (0.022)	0.08 (0.008)	0.08 (0.012)	0.02 (0.006)	-0.06 (0.005)	-0.13 (0.005)	-0.16 (0.007)
	Closure explicit	-0.01 (0.012)	-0.08 (0.009)	-0.09 (0.010)	0.19 (0.019)	0.08 (0.010)	0.03 (0.010)	-0.01 (0.007)
	Closure imputed	0.03 (0.013)	-0.06 (0.008)	-0.08 (0.010)	0.08 (0.007)	0.03 (0.005)	0.02 (0.006)	0.03 (0.004)
n	Control	0.09 (0.008)	0.09 (0.008)	0.00 (0.006)	-0.02 (0.004)	0.00 (0.005)	-0.04 (0.002)	-0.01 (0.001)
	Raw	0.20 (0.015)	0.13 (0.008)	0.06 (0.006)	0.04 (0.004)	-0.07 (0.003)	-0.11 (0.004)	-0.14 (0.004)
	Habitat	0.17 (0.012)	0.10 (0.009)	0.07 (0.005)	0.04 (0.004)	-0.07 (0.004)	-0.11 (0.004)	-0.12 (0.005)
	Continuous fishing	0.18 (0.014)	0.10 (0.012)	0.07 (0.006)	0.05 (0.004)	-0.07 (0.003)	-0.11 (0.004)	-0.12 (0.005)
	Closure explicit	-0.01 (0.011)	-0.07 (0.009)	-0.09 (0.006)	0.20 (0.013)	0.10 (0.009)	0.04 (0.006)	0.02 (0.005)
	Closure imputed	0.02 (0.009)	-0.02 (0.008)	-0.06 (0.005)	0.10 (0.004)	0.05 (0.004)	0.02 (0.003)	0.04 (0.003)
o	Control	0.10 (0.010)	0.05 (0.004)	0.03 (0.004)	-0.01 (0.003)	-0.03 (0.003)	-0.04 (0.004)	-0.04 (0.003)
	Raw	0.20 (0.012)	0.15 (0.008)	0.06 (0.005)	0.02 (0.005)	-0.06 (0.004)	-0.13 (0.005)	-0.13 (0.006)
	Habitat	0.16 (0.009)	0.11 (0.010)	0.06 (0.007)	0.01 (0.005)	-0.06 (0.004)	-0.10 (0.005)	-0.12 (0.007)
	Continuous fishing	0.18 (0.015)	0.10 (0.010)	0.05 (0.007)	0.01 (0.005)	-0.06 (0.004)	-0.11 (0.005)	-0.12 (0.006)
	Closure explicit	-0.03 (0.013)	-0.08 (0.012)	-0.12 (0.010)	0.17 (0.017)	0.09 (0.011)	0.05 (0.010)	0.01 (0.012)
	Closure imputed	-0.01 (0.010)	-0.05 (0.009)	-0.10 (0.008)	0.08 (0.006)	0.05 (0.005)	0.04 (0.005)	0.05 (0.005)
p	Control	0.11 (0.005)	0.07 (0.005)	0.02 (0.002)	-0.02 (0.002)	-0.04 (0.001)	-0.04 (0.001)	-0.05 (0.001)
	Raw	0.23 (0.013)	0.15 (0.005)	0.09 (0.003)	0.02 (0.004)	-0.09 (0.003)	-0.13 (0.003)	-0.15 (0.003)
	Habitat	0.18 (0.006)	0.11 (0.004)	0.08 (0.004)	0.03 (0.002)	-0.07 (0.003)	-0.10 (0.003)	-0.13 (0.003)
	Continuous fishing	0.19 (0.007)	0.12 (0.004)	0.06 (0.005)	0.03 (0.003)	-0.07 (0.003)	-0.10 (0.003)	-0.13 (0.003)
	Closure explicit	0.01 (0.005)	-0.05 (0.004)	-0.09 (0.004)	0.18 (0.009)	0.08 (0.003)	0.03 (0.004)	0.00 (0.004)
	Closure imputed	0.04 (0.004)	-0.03 (0.003)	-0.05 (0.003)	0.07 (0.003)	0.03 (0.002)	0.04 (0.002)	0.03 (0.002)
q	Control	0.13 (0.010)	0.05 (0.010)	0.03 (0.007)	-0.01 (0.006)	-0.01 (0.007)	-0.06 (0.005)	-0.07 (0.004)
	Raw	0.20 (0.014)	0.14 (0.007)	0.08 (0.007)	0.02 (0.005)	-0.07 (0.003)	-0.11 (0.005)	-0.16 (0.005)
	Habitat	0.15 (0.014)	0.11 (0.014)	0.08 (0.010)	0.02 (0.010)	-0.05 (0.004)	-0.09 (0.008)	-0.13 (0.007)
	Continuous fishing	0.15 (0.021)	0.12 (0.014)	0.08 (0.012)	0.01 (0.010)	-0.06 (0.004)	-0.10 (0.008)	-0.13 (0.007)
	Closure explicit	-0.02 (0.020)	-0.07 (0.015)	-0.07 (0.010)	0.18 (0.022)	0.10 (0.011)	0.06 (0.009)	-0.02 (0.014)
	Closure imputed	0.02 (0.015)	-0.05 (0.013)	-0.03 (0.008)	0.09 (0.010)	0.05 (0.006)	0.04 (0.004)	0.04 (0.007)
r	Control	0.13 (0.006)	0.07 (0.005)	0.01 (0.003)	0.00 (0.002)	-0.02 (0.002)	-0.05 (0.001)	-0.06 (0.002)
	Raw	0.28 (0.018)	0.19 (0.007)	0.10 (0.006)	0.04 (0.004)	-0.08 (0.002)	-0.16 (0.002)	-0.22 (0.005)
	Habitat	0.20 (0.016)	0.14 (0.005)	0.09 (0.005)	0.04 (0.003)	-0.08 (0.003)	-0.14 (0.004)	-0.19 (0.005)
	Continuous fishing	0.21 (0.019)	0.15 (0.008)	0.09 (0.006)	0.03 (0.003)	-0.08 (0.003)	-0.14 (0.004)	-0.19 (0.005)

Closure explicit	0.01 (0.008)	-0.04 (0.005)	-0.10 (0.005)	0.21 (0.015)	0.08 (0.009)	0.03 (0.006)	-0.05 (0.008)
Closure imputed	0.02 (0.007)	-0.03 (0.003)	-0.09 (0.004)	0.09 (0.006)	0.05 (0.005)	0.05 (0.003)	0.04 (0.004)

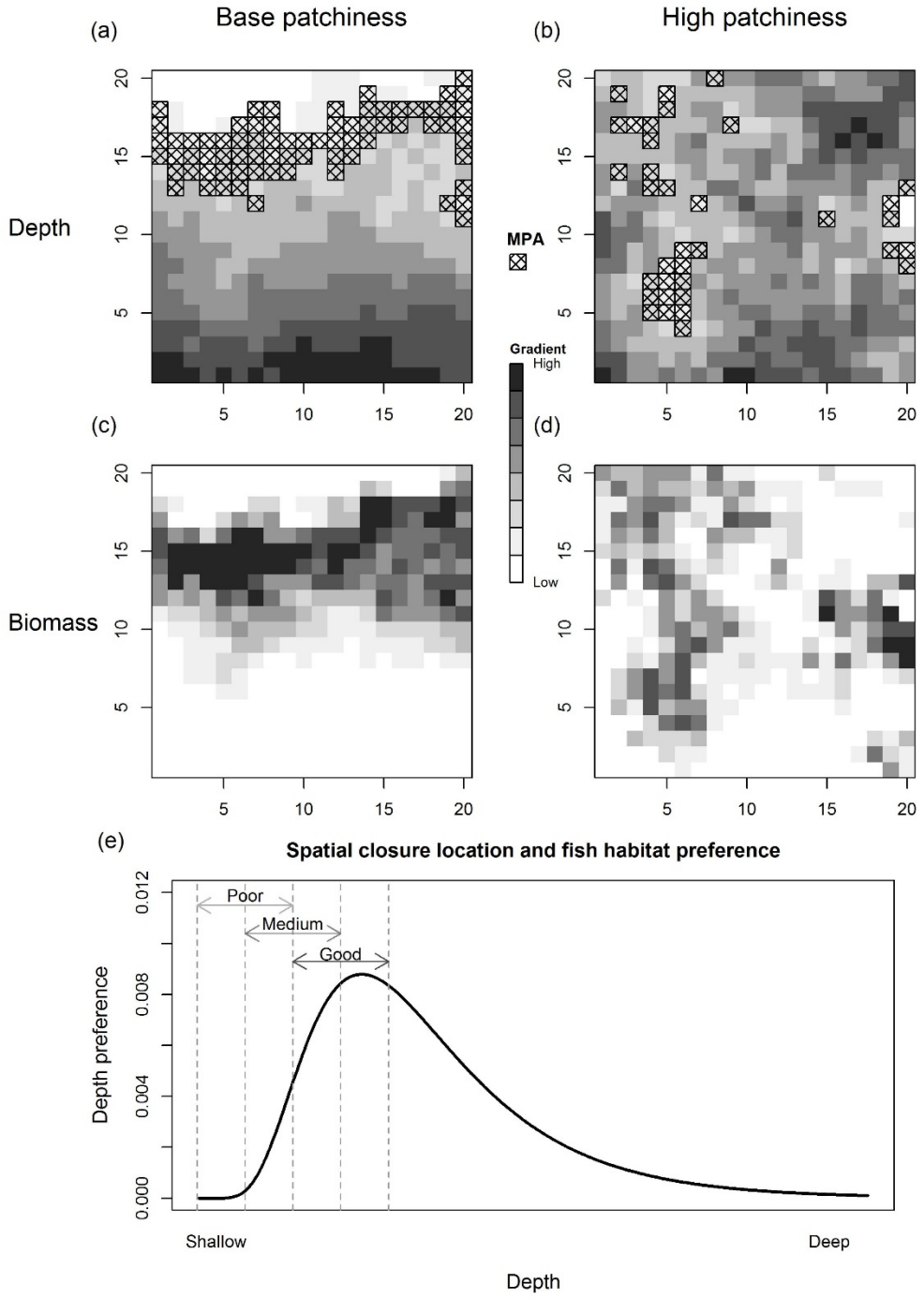

Figure 2.1: Patchiness as a function of depth: (a) example of a uniform depth distribution ("Base" patchiness), (b) example of a patchier depth distribution ("High" patchiness), and the associated closed area locations for the Base case spatial closure. (a) and (b) are both based on a single replicate of a scenario. (c) Fish habitat preference and the location of spatial closures: Poor [0; 50m], Medium [25; 75m], and Good habitat [50; 100m]

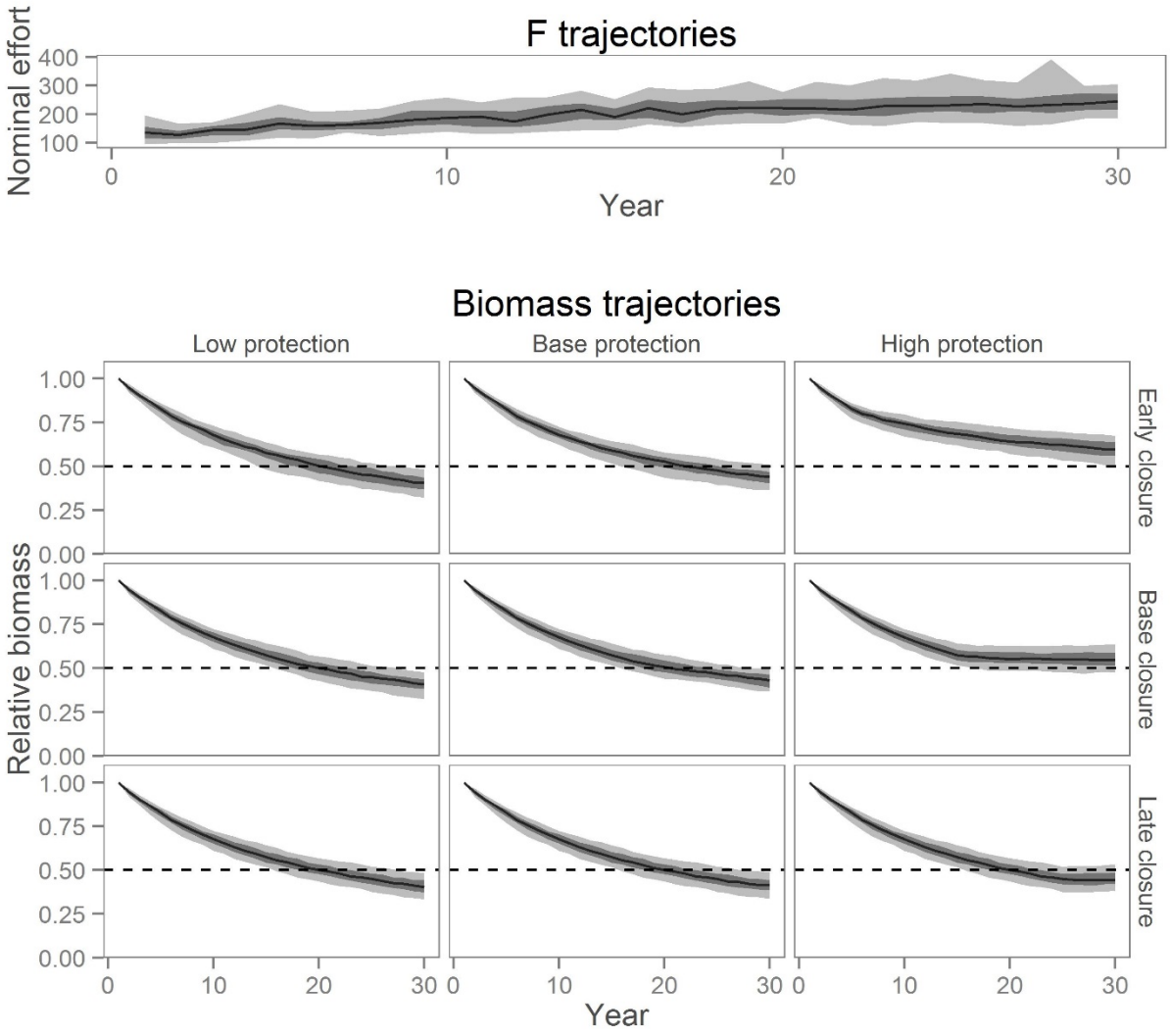

Figure 2.2: Fishing mortality and biomass trajectories for various combinations of species protection and timing of area closure based on the base case parameter settings. The dark and light grey areas show respectively 50% and 90% intervals. A horizontal line was drawn at 0.5 to facilitate case comparison.

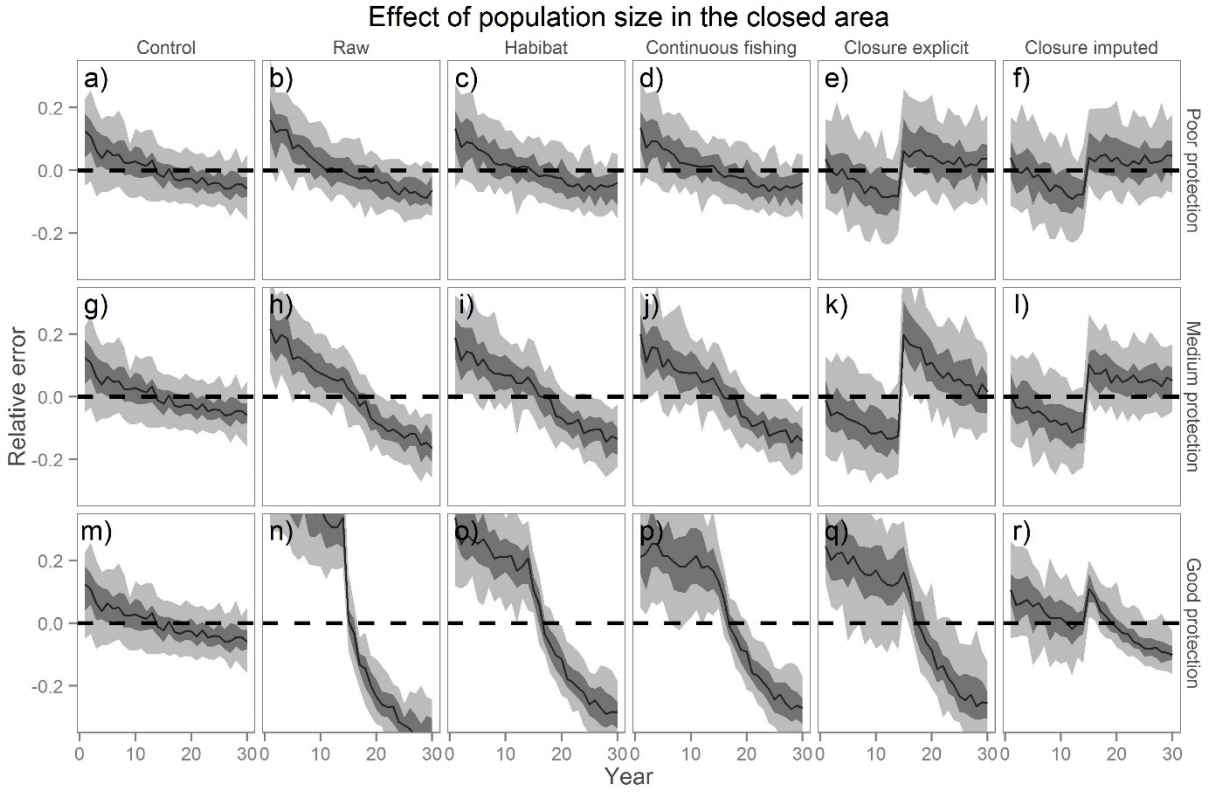

Figure 2.3: Relative error rates for the indices of abundance by standardization method ("Control", "Raw", "Habitat", "Continuous fishing", "Closure explicit", and "Closure imputed") for three levels of protection (Poor, Medium, and Good), for the base case parameter settings. The dark and light grey shading indicates 50% and 90% intervals respectively.

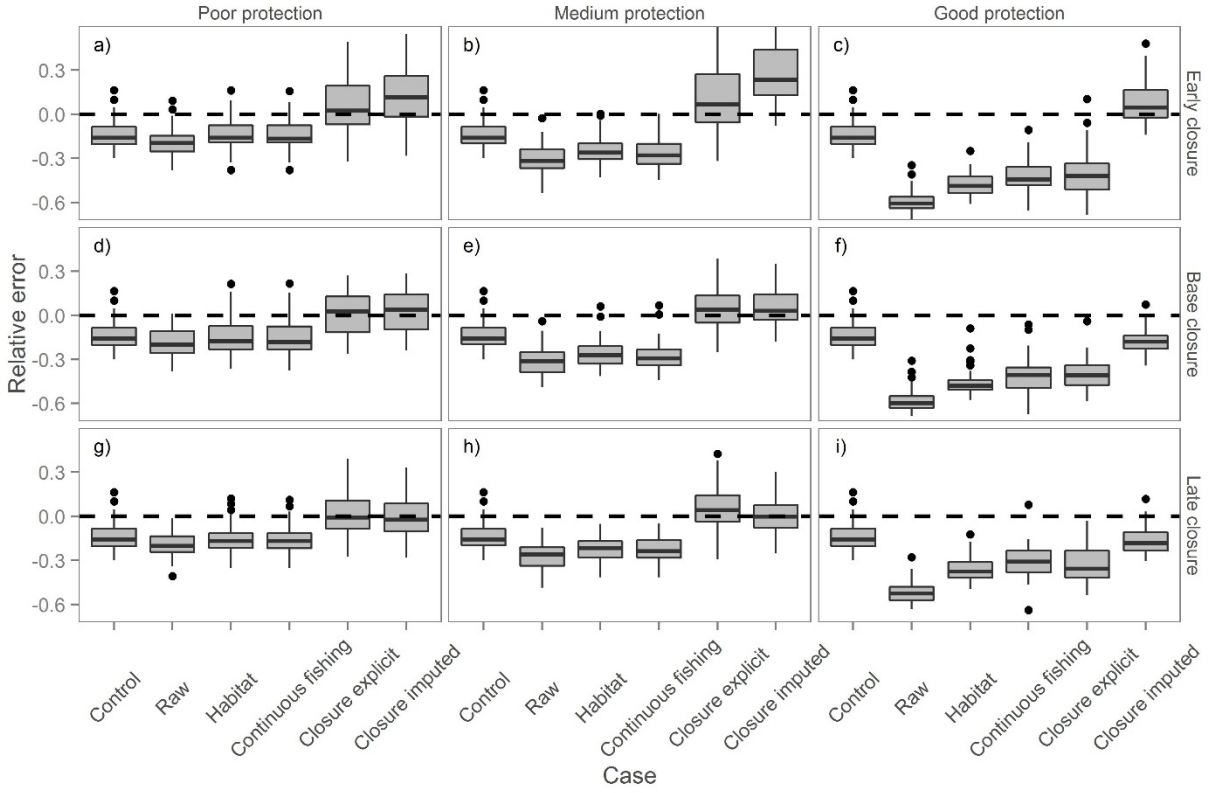

Figure 2.4: Relative error rates for final year depletion by standardization method ("Control", "Raw", "Habitat", "Continuous fishing", "Closure explicit", and "Closure imputed") for three levels of protection (Poor, Medium, and Good), for the base case parameter settings.

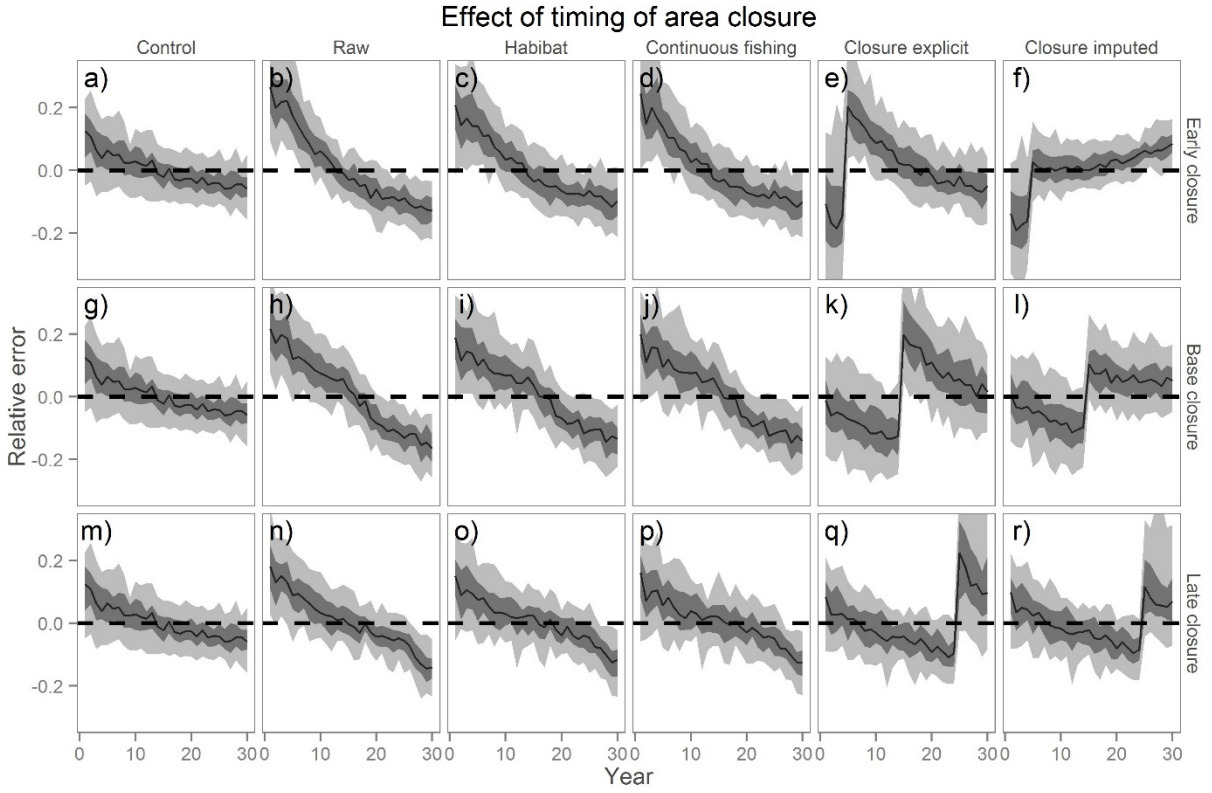

Figure 2.5: Relative error rates for the indices of abundance by standardization method ("Control", "Raw", "Habitat", "Continuous fishing", "Closure explicit", and "Closure imputed") as a function of when the closures were implemented (Early = year 5, Base = year 15, and Late = year 25), for the base parameter settings. The dark and light grey shading indicates 50% and 90% intervals respectively.

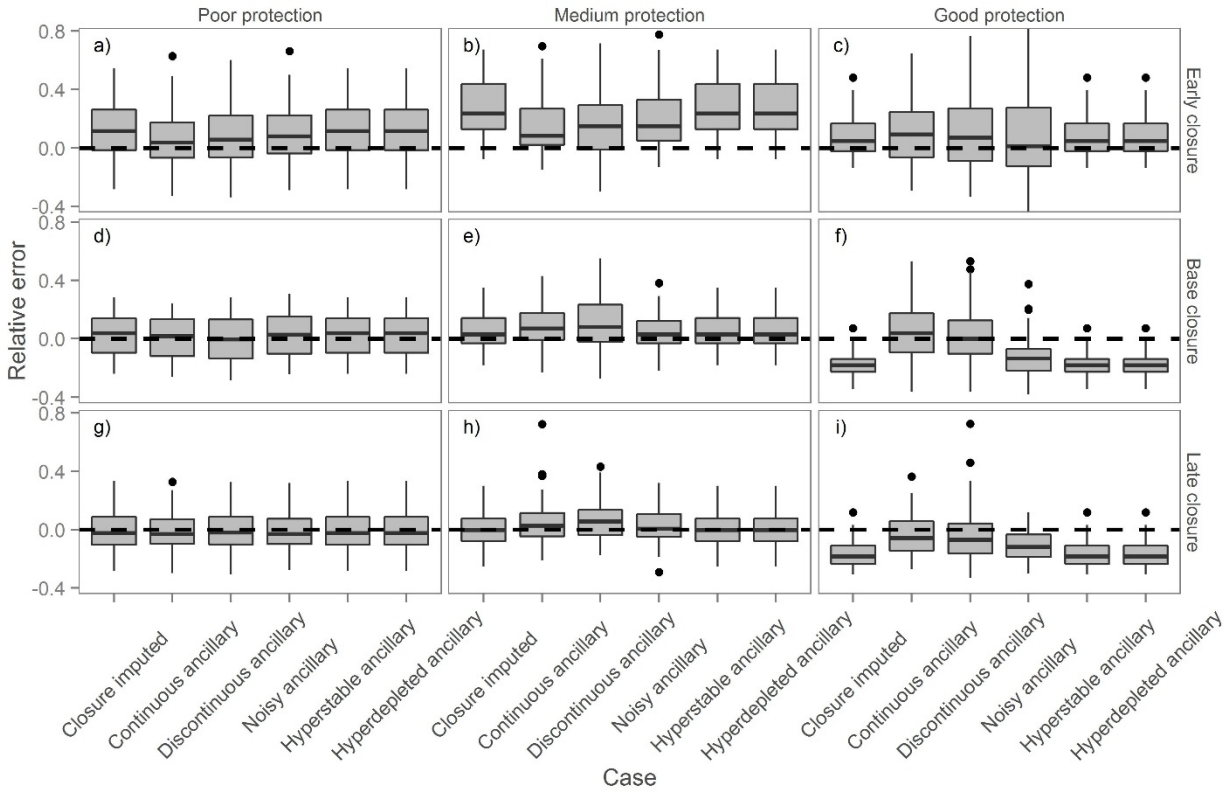

Figure 2.6: Relative error rates for the final year depletion estimate for six methods for three levels of protection (Poor, Medium, and Good), for the base parameter settings.

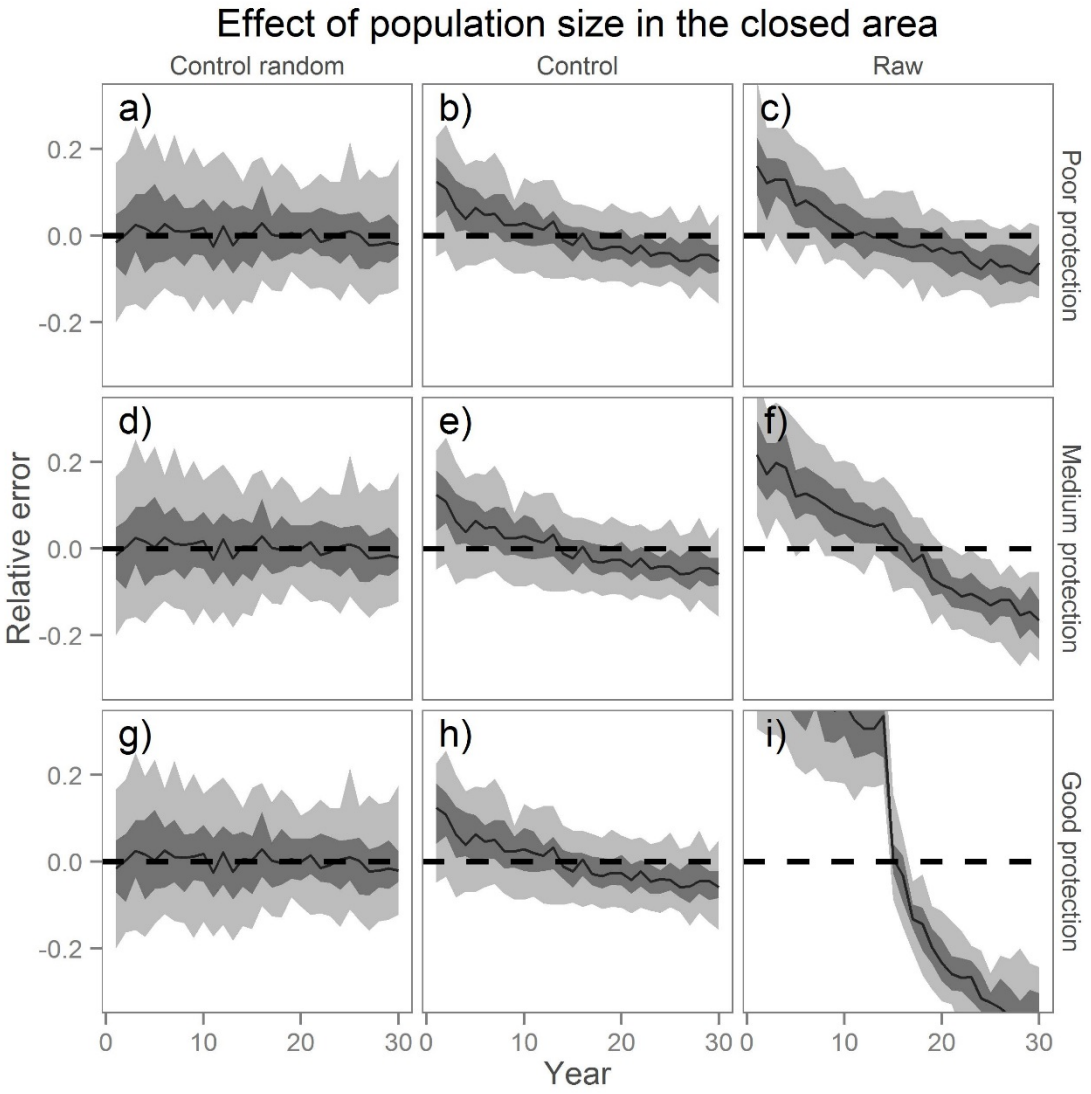

Figure A2.1: Relative error rates for the derived indices of abundance for three standardization methods ("Control random", "Control", and "Raw) for three levels of protection (Poor, Medium, and Good), for the base case parameter settings. "Control random" is based on simulations with a random distribution of fishing effort, while "Control" and "Raw" are both based on targeted fishing behavior. The dark and light grey shading indicates 50% and 90% intervals respectively.

Chapter 3 - Think outside the grids: a biologically meaningful method to define spatial strata for catch and effort analysis

Abstract

A method is developed to objectively stratify a fished area for standardizing catch per unit effort (CPUE) data for use in a generalized linear modelling framework. The method involves two steps: 1) subdividing the study area into grids and applying a boosted regression tree method based on the full model to reconstruct a rough population pattern among grids, and 2) applying a *k*-medoids algorithm to partition the grids into discrete strata based on the trend and magnitude of expected CPUE in each grid (time series clustering) or the spatial proximity and average CPUE in each grid (spatial clustering). The main advantage of this method compared to other area stratification approaches is that the shape of the resulting strata best matches the population structure as inferred from CPUE. This approach reduced bias in indices of abundance compared to ad-hoc methods. The variant of the area stratification method based on time series clustering performed best. However, this approach often performed more poorly than ad-hoc methods when there was a shift in fishing locations over time. In this case, strata needed to be organized to capture the shifts in fishing grounds over time, which was not necessarily accomplished using clustering-based area stratification. Finally, the study showed that goodness of fit criteria (AICc or BIC) can be used to select the optimal number of strata for CPUE standardization, but this does not guarantee improved accuracy of the derived index of abundance compared to a pre-specified number of strata. The importance of conducting sensitivity analysis to the choice of strata is highlighted.

Introduction

Considerable effort has been put into assessing natural populations and evaluating their status due to the increasing concern about the health of the oceans. These assessments are often performed using generic and standardized models and platforms which include, for example, VPA (Gulland 1965), MULTIFAN-CL (Fournier et al, 1998), and Stock Synthesis (Methot and Wetzel 2013) and attempt to make the best use of the available science and data. Catch data are a central piece of information for most of these methods and are used in two ways: as information on removals from the population or as a time series that provides information about relative abundance. Indices of abundance based on catch and effort data are constructed using a "catch per unit effort standardization" (Hilborn and Walters 1992, Campbell 2004, Maunder and Punt 2004). The catch data are first transformed into catch per unit effort (CPUE) (e.g. catch in tons per hour fishing) then "standardized" to account for the effects of any available variables that can influence CPUE. These variables can relate to changes in gear, vessel power, skipper, and vessel dynamics among others (Maunder 2006). "Standardization" has been frequently performed by regressing CPUE against these covariates using the fixed or mixed effect versions of the generalized linear/additive model (see Maunder and Punt 2004 for a review). Area strata are one of the variables that are often included in a CPUE standardization. In theory, each area stratum should be as homogenous in terms of density as possible (Bishop 2006) (higher density areas versus lower density areas for example). However, this is seldom the case, and many analysts use ad-hoc sets of grids as strata in CPUE standardizations (Nakano 1998). This can lead to "Simpson's paradox" (Simpson 1951): a trend that appears in different subgroups of areas

disappears when these subgroups are aggregated, and the reverse trend appears instead. This "paradox" could potentially result in a biased index of abundance, which could lead to erroneous advice given to fishery managers.

Recently, new strategies have been developed to create more meaningful area stratifications for use in CPUE standardization. For example, Ichinokawa and Brodziak (2010) proposed a binary recursive area partitioning approach to objectively stratify a study area based on model selection criteria (e.g., AIC or BIC) and Candy et al. (2014) proposed the use of ancillary data such as the empirical length distributions to help stratifying areas for CPUE analysis. While these methods are objective, there are drawbacks associated with each of them. The Ichinokawa and Brodziak method is limited to producing rectangular strata due to the nature of binary partitioning. However, populations are rarely structured this way. The Candy et al (2014) approach is attractive but it requires data on fish lengths, which are not always available. In addition, while the best area stratification can be selected based on goodness of fit criteria (Maunder and Punt 2004), there is no guarantee that the selected stratification leads to the least biased index of abundance, with the latter being the ultimate objective of CPUE standardization. It is therefore important to conduct a simulation analysis to explore alternative area stratification methods that do not require additional data, and examine the reliability of goodness of fit criteria in selecting a basis to develop indices of abundance.

In this paper, we propose an intuitive, but objective, area stratification method based on *k*-medoid partitioning that only uses the CPUE data. *k*-medoid partitioning has been used to define fishery management units (Cope and Punt 2009). This paper is divided into the following sections: (a) description of the simulation model that generates the CPUE data used to test CPUE

standardization methods; (b) presentation of the alternative CPUE standardization and the area stratification methods; (c) comparison of the performance of these methods; and (d) application of the methods to data for petrale sole (*Eopsetta jordani*).

Materials and methods

The simulation model

A spatially-explicit model (20 x 20 grids; n_a=400) of a single fish stock, coupled with a vessel dynamics model is used to generate the CPUE data (Fig. 3.1). The model works as follows. For each year of an arbitrarily chosen 30-year projection (n_y=30) period: (1) fishing effort is distributed to each grid given the population distribution at the start of the year, and the catch in each grid is calculated, (2) population abundance by grid is adjusted for catch and growth, and (3) fish are redistributed spatially based on movement probabilities. This generates catch and effort data on the 20 x 20 grid which are then used for CPUE standardization. Details are given in section 3.4.

Population dynamics

The underlying population dynamics are governed by a deterministic logistic model with a yearly time step, referred to as a Schaefer model in fisheries (Schaefer 1954) with movement dynamics controlled by habitat (depth) preference and mobility. This model has often been used in combination with indices of abundance to estimate population abundance (Hilborn and Walters 1992). The population biomass $B_{a,t}$ in grid a at time t evolves through time as a function of the catch $C_{a,t}$ in grid a during year t, the intrinsic rate of growth of the stock r, the carrying

capacity of grid *a, K_a* (as in Carruthers et al. 2011b), the biomass of animals emigrating $EM_{a,t}$, and the biomass of animals immigrating $IM_{a,t}$:

$$B_{a,t+1} = B_{a,t} + rB_{a,t}(1-\frac{B_{a,t}}{K_a}) - C_{a,t} - EM_{a,t} + IM_{a,t} \quad (3.1)$$

Movement among grids during year *t* is calculated as follows. The probability M_{ab} of moving from grid *a* to grid *b* is a function of (1) the Euclidian distance d_{ab}=||*a*-*b*|| between the centers of gravity of the two grids, (2) the coast-wide (x-axis) distribution range of the species, and (3) the relative preference for the habitat in grid *b* compared to that in the rest of grids. Fish movement is represented by an exponential decay function that depends on the distance d_{ab} and a rate parameter λ (Moilanen and Nieminen 2002, Ono et al. 2013), fish depth preference which follows a lognormal distribution with parameters (μ_d, σ_d) where z_x is the depth of grid *x* (Ono et al. 2013), and fish distribution range (x-axis wide) which is modeled using a lognormal distribution with parameters (μ_r, σ_r) where *x(x)* is the x-axis coordinate of the grid *x* (Table 3.1).

$$M_{\mathrm{ab}} = \frac{e^{-\lambda d_{ab}} \frac{1}{z_b} e^{-\frac{(\ln z_b - \mu_d)}{2\sigma_d^2}} e^{-\frac{(x(b)-\mu_r)}{2\sigma_r^2}}}{\sum_{x=1}^{n_a} e^{-\lambda d_{ax}} \frac{1}{z_x} e^{-\frac{(\ln z_x - \mu_d)}{2\sigma_d^2}} e^{-\frac{(x(x)-\mu_r)}{2\sigma_r^2}}} \quad (3.2)$$

Depth is simulated from a multivariate normal distribution with a mean that changes linearly with the y-coordinate of the grids and an exponential decay covariance function that depends on distance *d* between grids (eq 3.3). The linear increase in depth with the y-coordinate mimics a coastline (represented by the x-coordinate) that slowly increases in depth with the distance from coast.

(3.3) $$Z \sim MVN(\underline{\mu}, \mathbf{\Sigma}); \quad \mu_b = \alpha y_b; \quad \Sigma_{a,b} = \tau^2 \exp(-\xi d_{ab})$$

where Z is the depth variable (Fig. 3.1), y_b is the y-coordinate of grid b, α is the trend parameter for depth (which also determines the patchiness of the depth distribution), τ^2 is the variance parameter, and ξ controls the rate at which the spatial correlation declines with distance (Table 3.1). The simulated depth is then standardized so that it spans a specific range (Table 3.1).

The biomass of emigrants from grid a ($EM_{a,t}$) and that of immigrants to grid a ($IM_{a,t}$) at time t is calculated as:

(3.4) $$EM_{a,t} = \sum_{b \neq a} M_{ab} B_{a,t} \; ; \; IM_{a,t} = \sum_{b \neq a} M_{ba} B_{b,t}$$

The biomass in each area a, at the start of the simulation is assumed to be K_a, which is obtained by determining the stationary distribution of the population over areas **d** that satisfies the conditions:

(3.5) $$\begin{aligned} K_a &= K d_a \\ d &= M d \end{aligned}$$

where K is the total (across populations) carrying capacity, **d** is the positive eigenvector of the movement probability matrix **M** corresponding to the first eigenvalue.

Fleet dynamics

The total amount of nominal effort across all grids and all vessels during year t, $E_{.,t}$, is generated from a lognormal distribution with mean given by a logistic function of time and a CV of 0.2, where $\overline{E_T}$ is the final year effort, i.e.:

(3.6) For t∈[1;T], $E_{.,t} = \lfloor \log N(\frac{\overline{E_T}}{1+\exp(-0.1t)}, CV = 0.2) \rfloor$

These integer effort levels are then distributed randomly among twenty vessels (n_v=20). Each vessel has its own catchability coefficient q_v generated from a lognormal distribution with parameters ($\bar{q}$=0.1, CV_q=0.2). The differences in q_v among vessels reflect differences in vessel characteristics or skipper skill among vessels and each q_v is time-invariant.

Vessel v distributes its effort during year t, $E_{,t,v}$, to each grid a with a probability $p_{a,t,v}$ that depends on the mean expected catch in each grid. This approach is a stochastic version of the gravity model of Caddy (1975). It is assumed that vessels have perfect information about the biomass in each grid, but their catch rate is variable by grid cell.

(3.7) $$p_{a,t,v} = \frac{B_{a,t}\left(1-e^{-q_{a,v}}\right)}{\sum_{x=1}^{n_a} B_{x,t}\left(1-e^{-q_{x,v}}\right)}$$

The amount of effort (trips) for vessel v in grid a during year t, $E_{a,t,v}$, follows a multinomial distribution with probability $p_{a,t,v}$. :

(3.8) $$E_{a,t,v} \sim Multinomial(E_{.,t,v}, p_{a,t,v})$$

One consequence of this effort allocation algorithm is that several areas will be unfished throughout the time series and fishing areas will change over time. Specifically, the number of high CPUE areas will decrease over time due to fishing, which increases the number of fished areas over time.

Randomness in the catch was introduced by sampling the realized catchability for trip e by vessel v, $q'_{v,e}$, from a Tweedie distribution with a mean $\mu=q_v$ and values for p and Φ of 1.2 and 0.1 respectively. The Tweedie distribution belongs to the exponential family, and has mean μ and variance $\Phi\mu^p$. It is a continuous distribution with an added mass at 0 when $1<p_v<2$. This distribution is therefore a good candidate to simulate zero-inflated CPUE data, as a high fraction of zero catches are often observed in practice (Maunder and Punt 2004). The total (over vessels) catch $C_{a,t}$ in grid a and time t is determined as follows:

$$(3.9) \quad C_{a,t} = B_{a,t}\left(1 - e^{-\sum_{v=1}^{n_v}\sum_{e=1}^{E_{a,t,v}} q'_{v,e}}\right)$$

$C_{a,t}$ is redistributed among vessels and fishing events to generate catch per unit effort for the e^{th} trip by vessel v, in grid a, during year t, $C_{a,t,v,e}$, used for the CPUE standardization, as follows:

$$(3.10) \quad C_{a,t,v,e} = C_{a,t}\frac{q'_{v,e}}{\sum_{v=1}^{n_v}\sum_{e=1}^{E_{a,t,v}} q'_{v,e}}$$

The well-known Baranov catch equation arises from the combination of equations 9 and 10.

Standardizing the CPUE data

General approach

CPUE standardization was performed using the generated catch and effort data, in addition to the vessel number. Depth was not considered as possible covariate: 1) to focus on the effect of area stratification, and 2) to mimic reality where the variables affecting species distribution are rarely

known and available. In addition, incorporating depth as a covariate would attenuate the effect of area stratification.

A delta model (also called hurdle model) was used to analyze the data since the generated data contain many zero catches (Maunder and Punt 2004). In this analysis, the presence/absence of a non-zero catch was modeled using a binomial model (eq 3.11), and the positive catch rates using a lognormal distribution (eq 3.12). Model selection using AICc was used to select between lognormal, normal and gamma distributions for the positive catches; the gamma model was usually the best (>95% of simulations), followed by the lognormal then the normal, but gamma model often (>25% of simulations) failed to converge. Therefore, the lognormal model was chosen to model the positive catch data for all analyses for consistency. The statistical analyses were performed using the generalized linear modeling (glm) framework in the programming language R (R Core Team 2013). The final standardization model was:

$$(3.11)\quad \mathrm{p}(\mathrm{CPUE}_{\mathrm{a,t,v}} > 0) = \frac{e^{\mu' + \alpha_t' + \beta_a' + \alpha_t'\beta_a' + \delta_v'}}{1 + e^{\mu' + \alpha_t' + \beta_a' + \alpha_t'\beta_a' + \delta_v'}}$$

$$(3.12)\quad \mathrm{E}(\mathrm{CPUE}_{\mathrm{a,t,v}} \mid \mathrm{CPUE}_{\mathrm{a,t,v}} > 0) = e^{\mu + \alpha_t + \beta_a + \alpha_t\beta_a + \delta_v}$$

where μ (and μ') is the mean, α_t (and α_t') the year effect, β_a (and β_a') the area stratum effect for grid a, and δ_v (and δ_v') the vessel effect. $\alpha_t\beta_a$ represents the interaction effect between year and area. The results of the delta model were used to create an index for year t, $\hat{I}_t'$, that is the sum of the predicted CPUE (predicted probability of catch multiplied by the expected CPUE) for each grid for an arbitrary vessel 1 (Maunder and Punt (2004) suggest using the vessel that is the most

representative of the fishery, but in this simulation any vessel is equally likely to go fishing, hence they are equally representative of the fishery):

$$(3.13)\quad \hat{I}_t' = \sum_{a=1}^{n_a} p(CPUE_{a,t,v=1} > 0) E(CPUE_{a,t,v=1} \mid CPUE_{a,t,v=1} > 0)$$

For any given simulated data set, some year-area strata could be unfished due to the dynamics of the fishery. In these cases, the method of Walters (2003) and Carruthers et al. (2011a) was used to linearly interpolate the CPUE for any missing year-area strata based on the nearest predictions before and after the missing years (the GLMi/IMP approach of Carruthers et al. 2011a). The final index of abundance $\widehat{I_t}$ was obtained by dividing $\hat{I}_t'$ by its geometric mean over time (Francis 1999). The steps of the simulation-estimation procedure are summarized in Fig. 3.2.

Competing models to standardize CPUE data

Indices of abundance are computed for some commonly-used CPUE standardization approaches:

(1) The Raw CPUE model ("Raw") is just the total catch divided by the total effort. This is the unstandardized index of abundance.

(2) GLM, with arbitrary area stratification ("Arbitrary"). It is common to (arbitrarily) stratify fishing grounds into a small number of pre-established areas (e.g. state boundaries) when creating strata from logbook data. We examined cases when fishing grounds were divided arbitrarily into 2 (n=2), 4 (n=4) or 8 (n=8) regions (Fig. 3.1).

(3) GLM with clustering based area stratification. Two types of clustering are used in this study: (a) a spatial clustering that groups grid cells based on the mean animal density (or presence) in the grid cell and their spatial proximity, and (b) a time series clustering approach that

groups grids based on the similarity in the trend and magnitude of fish density (or presence). Both spatial and time series clustering are conducted using partitioning around medoids (*pam*) (Kauffman and Rousseeuw 1990). Clustering based on area stratification works as follows:

1) The study area is divided into a large number of equal sized areas to allow patterns to be detected (in this study, the 400 grid cells were divided into 100 larger grid cells; Fig. 3.2).

2) Boosted regression tree (Elith et al. 2008), a machine learning method, is applied to the CPUE data (using "Year", "Area", and "Vessel" as covariates) to predict the probability of fish presence and density in each of the 100 grid cells, over the simulation period. Boosted regression tree (BRT) was chosen because it is a flexible method that accommodates missing predictors (no catch in a grid during a specific year), interaction between predictors, and nonlinear relationship between predictors. BRT was applied with a learning rate[2] of 0.005 and 0.0001 for the lognormal and binomial models, respectively, and with a bag fraction of 0.5. In short, BRT is a linear combination of many regression

[2] The bag fraction determines the proportion of data to randomly draw from the full data at each iteration before fitting the regression model. The learning rate is the contribution of each regression model to the final model which is a linear combination of all previous models.

trees fitted to a fraction of the data (i.e. 50% of the data with a bag fraction of 0.5) to improve model accuracy and reduce overfitting (see Elith et al. 2008 for more details on boosted regression). For actual applications, this step would be based on using the full model (i.e. all covariates) without performing a model selection as we only seek to reconstruct roughly the pattern of CPUE in each grid.

3) Use the fitted BRT to predict the probability of fish presence and fish density in each of the 100 grids, over the simulation period. A reference level is chosen for each covariate in addition to the "Year" and "Area" effects. For the simulation study, vessel 1 was chosen arbitrarily as the reference level (any vessel is equally likely to go fishing in this study, hence is equally representative of the fishery). For actual applications, reference levels could be chosen to be the most representative of the fishery e.g. the most frequently observed level for a categorical variable (Punt et al. 2000) or the mean value for a continuous variable (Maunder and Punt 2004).

4) Calculate a distance matrix for the 100 grids based on the data from step 3) and run the cluster analysis to group grids based on their similarity. This is done separately for the predicted fish density given presence and predicted fish presence. The strata for the lognormal and binomial models are then selected by applying a cluster analysis with a specified number of strata. For the spatial clustering, the Euclidean distance between grids p and q, $d(p,q)$ was calculated using either the average (over time) predicted fish density or the average predicted fish presence for each grid i, z_i, and the 2D spatial coordinates (x_i,y_i) of grid i, depending on whether the binomial r lognormal models are being applied. Fish density estimates and spatial coordinates were standardized (i.e. demeaned and divided by their standard deviations) and multiplied by a weighting factor,

w to emphasize (or de-emphasize) the importance of spatial proximity with respect to the difference in underlying population density (or probability of fish presence):

$$(3.14)\quad d(p,q)=\sqrt{w^2\left[(x_p-x_q)^2+(y_p-y_q)^2\right]+(z_p-z_q)^2}$$

The "Spatial0.1" approach sets *w*=0.1 i.e. a difference of one standardized unit in either spatial coordinate has 100 times less influence than one unit change in population density or presence. The "Spatial1" approach assigns equal weight to spatial proximity and to the average population density (or presence). The "Time" method uses the CORT algorithm (eq 3.15; Chouakria-Douzal and Nagabhushan, 2007), which combines both temporal correlation and the raw values to calculate a dissimilarity matrix.

$$(3.15)\quad d(p,q)=\frac{2}{1+\exp\left(2\dfrac{\sum(v_{p,2:T}-v_{p,1:(T-1)})(v_{q,2:T}-v_{q,1:(T-1)})}{\sqrt{\sum(v_{p,2:T}-v_{p,1:(T-1)})^2}\sqrt{\sum(v_{q,2:T}-v_{q,1:(T-1)})^2}}\right)}\sqrt{\sum(v_{p,1:T}-v_{q,1:T})^2}$$

where $v_{p,1:T}$ is the predicted fish density estimate (or probability of fish presence) of area *p* from year 1 to T (T=30).

AICc and BIC were used for model selection to select the optimal number of spatial strata (choice between 2 to 10 strata) for both the binomial (eq 3.11) and lognormal models (eq 3.12).

Performance evaluation

The performances of the CPUE standardization approaches are evaluated using three metrics: 1) the relative error (RE) in the derived index of abundance ($\hat{I}_t$) over time (eq 3.16) and the RE of the final year depletion estimate (B_{30}/B_1), which is often a quantity of management interest (eq

3.17), and 2), the median relative error (MRE) and the median absolute relative error (MARE) of the derived index of abundance (eq 3.18), which provide information about bias and accuracy respectively. The true biomass was rescaled by its geometric mean, B_t' to match the scale of the derived indices of abundance when evaluating model performance.

$$RE_t = \frac{(\widehat{I}_t - B_t')}{B_t'} \tag{3.16}$$

$$RE_{depletion} = \frac{(\widehat{I_{t=30}} / \widehat{I_{t=1}} - B'_{t=30} / B'_{t=1})}{B'_{t=30} / B'_{t=1}} \tag{3.17}$$

$$\begin{aligned} MRE &= median(RE_{t=1}, ..., RE_{t=30}) \\ MARE &= median(|RE_{t=1}|, ..., |RE_{t=30}|) \end{aligned} \tag{3.18}$$

Simulation scenario

The performances of five area stratification methods ("Raw", "Arbitrary", "Spatial 0.1", "Spatial 1", and "Time") were explored given different levels of patchiness in fish distribution and fisher behavior:

(1) The patchiness of fish distribution. Fish are usually not distributed uniformly as their habitat is limited and often fragmented. Model performance is compared between situations where fish distribution is patchy (α=0; "Base patch") or less patchy (α=5; "Less patch") (Fig. 3.1).

(2) A shift in the fishing grounds. Several factors can cause this such as a progressive change in species targeting over time or, in the context of climate change, a species range shift. For the purpose of this study, we mimicked this by shifting the distribution range of the species. Model performance is evaluated for situations where animals do not show any directional

movement ("Base") and where they shift their ranges during the simulation period ("Range shift"). Directional movement was modeled by changing the species' center of distribution by 1.5 cells every year along the coast (x-axis).

This led to four scenarios that formed the basis for model comparison and which were subsequently used to evaluate sensitivity to the study assumptions:

(1) Sensitivity to the number of spatial strata for the analysis. Cases with "2 areas", "Base areas" (4 areas), and "8 areas" (Fig. 3.1) were compared.
(2) Sensitivity to the amount of data available for the CPUE standardization. The amount of data available for the analysis depends on the fishery. We examined a 50% change in the amount of data: from roughly 200 data points per year on average ("Base data") to 300 data points per year on average ("More data")
(3) Sensitivity to the expected proportion of zeros in the data set. Some species are widely distributed (or easier to catch) than others depending on life history and the type of gear used in the fishery. Cases were examined when the amount of zero inflation is about 14% ("Base zero") and when there were twice as many zero catches ("More zeros").

The term "Base case" refers to a case with "Base areas", "Base data", and "Base zero".

Case study application: the U.S. west coast petrale sole

The area stratification methods were applied to data for petrale sole off the U.S. west coast. We used the same data as in the 2013 stock assessment (see Haltuch et al. 2013 for more details about the data). Two fisheries are structured seasonally based on winter (November to February) and summer (March to October) fishing seasons, and the data are divided into northern (Washington and Oregon) and southern (California) regions. There are a total of 18,627 trip level

data points for the summer fishery in the northern region, 6,645 for the summer fishery off California, 3,983 for the winter fishery off Washington and Oregon, and 1,307 for the winter fishery off California. The covariates that were available for the analysis were: year, spatial stratum, bimonth period, port of landing, fishing gear, vessel number, and species composition data (summarized into a few principal component axes to reflect targeting behavior; Winkler et al. 2011). The fishing grounds were divided into a small grid system of 0.2x0.2 degrees (Fig. 3.3) before the boosted regression (using all covariates) was applied to predict fish density and fish occurrence in each grid over time. Predictions were based on reference levels chosen as the most frequently observed level for a categorical variable (Punt et al. 2000), the mean value for a continuous variable (Maunder and Punt 2004), and the combination of principal component loadings that predicted a catch composition close to (or exactly) 100% petrale sole so that predictions are representative of a fishery that targets petrale sole. Boosted regression was performed with a learning rate of 0.005 and 0.001 for the lognormal and binomial models respectively and with a bagging fraction of 0.5 which led to more than 1000 trees, as recommended by Elith et al. (2008). The fishing grounds were then stratified into 1 to 10 areas and a generalized linear regression applied. The best model (both covariates and stratum numbers) was then selected for each component of the model (i.e. binomial and lognormal) using AICc and BIC. All models included the "Year x area" interaction. Finally, the best model was used to create an index of abundance. This index was compared with the index of abundance used by Haltuch et al. (2013), and the sensitivity of the results was examined to the choice of model selection criteria (for choosing the number of spatial strata). We compared the results between the use of AICc, BIC, and an ad-hoc (five strata) method for stratifying areas (the rest of covariates were chosen based on BIC when there were five strata).

Results

Performance comparison between the CPUE standardization methods

In general, the "Raw" method led to the most biased indices of abundance among the evaluated methods (Fig. 3.4, a,f,k,p). The bias was positive at the start of the time series and negative at the end, for the "Base" and "Less patch" scenarios (Fig. 3.4, a,f), leading to a negatively biased estimate (-20%) of final year relative biomass (Fig. 3.5, a,b). On the other hand, bias was U-shaped over time for scenarios with changing fishing grounds (Fig. 3.4, k,p), leading to a positive bias (+25%) in the estimate of final year relative biomass (Fig. 3.5, c,d).

While the "Raw" method was generally the most biased, the "Arbitrary" stratification approach led on average to a less accurate index of abundance (higher MARE) for the "Base patch" and "Less patch" scenario (Fig. 3.6, a,b). The pattern of bias for the "Arbitrary" method was similar to that for "Raw" method for the "Base" and "Less patch" scenarios (Fig. 3.4, b,g), leading to an underestimation (-10%) of the relative biomass at the end of the time series (Fig. 3.5, a,b). Nonetheless, the "Arbitrary" method led to an index of abundance that was almost unbiased for scenarios in which the fishing grounds changed over time (Fig. 3.4, l,q).

Two of the three clustering based CPUE standardization methods ("Spatial 0.1" and "Time") performed equally well, and the derived indices of abundance were almost unbiased and more accurate than those form the "Raw" and "Arbitrary" methods for the "Base" and "Less patch" scenarios (Fig. 3.4, c,d,e,h,i,j, Fig. 3.5 and 6, a,b). "Spatial 1" had more bias over time than the other two clustering based methods for the "Base" and "Less patch" scenarios (Fig. 3.4, d *vs.* c,e and i *vs.* h,j), but was also the only clustering-based stratification method that produced an index of abundance that was close to unbiased for scenarios with shifting fishing grounds, and with

bias and accuracy that were comparable to that of the "Arbitrary" method (Fig. 3.4, n,s *vs* l,q, Fig. 3.5 and 6, c,d). The "Spatial 0.1" and "Time" methods resulted in an index of abundance with a marked U-shaped bias similar to the "Raw" method (Fig. 3.4, m,o,r,t *vs* k,p), with less accuracy (Fig. 3.6, c,d), and a positive bias (+10%) in the estimate of final year relative biomass (Fig. 3.5, c,d).

Sensitivity analysis of the CPUE standardization methods

The effect of number of strata

The number of strata had a different effect on model performance depending on the patchiness of fish distribution and whether fishing grounds shifted location over time. The accuracy of abundance indices and the bias in final year relative biomass estimates did not change much between different numbers of strata (2, 4, 8) for the "Base patch" scenario and for all CPUE standardization methods (Fig. 3.5 and 6, a,e,i). The "Time" approach was the least sensitive to the number of strata among all methods, and was best in terms of predicting the indices of abundance and final year biomass estimate for the "Base patch" and "Less patch" scenarios (Fig. 3.5 and 3.6, a,b,e,f,i,j). On the other hand, using a larger number of strata decreased accuracy for the rest of methods for the "Less patch" scenario (Fig. 3.6, b,f,j). Changes were largest for the "Spatial 1" method which had the poorest accuracy among all methods with 8 strata (Fig. 3.6, j) followed by the "Arbitrary, "Spatial 0.1" and "Time" methods.

The performances of the clustering-based methods were more sensitive to the number of spatial strata when fishing grounds shifted over time. Bias was generally U-shaped over time but it decreased with larger number of strata and the accuracy increased, except for the "Spatial1" method for the "Less patch range shift" scenario (Fig. 3.6, c,d *vs.* g,h *vs.* k,l). "Spatial 1" had a

less distinct U-shaped bias over time, the least biased estimates of final year relative biomass, and the most accurate index of abundance compared to the other clustering-based methods, except for the "Less patch range shift" scenario with 8 strata (Fig. 3.5 and 6, k,l). However, bias was lower for the "Arbitrary" method (Fig. 3.4) than for "Spatial 1", and the indices of abundance were more accurate with 4 or 8 strata (Fig. 3.6, c,d,k,l). Nonetheless, the "Arbitrary" method was more biased and less accurate than any clustering based methods when there were only two strata (Fig. 3.5 and 6, e,f,g,h).

The effect of data quantity and zero inflation

Increasing the amount of data increased the overall accuracy of the indices of abundance and decreased the amount of bias in the estimate of final year relative biomass for all methods except the "Raw" method (Fig. 3.5 and 6, m,n,o,p *vs.* a,b,c,d). The overall accuracy of the abundance indices decreased with a greater proportion of zeros in the data (Fig. 3.6, q,r,s,t). The bias in final year relative biomass did not change much compared to the Base case, except for "Spatial 1" which now had a slight negative bias (-5%) (Fig. 3.5, t).

Model selection and accuracy of derived index of abundance

The model selected using AICc or BIC did not necessarily lead to more accurate abundance indices (lower MARE) compared to basing the CPUE standardization on four strata. The estimates of the abundance time-series were more accurate in 36 to 74% of the 50 simulations depending, on the scenario, model selection tool and CPUE standardization method (Fig. 3.7). Similarly, the estimates of final year relative biomass based on the models selected using AICc and BIC were less biased than those based on four strata in 38 to 72% of simulations (Fig. 3.8). Model selection based on AICc and BIC led to slightly different outcomes. The best model based

on BIC led on average to a more accurate index of abundance (6 out of 6 comparisons) than that selected using AICc (Fig. 3.7 a,b *vs.* e,f) for the "Base patch" and "Less patch" scenarios. On the other hand, model selection based on AICc led to more accurate indices of abundance (4 out of 6 comparisons) and less biased estimates of final year relative biomass (4 out of 6 comparisons) than model selection based on BIC for scenarios with shifting fishing grounds.

Petrale sole CPUE standardization

The "Spatial 0.1" and "Time" methods led to similar indices of abundance to those used in the 2013 petrale sole assessment for all four fisheries: the correlation between these indices with the results from the 2013 assessment were larger than 81% for the AICc-selected models, 91% for the BIC-selected models, and 89% for the 5 strata models (Fig. 3.9). On the other hand, the index of abundance derived from the "Spatial 1" method differed from those produced by the other methods and was sensitive to how model selection was conducted (Fig. 3.9). The index of abundance for the summer WA/OR fishery is the only one that did not change much between the use of AICc, BIC or fixed strata for "Spatial 1", while the other fisheries showed large differences in the index of abundance (Fig. 3.9).

Discussion

Which area stratification to use for CPUE standardization?

The accuracy of abundance indices can be improved by using an objective area stratification method based on spatial or time series clustering. This approach is most beneficial when the fishery has been stable spatially over time. Indeed, clustering based area stratification removed the time bias in the indices of abundance observed in the "Raw" and "Arbitrary" methods. This

trend was most likely due to the fishing dynamics where vessels targeted preferentially areas of high abundance (Hilborn et al. 1992, Ono et al. in review). Nonetheless, the proposed methodology was able to capture the underlying population structure and removed the time series bias in the indices of abundance. Additionally, the clustering based approach did not limit strata to rectangular shapes as in Ichinokawa and Brodziak (2010), but expanded the concept of strata from a contiguous "chunk" of space to fishing grounds that show a similar CPUE history, where the similarity was either based on average CPUE over time and spatial proximity of areas, or on the whole time series. Time series clustering was the most promising of the methods as it was the least sensitive to the choice of number of strata, consistently produced one of the least biased indices of abundance, and model selection most consistently improved index accuracy. However, the cluster-based area stratification approach performed poorer with increasing changes in fishing ground over time (Fig. 3.A1). The arbitrary area stratification led to the least biased abundance index of all as long as there were enough spatial strata to cover the shifts in fishing grounds i.e. be sure that the grounds where changes happened (effort moved in or moved out) are defined as their own strata. Changes in fishing grounds could be detected in actual applications by tracking the location of effort range centroids for example (Pinsky et al. 2013).

To summarize, an arbitrary area stratification might be sufficient for CPUE standardization if there is evidence for changes in fishing grounds over time and if there are enough spatial strata to capture these changes. On the other hand, the clustering-based area stratification method (especially the time series based variant) is most appropriate if the fishery has been spatially stable over time (no shifts in fishing grounds).

How should the number of strata in CPUE standardization be selected?

Based on the simulation study, both AICc and BIC are potentially helpful in selecting the number of strata for a CPUE standardization. However, there is also about a 50% chance that the index selected using AICc and BIC is less accurate and more biased than that based on an ad-hoc choice of strata number. We therefore recommend examining the sensitivity of the results of a CPUE standardization to the method used to select the number of spatial strata i.e., ad-hoc *vs.* using goodness of fit criteria such as AICc and BIC. An appropriate way to handle cases in which the results differ among standardization methods would be to take the average index of abundance among methods and inflate the confidence interval around it to account for model uncertainty.

Indices of abundance for the U.S. west coast petrale sole

The indices of abundance based on "Spatial 0.1" and "Time" methods resembled those from the 2013 petrale sole assessment for all fisheries. However, there were a few noticeable differences between the alternative indices and the 2013 indices. For example, the indexes differed markedly after 2003 (WA/OR) and 2002 (CA). While it is impossible to know which index is more "correct", the simulation exercise showed that the cluster-based method (especially the "Time" variant) generally performed best if the fishery did not change spatially over time. However, 2002/2003 corresponds to when various area closures were implemented along the U.S. west coast to protect several overfished rockfish species (e.g. the yelloweye rockfish conservation area and rockfish conservation area; Haltuch et al. 2013). This could have shifted the fishing grounds for the summer fishery as vessels had to avoid fishing in certain depth zones. However, these area closures had a minor impact to the winter fishery as it mainly targeted spawning

aggregations found in waters deeper than the rockfish conservation areas. The index of abundance derived from clustering-based area stratification might therefore be more accurate than the 2013 index (which used arbitrary area stratification) for the winter fishery. Finally, the "Spatial 1" approach produced very different indices than the other methods. However, based on the simulation testing, these indices should be ignored as the simulation testing showed that this method was more sensitive than the other two clustering-based methods.

Limits and future research

CPUE standardization is an important component of a stock assessment and a standardized CPUE index is often the major source of data to assess the stock status in commercial or recreational fisheries (Hilborn and Walters 1992). This study investigated a way to improve the accuracy of indices of abundance through the use of more objective area stratification. However, there are other aspects of CPUE standardization that need additional research as CPUE is a rich but complex data type influenced by interactions between the environment, fishery and fish biology (Maunder et al. 2006). For example, future studies should investigate the utility of non-parametric models such as boosted regression tree (Elith et al. 2008) or random forest (Breiman et al. 2001, Cutler et al. 2007, Prasad et al. 2006) in lieu of more traditional parametric models such as GLM(M) and GAM(M) for CPUE standardization. These non-parametric models have been used increasingly in ecology to model species distribution (Elith et al. 2008) and it might be worth investigating their performance for CPUE standardization. Furthermore, the use of spatio-temporal models is also expanding in ecological studies (Dormann et al. 2007, Ono et al. in review, Shelton et al. in review) and the use of these models for CPUE standardization should be explored. Finally, CPUE standardization might benefit from an extended analysis on model

selection criteria and their relationship to the accuracy of abundance indices (expanding on the study of Shono et al. 2005). Model selection is now a necessary step in CPUE standardization but our study showed that the best model based on AICc or BIC does not guarantee a more accurate index of abundance.

Tables

Table 3.1: Table of model specifications

Parameters	Values
Depth distribution (exponential covariance function)	
Variance (τ^2)	200
Range (ξ)	10
Trend/patchiness (α)	Less patchy (0), Base (5)
Standardized depth range	[0-300]
Fish habitat preference	
Mean depth preference (μ)	140
Variance of depth preference on log scale (σ^2)	0.29
Movement range (λ)	Base (0.4), Range shift (3)
Center of distribution along the coast	20
Variance in distribution along the coast	Base (10000), Range shift (15)
Population parameters	
Total carrying capacity (K)*	100000
Intrinsic rate of growth (r)*	0.15 yr^{-1}
Fish mobility	No, Yes
Fleet dynamics parameters	
Number of vessels (n_v)	20
Mean catchability ($\bar{q}$)	0.1
Coefficient of variation of catchability (CV_q)	0.2
Catch zero inflation parameter (ϕ)	Base (0.1), More zeros (0.15)
Ending year fishing effort ($\overline{E_T}$)	Base (250), More data (400)

*: this value is an average based on 22 West Coast groundfish species

Figures

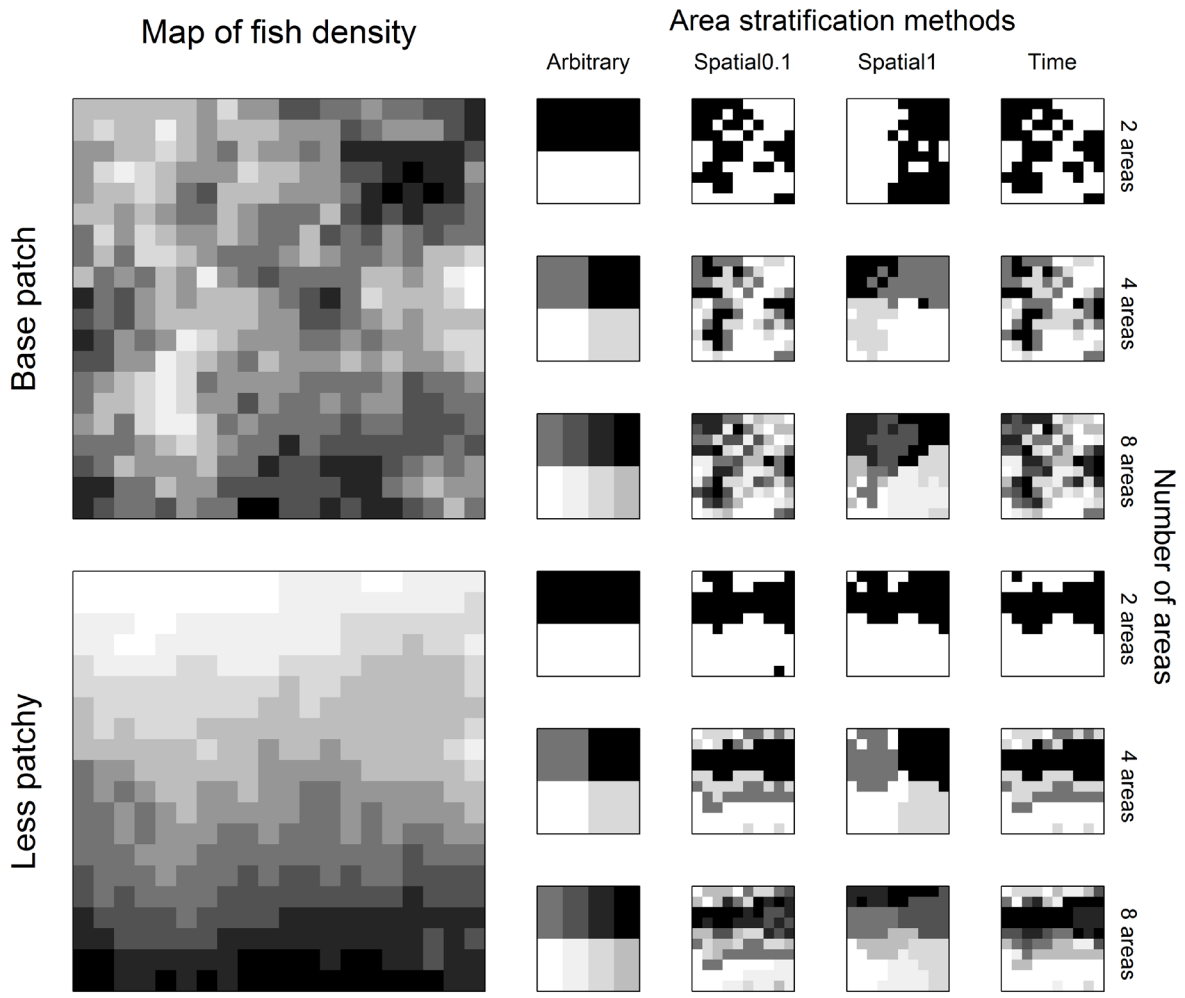

Figure 3.1: Example of fish density maps ("Base patch" and "Less patchy"), with the corresponding area stratification based on four methods ("Arbitrary", "Spatial 0.1", "Spatial 1", and "Time").

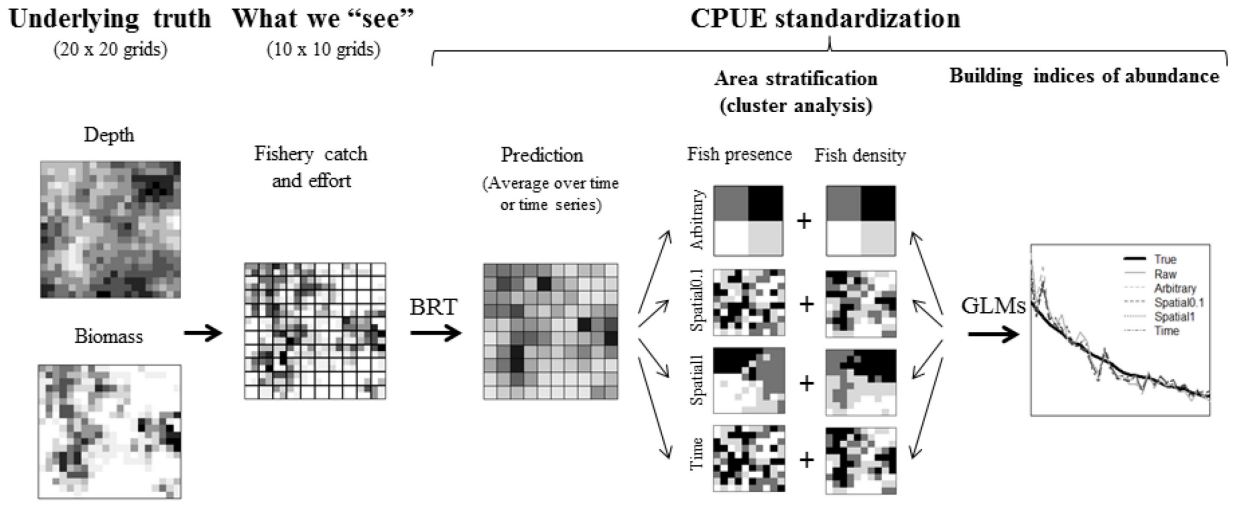

Figure 3.2: Simulation-estimation steps. Boosted regression tree (BRT) is applied to the catch and effort data to create a predicted map of fish density and fish presence. The maps are then used to stratify areas based on an ad-hoc area stratification method or based on cluster analysis using partitioning around medoids. The derived strata are used as a covariate in the generalized linear model (GLM) to standardize the catch per unit effort (CPUE) data which is used to create an index of abundance.

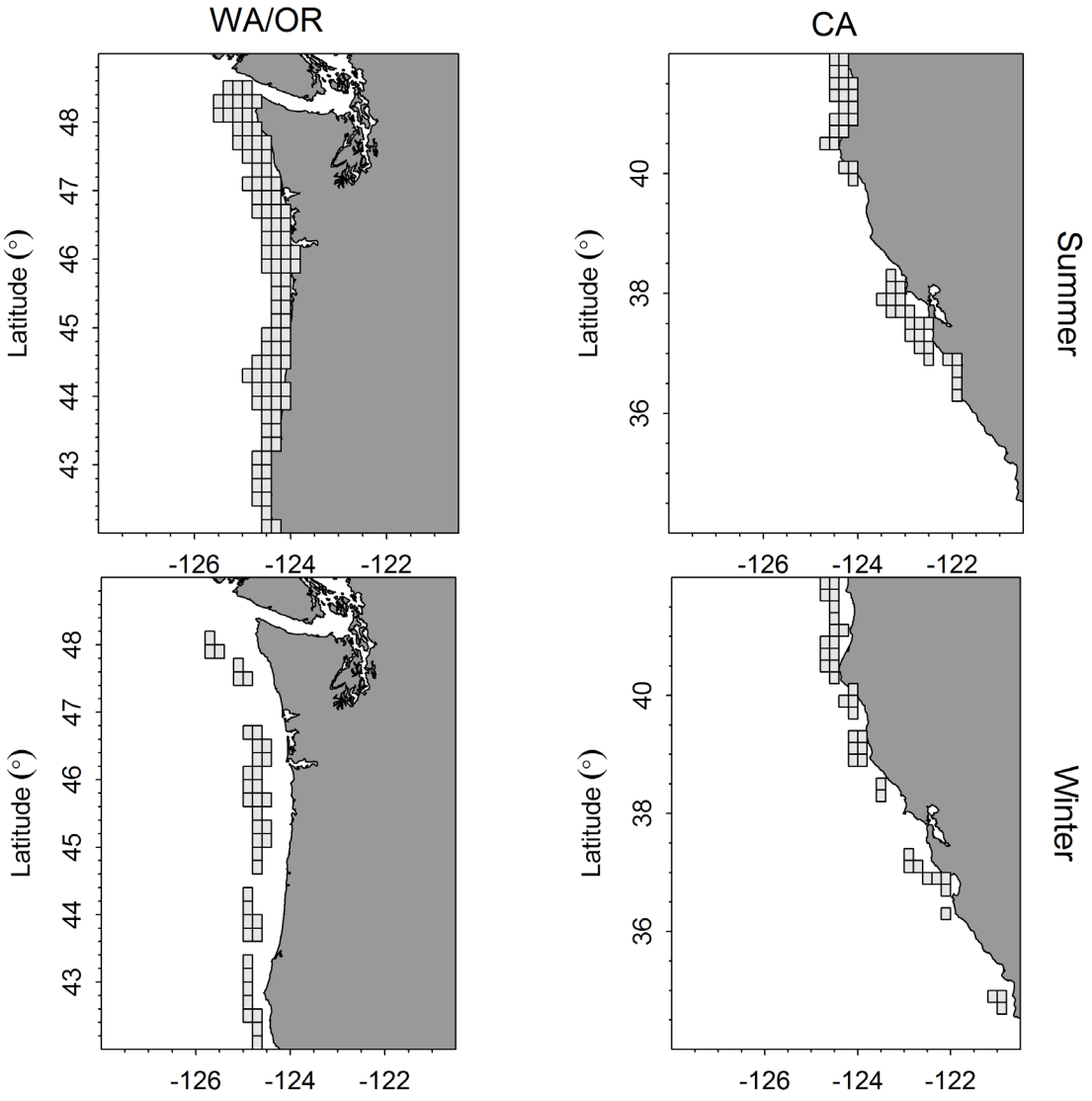

Figure 3.3: Grid system used to perform the spatial stratification of the petrale sole data set (1987-2009).

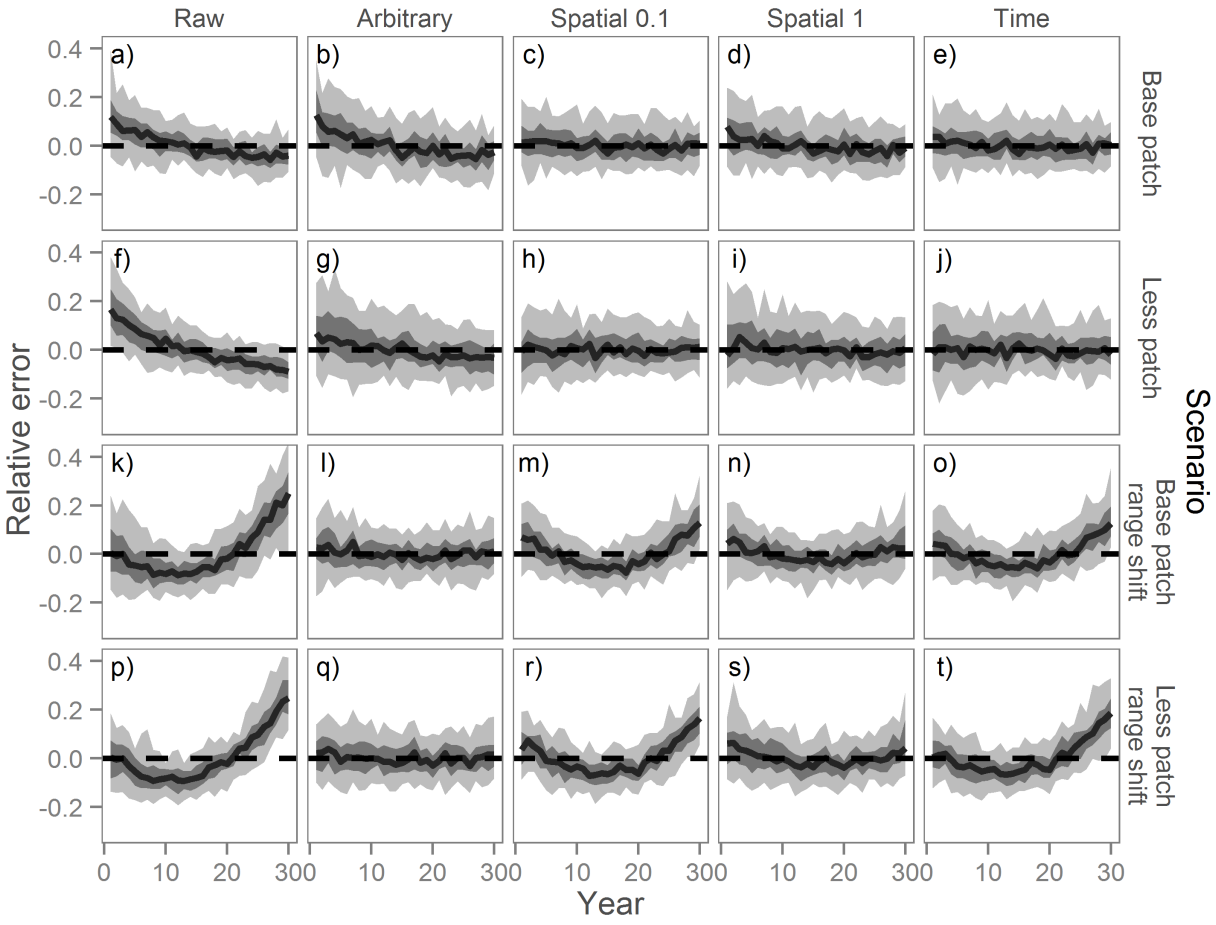

Figure 3.4: Time series of relative error in the index of abundance for five area stratification methods (Raw, Arbitrary, Spatial0.1, Spatial1, and Time) and four scenarios (Base patch, Less patch, Base patch range shift, Less patch range shift) for the Base case (= 4 areas).

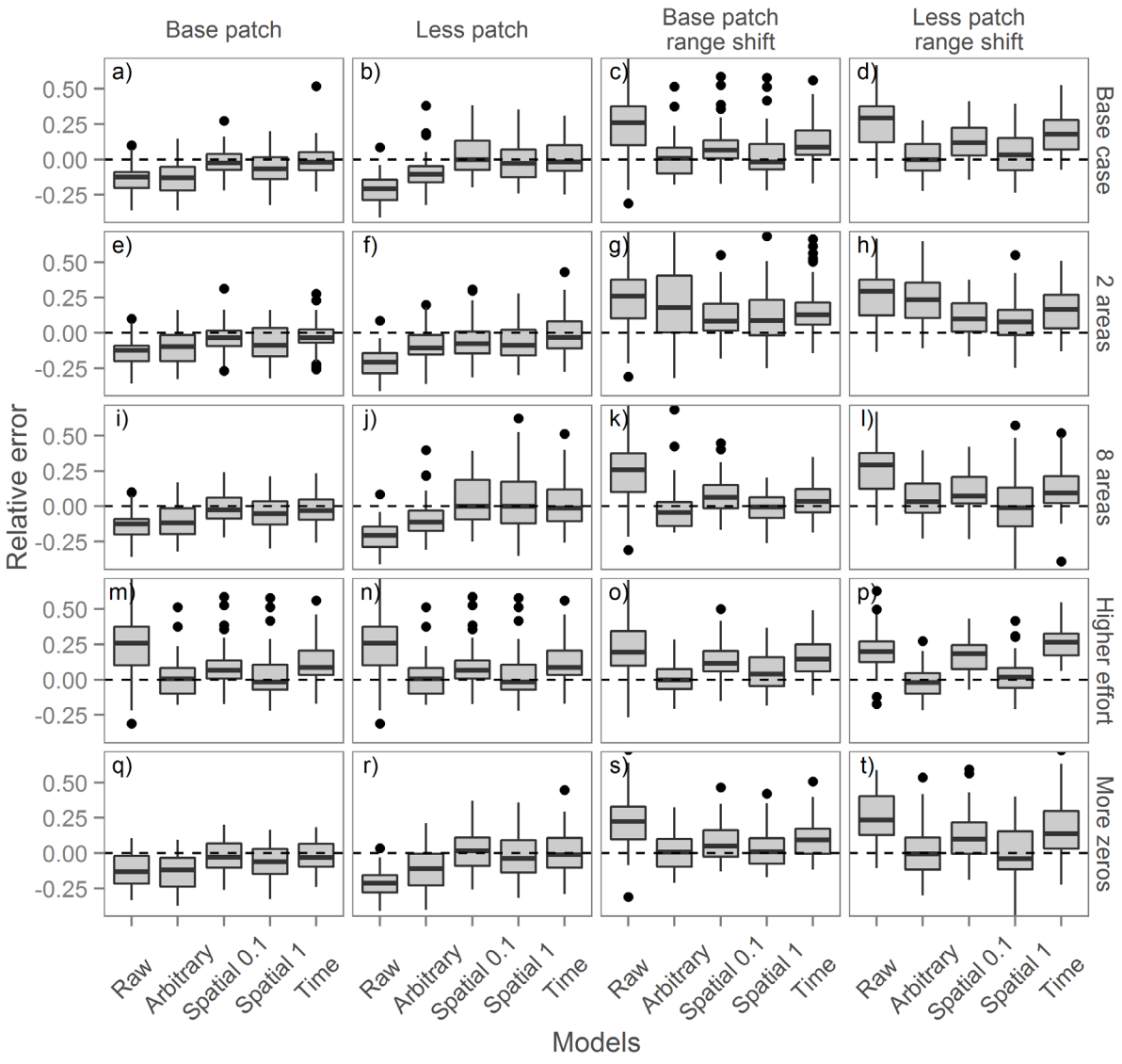

Figure 3.5: Relative error in final year relative biomass for five area stratification methods (Raw, Arbitrary, Spatial0.1, Spatial1, and Time), four scenarios (Base patch, Less patch, Base patch range shift and Less patch range shift) and base case (= 4 spatial strata) + four sensitivity tests (2 areas, 8 areas, More data, and More zeros).

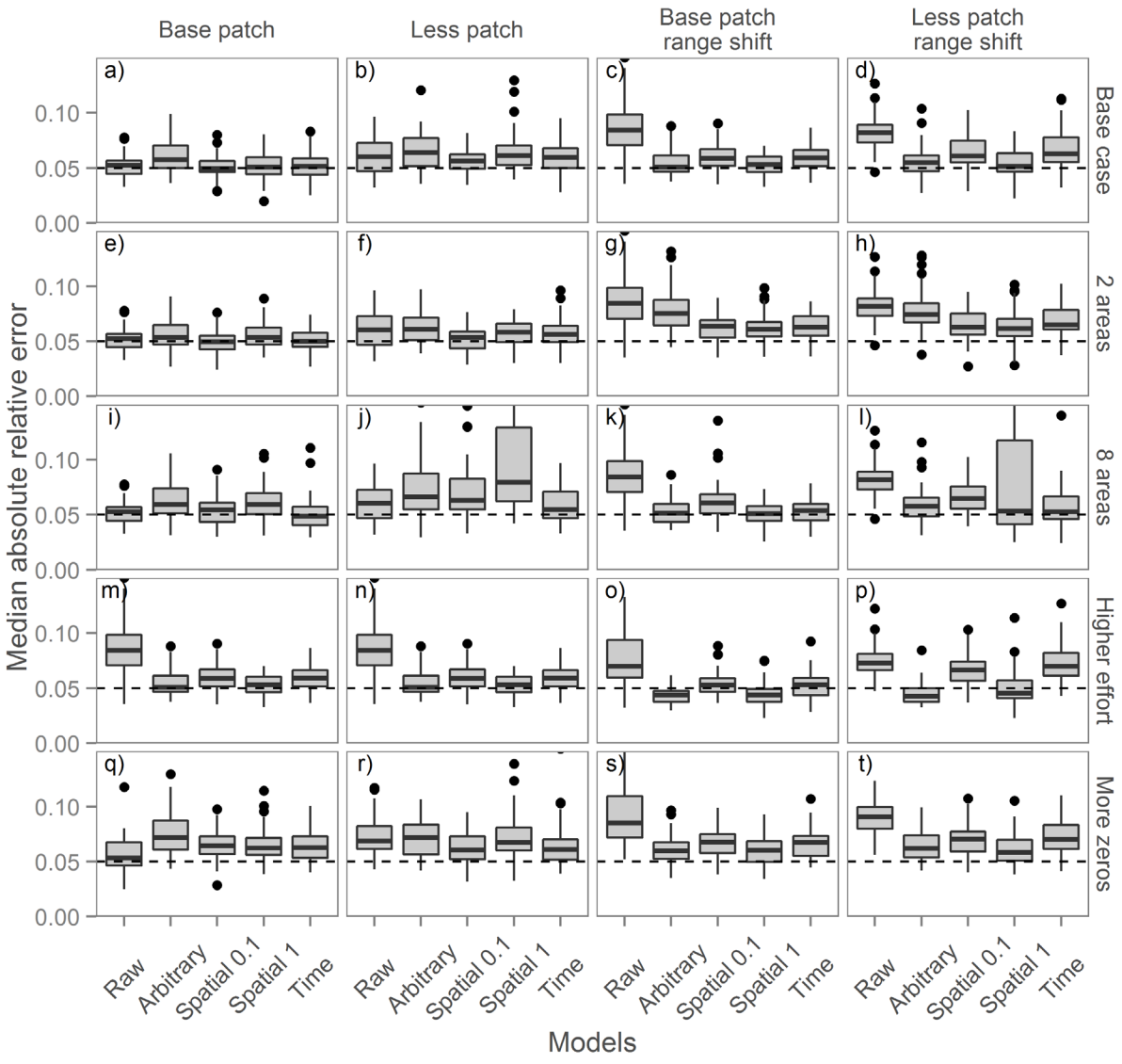

Figure 3.6: Median absolute relative errors of the time series of abundance indices for five area stratification methods (Raw, Arbitrary, Spatial0.1, Spatial1, and Time), four scenarios (Base patch, Less patch, Base patch range shift and Less patch range shift) and base case (= 4 spatial strata) + four sensitivity tests (2 areas, 8 areas, More data, and More zeros). The horizontal line at 0.05 is to facilitate case comparison.

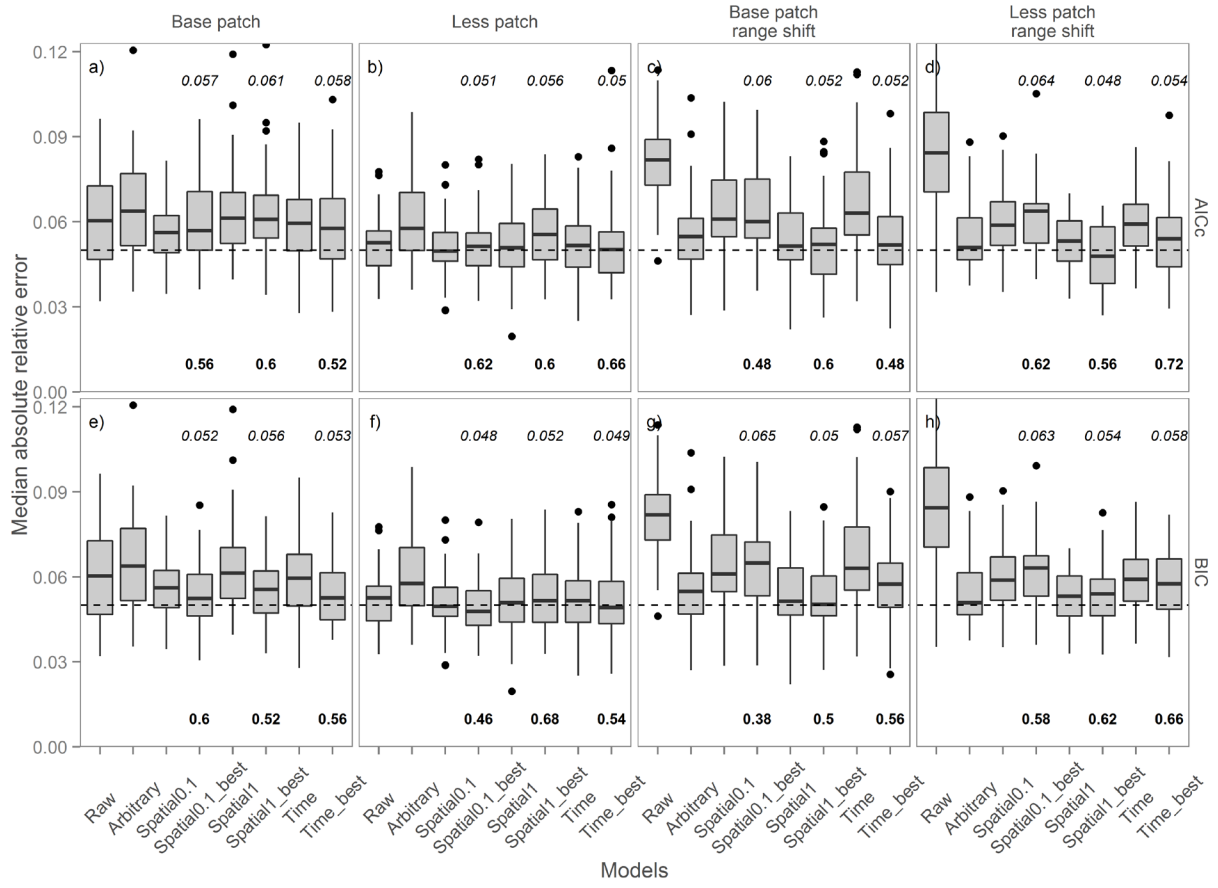

Figure 3.7: Median absolute relative error (MARE) of the time series estimate of abundance for eight area stratification methods (Raw, Arbitrary, Spatial0.1, Spatial0.1_best, Spatial1, Spatial1_best, Time, and Time_best), four scenarios (Base patch, Less patch, Base patch range shift and Less patch range shift) and two model selection methods (AICc and BIC) for the Base case (= 4 spatial strata). Spatial0.1_best, Spatial1_best, and Time_best are derived from models where the optimal number of spatial strata was chosen for the binomial and lognormal components (independently) using the associated metric. The numbers in italics above some plots are the median of the MARE and the numbers under some boxplots indicate the proportion of times the best model led to a lower MARE than the fixed strata (4 strata) counterpart. For example, for the "Base patch" scenario and using AICc, "Spatial0.1_best" had a MARE of 0.057 and led to an index of abundance that was more accurate than "Spatial0.1" in 46% of the simulations. A horizontal line is drawn at 0.05 to facilitate cases comparison.

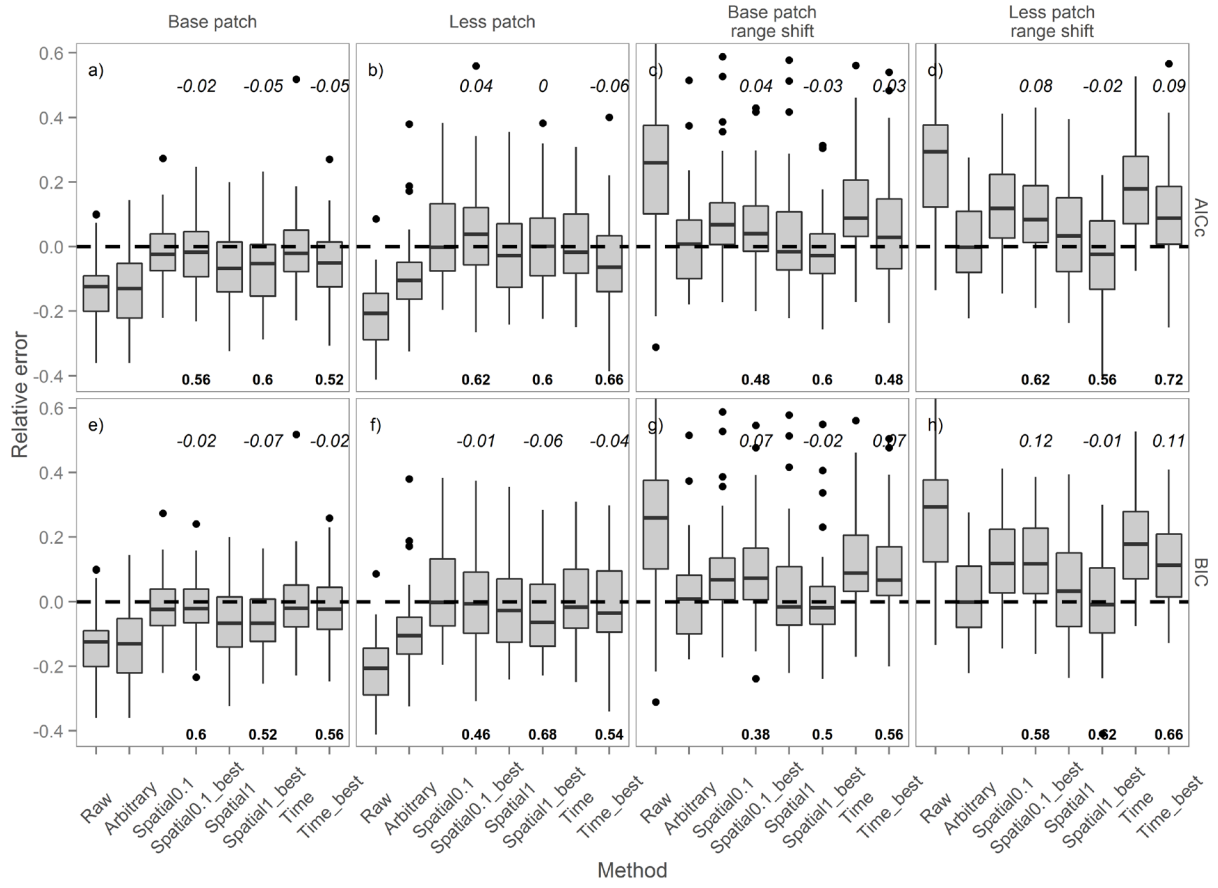

Figure 3.8: Relative error in final year relative biomass for eight area stratification methods (Raw, Arbitrary, Spatial0.1, Spatial0.1_best, Spatial1, Spatial1_best, Time, and Time_best), four scenarios (Base patch, Less patch, Base patch range shift and Less patch range shift) and two model selection methods (AICc and BIC) for the Base case (= 4 strata). Spatial0.1_best, Spatial1_best, and Time_best are derived from models where the optimal number of spatial strata was chosen for the binomial and lognormal components (independently) using the associated metric. The numbers in italics above some plots are the median of the relative error (MRE) and the numbers under some boxplots indicate the proportion of time the best model was less biased (in absolute value) than the fixed strata (4 strata) counterpart. For example, for the "Base patch" scenario and using AICc, "Spatial0.1_best" had a MRE of -0.02 and led to an estimate of final year relative abundance that was less biased than "Spatial0.1" in 56% of the simulations.

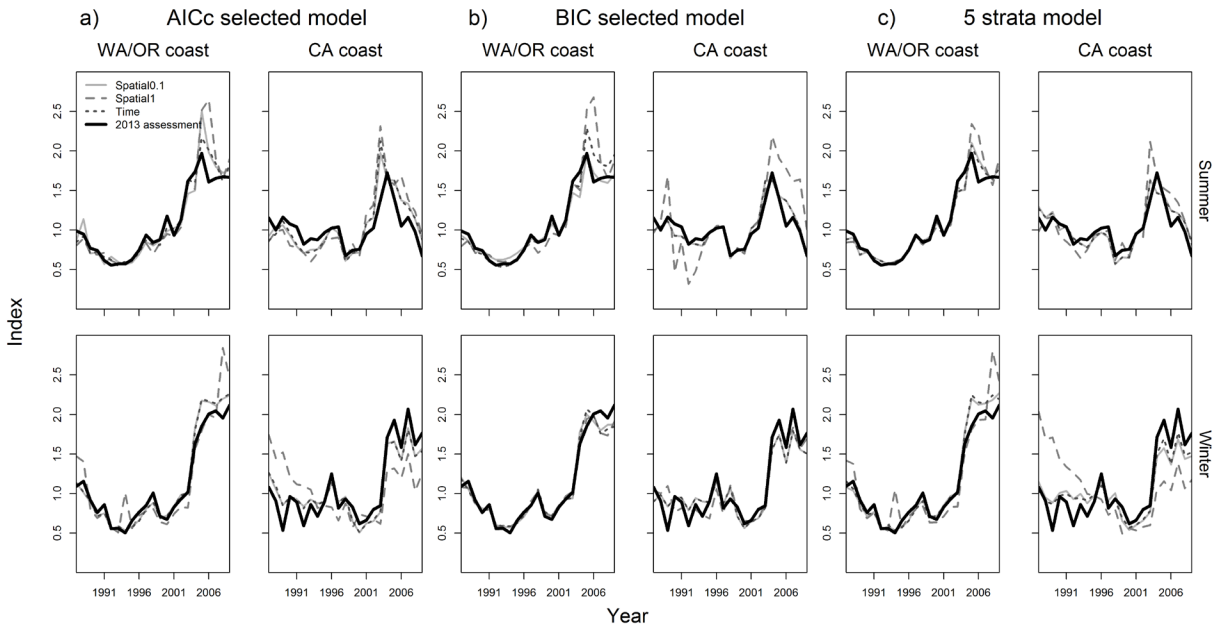

Figure 3.9: Indices of abundance for the petrale sole fishery. Indices are calculated for the summer and winter fisheries, and for the WA/OR and CA regions. For each fishery, the indices of abundance from the 2013 assessment are compared with the three clustering-based methods. Sensitivity of the results to the model selection approach is examined between a) AICc *vs*. b) BIC *vs.* c) 5 strata model.

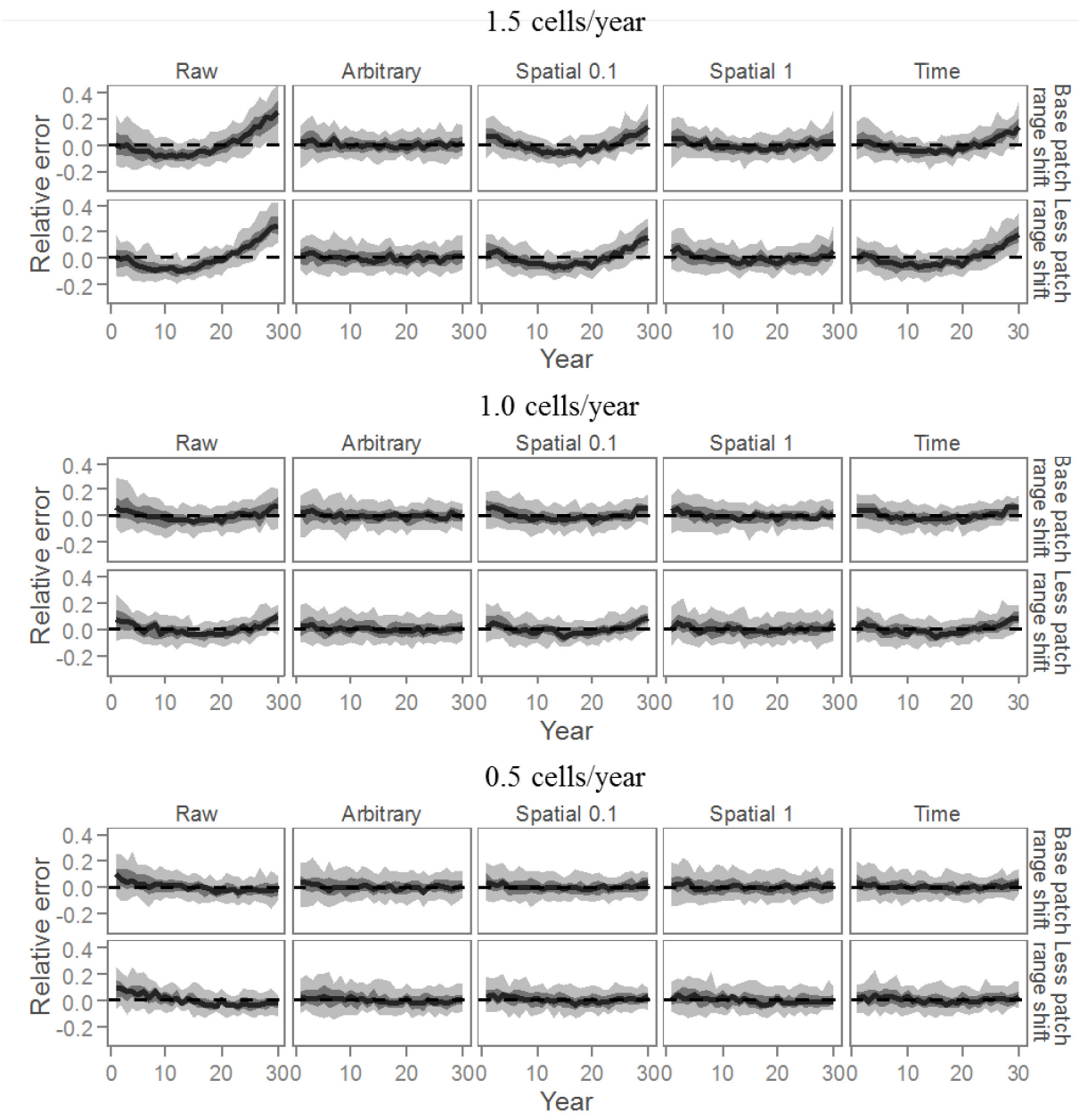

Figure A3.1: Influence of fish migration rate on the bias in the index of abundance: cases when fish center of distribution shifts by 1.5, 1.0, 0.5cells/year.

Chapter 4 - How do populations respond to fishing? A spatio-temporal investigation of population seasonal dynamics.

Abstract

Species distribution modeling (SDM) is an important statistical tool for obtaining ecological insight into species-habitat relationships, and providing advice for natural resource management. Many SDMs have been developed over the past decades, with a focus on space- and more recently, time-dependence. However, most of these studies have been on terrestrial species and applications to marine species have been limited. In this study, we used three large spatio-temporal data sources (habitat maps, survey-based fish density estimates and fishery catch data) and a novel spatio-temporal model to study how the distribution of fishing effort may affect the seasonal dynamics of a commercially important fish species (Pacific Dover sole, *Microstomus pacificus*) commonly found off the U.S. West coast. Dover sole seasonal dynamics were primarily driven by movement and the effect of fishing could not be detected. They showed a large scale change in seasonal and annual distribution but also displayed a consistent seasonal flux of biomass across years. They appeared to move inshore or to deeper waters during late summer/early fall, leaving the mid-depth zones. They also consistently congregated or left some areas along the coast during the same time period. Additionally, results suggest that the population might be moving outside the range of the survey area during the survey season. The availability of appropriate data and spatio-temporal modeling software should facilitate extending this work to many other species – particularly those in marine ecosystems – and identifying the role of growth, recruitment, movement and fishing on spatial patterns of species distribution in marine systems.

Introduction

A central aim in conservation is to preserve important habitats for organisms to ensure species and population persistence in the face of anthropogenic threats (U.S., Public Law 93–205, Kareiva et al. 2008). Species distribution models have proven vital as tools for expanding our understanding of species habitat associations and for conservation planning and resource management (Guisan and Thuiller 2005, Elith and Leathwick 2009). Many methods have been developed over the past several decades to model the distribution of species in relation to habitat. Statistical techniques include generalized linear models (GLMs), generalized additive models (GAMs), quantile regression, artificial neural networks, regression trees, and genetic algorithms (see reviews by Guisan and Thuiller 2005, Elith and Leathwick 2009). To date, however, many of these models fail to consider space and time dependence (Dormann 2007). Being able to explicitly account for spatio-temporal dependence is crucial for understanding current and future threats from anthropogenic forces, and for reducing the risks of erroneous results as many exogenous (e.g. climate, habitat) and endogenous (e.g. dispersal, predation, breeding) drivers of species distributions are likely to vary through time and space (Legendre 1993, Dormann 2007, Elith and Leathwick 2009, Beale et al. 2010, Saas and Gosselin 2014).

Despite the importance of spatial and temporal dependence in the field of environmental and biological science, the use of spatio-temporal models has remained limited due to their presumed complexity and possible computation burden. The number of numerical operations increases quickly as the dimensionality of models in space and time increases, rendering the computation tedious and sometimes infeasible for large datasets. Nonetheless, spatio-temporal modeling has

become more feasible and accessible through the availability of several statistical software packages in the last decade, owing to the increasing computational power and advances in numerical techniques (e.g. R, WinBUGS, Matlab, SAS). Some (but not all) of the methods that have been developed to deal with spatio/temporal dependence include dimension reduction (e.g. covariance tapering (Furrer et al. 2006), or the predictive approach (Banerjee et al. 2008, Latimer et al. 2009, Finley et al. 2009)), numerical approximation to the likelihood (e.g. the spectral method (Fuentes 2007)), or the use of Markov random fields to approximate the spatial process (Rue and Martino 2007). The use of Markov random fields has been extended to develop an analytical solution to the marginal posterior distributions using the Integrated Nested Laplace Approximation (Rue et al. 2009). Several biological, environmental and natural resource studies have used these techniques to model the distribution of disease (e.g. Schrödle and Held 2011), weather (e.g. Finley et al. 2012), heritability (e.g. Holand et al. 2013), animals and plants (e.g. Latimer et al. 2009), at a variety of geographical and temporal scales.

In marine ecosystems, many factors could potentially affect the distribution of fish over time and space (Whittaker et al. 1973). Fish may have a specific habitat preference (that can vary with life stage). The mobility of a species can also vary with ontogeny and scale (sedentary fish *vs* mobile species with diurnal movement, ontogenetic movement, or seasonal migration), and they interact with their prey and predators. Humans are one of the central predators in marine ecosystems and can alter fish communities substantially (e.g. Worm et al. 2009). Moreover, fishing does not occur randomly in space and time as fishers choose the location and timing of fishing based on their knowledge and the rules that regulate fisheries (Holland and Sutinen 2000, Branch et al. 2006a, Salas and Gaetner 2004, van Putten et al. 2012). As a consequence, marine species

distributions can potentially change over relative short periods of time, with the change in distribution reflecting the joint effect of fishing activity, environment, and species life history.

Here, to document spatial and temporal changes in the distribution of an important marine species, we integrate three large scale spatio-temporal data sources: detailed benthic habitat data from the continental shelf and slope off the U.S. West coast, fish density estimates from an extensive fishery-independent research survey, and commercial fishing catch data. We take the example of Pacific Dover sole (*Microstomus pacificus*), an abundant and commercially-important species off the U.S. West coast, to illustrate the applicability of our methodology to study the seasonal dynamics of marine species. We make use of the unique design of the research survey - parallel surveys conducted three months apart in the summer and fall - to address how the distribution of fishing effort may affect the distribution and biomass of Dover sole within a year. We document changes in spatial distribution over time but also reveal geographical regions with consistent patterns in seasonal population dynamics. We then link the observed pattern in Dover biomass change to potential environmental and biological processes.

Material and methods

Motivational case study: Dover sole population of the U.S. West coast

Dover sole is a commercially-important flatfish species off the U.S. West coast that has been exploited since the early 20th century (Hicks and Wetzel 2011). The annual catch over the last fifty years averages 14,000 tons (~2% exploitation rate), and the landed value of the catch was estimated at over $6.5million in 2012. The species is long-lived (max. age ~60 years) and widely distributed from Alaska to southern California. It is commonly found on soft bottom in waters ranging from 37-1500m, and individual Dover sole tend to migrate to deeper waters in winter

(between November to March), during the spawning season (Hagerman 1952) and as they mature and age (Jacobson et al 2001). Summer is the main feeding/growing season for Dover sole off the U.S. West coast.

NOAA's Northwest Fisheries Science Center conducted a series of fishery-independent surveys using bottom trawling gear over 2004-present (we only use data from 2004-2011in this study) to inter alia assess the spatiotemporal distribution of Dover sole and other co-occurring species (Bradburn et al. 2011). The survey involves two 'passes' each year between mid-May and late October: the first 'pass' occurs between mid-May to August while the second 'pass' lasts from August to October. Approximately 700 hauls are conducted each year. The same fishing gear (net) is towed through the water for 15 minutes, and the number and biomass of all fish present are recorded. Benthic habitat information - such as average depth, bottom water temperature, sediment size, and distance to nearest rock outcrops - and spatial location are also recorded. Detailed descriptions of the sampling design, gear, and protocols used for this survey are found in Keller et al. (2012).

In addition to the spatially-referenced survey data, we also used nearly 200,000 spatially-referenced commercial Dover sole catch records by fishing vessels. While it is mandatory to report all trawl fishing events, the fishing vessel logbook data are incomplete and the sum of the reported catch in each year averages about 90% of the total catch. We therefore assumed that these missing catches in the logbook data were missing-at-random, and they were imputed based on the expected catch probabilities from the logbook data on a 2x2 km grid (a resolution small enough to be able to detect potential seasonal dynamics of the species). Catch data at the tow level were linearly distributed to each grid based on the portion of commercial vessel tracks

intersecting each of the 2x2km grids. As we only had the start and end coordinates of each fishing event, we interpolated the vessel track to the segment joining these two locations.

General approach

The objective of this study is to examine how Dover sole distribution changed during the summer months of 2004-2011 in response to fishing and habitat characteristics, and to identify potential causative mechanisms. In other words, we ask whether the fall research vessel survey (or second pass) shows any sign of a decrease from the spring survey (first pass) given the catches, and whether any such changes can be attributed to factors such as growth, movement or recruitment.

To study the problem, we need to i) determine the spatial distribution of the species by year and survey pass by fitting a statistical model to the survey data, ii) use the best model from step i) to predict the biomass of Dover sole along the coast for each pass and year, iii) examine the net change in biomass between the survey passes taking the catch into account, and iv) detect patterns of variation in the net change in biomass and associate them with environmental and/or biological factors.

Estimating population biomass at each survey pass

Description of the spatio-temporal regression model

We fitted a spatio-temporal generalized linear model to the survey data to create a predictive map of population biomass along the U.S. West coast for each survey pass and year. We modeled the species distribution in two stages: first, a spatio-temporal model was fitted to explain the variation in Dover sole presence/absence (based on Bernoulli distribution); and then

a model for positive data (based on lognormal distribution) was fitted to explain changes in Dover sole density given that a least one fish was observed. We used this modeling framework as survey data comprised a large portion of zeros and we expected different variables to be important to each stage of the model. These two pieces were assumed to be independent, and the general framework is often referred as a delta or hurdle model in ecology (Zuur et al. 2009). We constructed our model in a Bayesian framework (see Table 4.1 for prior specification). Separate models were created for each survey pass as the objective of the study was to determine changes in population distribution between the two survey passes. We defined the random variable $Y_p(s_i, t)$ as the Dover sole density (kg/km^2) at location s_i, time t and survey pass p. The notation P stands for probability.

(4.1) $$P(y_i = 0) = 1 - \pi_p(s_i,\ t)$$

(4.2) $$P(Y_p(s_i,\ t) = y_i \mid y_i > 0) = \frac{1}{\sqrt{2\pi}\sigma_p y_i} e^{-\frac{1}{2\sigma_p^2}(\ln(y_i) - \mu_p(s_i,\ t))^2}$$

where $\pi_p(s_i, t)$ is the probability of catching at least one fish at location s_i, time t, and pass p, $\mu_p(s_i, t)$ is the mean Dover sole density on the log-scale and σ_p^2 is the measurement error variance. We used a logit-link function to model the probability of fish occurrence.

(4.3) $$\log it(\pi_p(s_i,t)) = x_{1,p}(s_i,t)\beta_{1,p} + \varpi_{1,p,t}(s_i,t)$$

(4.4) $$\mu(s_i,t) = x_{2,p}(s_i,t)\beta_{2,p} + \varpi_{2,p,t}(s_i,t)$$

where $\boldsymbol{x_{1,p}(s_i,t)}$and $\boldsymbol{x_{2,p}(s_i,t)}$ are the vectors of covariates for haul i, time t, and pass p, $\boldsymbol{\beta_{1,p}}$ and $\boldsymbol{\beta_{2,p}}$ are the regression coefficients (shared across years for each pass p for continuous variables such

as the depth, temperature and sediment size; we assumed that fish preference for these habitat variables doesn't change between years for each pass p during this short study period), and $\boldsymbol{w_{1,p,t}}$ and $\boldsymbol{w_{2,p,t}}$ are the spatial fields for year t and pass p. We modeled $\boldsymbol{w_{p,t}}$ as a smooth spatial surface, $\boldsymbol{w_{p,t}} \sim MVN(0, \boldsymbol{\Sigma_{p,t}} = \tau_p^2 \boldsymbol{C_{p,t}}(h))$ where τ_p^2 is the spatial variance and $C_{p,t}(h)$ is the isotopic spatial correlation function that depends on location s_i and s_j only through the Euclidian distance $h=||s_i - s_j||$ and defined by the Matérn function

$$(4.5) \quad C_{p,t}(h) = \frac{1}{\Gamma(\nu)2^{\nu-1}}(\kappa h)^{\nu} K_{\nu}(\kappa h)$$

where K_ν is the modified Bessel function of second kind and with order ν=0.5 and κ>0 is the scaling parameter related to the range (distance at which the spatial correlation becomes close to zero). We constructed a block diagonal covariance matrix among years to avoid conflating spatial and temporal components of variation to account for the possibility for inter-annual changes in species distribution with a distinct clustering pattern for each year (as in Shelton et al. in review).

$$(4.6) \quad \sum_p = \begin{bmatrix} \sum_{p,2004} & 0 & \cdots & 0 \\ 0 & \sum_{p,2005} & \ddots & 0 \\ \vdots & \ddots & \ddots & 0 \\ 0 & 0 & 0 & \sum_{p,2011} \end{bmatrix}$$

Model fitting was performed using the R package INLA (Rue et al. 2013) and readers are referred to Rue et al. (2009) and Cameletti et al. (2013) for details about the underlying theory and computational approaches for spatio-temporal models such as INLA. Briefly, INLA is a computational approach to statistical inference for latent Gaussian Markov Random Field (GMRF) models that bypasses the use of MCMC to compute the marginal posterior distribution

of the latent field and hyperparameters. This method uses instead a combination of Laplace approximation and numerical integration to approximate the posterior marginals. We used the INLA implementation of a stochastic partial differential equation (SPDE) to the Gaussian random field. This SPDE approach approximates the inverse of the spatial covariance matrix $\Sigma_{p,t}$ using three sparse matrices, as calculated using a finite element analysis applied to a partial difference equation evaluated over the population's spatial domain (Lindgren et al. 2011).

Explanatory variables

We used existing geospatial data layers from the Essential Fish Habitat (EFH) Phase 1 report (NMFS 2013), which included depth, sediment grain size, bottom temperature, and distance to nearest rocky habitat. Distance to rock was calculated using ArcGIS software to calculate the distance from each of the trawl survey sites to the nearest rock habitat patch. Rock was defined as any grid cell in the substrate type data layer with a value of 1 or 4. We only used rocky patches greater than 1 ha in area.

Model selection

Model selection was conducted to decide which of the explanatory variables: log(depth), $\log^2$(depth), distance to nearest rocky habitat, sediment grain size, (sediment grain size)^2, temperature, and (temperature)^2 to include in the models. Model selection was based on the deviance information criteria (DIC) (Spiegelhalter et al. 2002) and the mean logarithmic score (Gneiting and Raftery 2007, Krnjajić et al. 2008); two metrics that are readily available from the INLA model output. In either case, the lower the metric, the more preferred the model. The DIC was directly obtained from the model output while the logarithmic score (LS) was calculated as the negative log of the conditional predictive ordinate (CPO). The CPO corresponds to the

position of the observed value y_i within the leave-one-out cross-validatory posterior predictive distribution evaluated at the observed value y_i. Gneiting and Raftery (2007) proposed ranking competing models based on their mean logarithmic scores. A paired permutation test based on the observation-level score provided a convenient approach to test if one model's mean logarithmic score was significantly different than another one.

$$\overline{LS} = \frac{\sum_{i=1}^{n_{obs}} -\log(CPO_i)}{n_{obs}} \quad (4.7)$$

where n_{obs} corresponds to the number of data points.

Moving up from density to estimate of population biomass along the coast

We generated a gridded (2x2 km) coast-wide representation of the model spatial domain using ArcGIS software. The U.S./Canada border and U.S./Mexico border marked the north and south extents, respectively, while the shoreline and seaward boundaries were defined by a vector shoreline geospatial data layer (NOAA 2001), and the 1,600 m isobath (NOAA 2003), respectively. We overlaid this gridded domain with the four habitat covariates geospatial data layers and calculated the corresponding values for each of the grid cells. Categorical covariates were summarized by the proportion, and continuous covariates were expressed as an area weighted mean (AWM) for each of the grid cells.

We computed the posterior predictive distribution for Dover sole biomass at each pass and year once the best models (one for the presence/absence and one for the positive catch data) for each pass was chosen. We generated a predictive distribution for each 2x2km grid along the coast, $I_p(s,t)$. This corresponded to a total of 38,047 grid cells. The posterior predictive distribution was created based on the product of the probability distribution of fish presence at each grid and the

probability distribution of fish biomass assuming that fish were present. The predictive distribution reflected the biomass susceptible to the trawl gear, not the entire population, because the bottom trawl does not catch fish of different sizes equally (i.e. fish selectivity varied with length), and fish population size structure was unknown. We therefore re-scaled the whole distribution to match the scale of the exploitable population size estimated in the latest Dover sole assessment (Hicks and Wetzel 2011). To do so, the scaling coefficient q (also called catchability coefficient in the fisheries literature; Maunder and Punt 2004) was calculated as the average ratio (between 2004 and 2011) between the average of the total population density estimated from passes 1 and 2 in year t and the population biomass in year t estimated in the actual assessment, $Biomass_t^{assesssment}$.

$$(4.8) \quad q = \frac{1}{8}\sum_{t=2004}^{2011}\left(\frac{\frac{1}{2}\sum_{p=1}^{2}\sum_{s=1}^{N} I_p(s,t)}{Biomass_t^{assessment}}\right)$$

Finally, Dover sole biomass at location s, $B_p(s,t)$, for each pass p and year t, was determined by multiplying the biomass index by the scaling coefficient q.

$$(4.9) \quad B_p(s,t) = qI_p(s,t)$$

Calculating the net change in biomass (NCB) between the two survey passes

There is a gap of roughly two and a half months between the two survey passes within a year, During that time, biomass at a given location can change due to fishing, growth, death, recruitment and movement. These factors were agglomerated in this study as a single factor referred to as net change in biomass, NCB. NCB can therefore change in time and space, and the

examination of its pattern could reveal areas of particular interest (area with consistently high or low NCB). NCB can be calculated for two time periods: i) between pass 1 and pass 2 of the same year, $NCB_1(s,t)$, or ii) between pass 2 or year *t* and pass 1 of the year *t+1*, $NCB_2(s,t)$. If the pattern in NCB_2 is exactly the opposite of that of NCB_1, seasonal movement is probably the main reason behind the observed pattern in NCB. We would not expect NCB_2 to mirror NCB_1 as winter patterns of growth and recruitment are not expected to be related to the summer pattern if growth or recruitment is the main factor driving the spatial patterns,.

$$\left.\begin{array}{c} NCB_1(s,t) = B_{p=2}(s,t) - B_{p=1}(s,t) + Catch_1(s,t) \\ NCB_2(s,t) = B_{p=1}(s,t+1) - B_{p=2}(s,t) + Catch_2(s,t) \end{array}\right\} = \text{(growth-death+recruitment+movement)} \quad (4.10)$$

where $Catch_1$ and $Catch_2$ are the total fishery removals from grid *s* between pass 1 and 2 of the same year or pass 2 of year *t* and pass 1 of year *t+1*, respectively.

Detecting pattern of variation in the net change in biomass along the coast

Whether the spatial pattern of NCB can be explained by biological phenomena is determined by performing a random forest (RF) analysis on the NCB estimates for all grids and for each year using the package "randomForest" in R (Liaw and Wiener 2002). RF is a powerful machine learning algorithm for classification and regression analysis that is increasingly being used in ecology (Cutler et al. 2007). We included the depth, the Northings (i.e. northward-measure of distance, similar to latitude), the distance to closest rock outcrops and a random variable varying from [0; 1] as explanatory variables for the analysis. We incorporated the random variable to test the significance of the other covariates: any variable with less predictive power than this random variable is considered "not significant". Finally, RF makes it easy to assess the importance of a

predictor and determine its marginal effect on the response variable (readers are referred to Breiman 2001 or Cutler et al. 2007 for detailed explanation about RF).

Results

How does Dover sole biomass change between survey passes and among years?

By creating maps of Dover sole biomass at each survey pass and year (based on the best models, Table 4.2), we not only revealed clusters of high biomass along the coast but also a high variability in Dover sole distribution among years and survey passes (Fig. 4.1). Dover sole was generally abundant in the 200-800m depth zone and in the central region between Cape Blanco and Eureka for both pass 1 and 2. Biomass was especially high in these locations for years 2004, 2005, 2007-2009 for pass 1 and 2004-2007 for pass 2. Another cluster of high Dover sole biomass was present in the northern region between Cape Flattery and Astoria. However, the years of high biomass did not coincide necessarily with years of high biomass in the central region, and the population was generally higher in the north during the second pass. Finally, Dover sole were also concentrated in areas southwest of San Francisco and north-west of Point Conception.

Does biomass change in response to fishing?

In general, changes in biomass due to fishing could not be detected (Fig. 4.2). While most of the catches were recorded below 2 tons in each grid (totaled across grids, catches averaged 8,500 tons annually over the last eight years), the scale of biomass change between the survey passes was an order of magnitude higher, and varied frequently from [-75; 75t].

How does the net change in biomass vary spatially and temporally? Are there consistent patterns of net change in biomass among years?

By mapping the net change in biomass for each survey year (both NCB_1 or NCB_2), we detected many changes in population biomass, with only a few areas with large positive or negative NCB values. While most of the NCB ranged between [-75; 75t] (Fig. 4.1), some locations along the coast had a NCB that was close to a magnitude higher (Fig. 4.3). Additionally, NCB changed in magnitude and distribution among years. For example, areas with negative NCB_1 were more widely spread along the coast in 2008 and 2009 compared to the other years, while 2005-2007 showed a larger NCB_1 around Cape Blanco than the rest of years (Fig. 4.3, a-h). Similarly, the distribution of NCB_2 varied among years, with a pattern that was often opposite of that of NCB_1. Despite the year to year variation in NCB_1 and NCB_2 (Fig. 4.3), few areas along the coast showed consistent negative or positive NCB between the survey passes (Fig. 4.3 and 4.4b,c). Some areas had a highly negative NCB_1 every year in regions southwest of Eureka and southwest of San Francisco. Likewise, NCB_1 was mostly positive southwest of Cape Flattery, northwest of Astoria, north of Cape Blanco, and west of San Francisco throughout the study period. NCB_2 showed generally the opposite pattern than that of NCB_1 (Fig. 4.4d). Notably, NCB_2 was positive northwest of Eureka and southwest of San Francisco and a negative estimate southwest of Cape Flattery, northwest of Astoria, and north of Cape Blanco.

Are there detectable patterns of variation in the net change in biomass along the coast?

Northings and depth were the main factors explaining variations in NCB according to the random forest analysis, but their importance changed among years (Fig. 4.5c). Distance to

nearest rock outcrops also explained some changes in NCB but to a lesser extent than the other two variables.

Northings (latitude) affected NCB_1 and NCB_2 in a complex manner (Fig. 4.5d and 4.6d). Northern regions (above 1500km north i.e. along the Washington coast) had a positive and higher NCB_1 than the rest of the coast (Fig. 4.5d). 2004 was notable with a net change in biomass 2-3 times higher than the rest of the years. Similarly, peaks in NCB_1 were observed around 700km and 1300km north with some year to year variability. All these locations corresponded to the regions previously identified with consistent positive NCB_1 across years (Fig. 4.4b). Two drops in NCB_1 were observed at around 600km and 900km north. These were located southwest of San Francisco and southwest of Eureka where NCB_1 was consistently negative across years (Fig. 4.4b), with 2006 and 2008 being particularly negative. NCB_2 showed almost exactly the opposite pattern than NCB_1 with negative estimates in northern areas for example (Fig. 4.6d).

Similarly to the effect of Northings on NCB_1, there was a large year to year fluctuation in the effect of depth to the NCB (Fig. 4.5e). On average, shallow (<100m) and deeper (>400m) areas had a much higher NCB estimates than intermediate-depth areas [100; 400m]. However, depending on the year, the depth range with negative NCB_1 varied: while the range was reduced to [100; 250m] for 2004 and 2010, it increased to [100; 800m] during 2008 and 2009 and stayed around the average for the rest of the study period. Here again, the pattern in NCB_2 was almost the opposite of that of NCB_1 (Fig. 4.6e).

Finally, NCB_1 was on average high near rocks and at 1-4km away from rocks, but low between 0-1 km from rocks. At distances >4km, NCB_1 became low again. While the effect of distance to

rock changed in absolute scale depending on the year, its general shape was the same among years (Fig. 4.5f). NCB_2 varied in the opposite manner compared to NCB_1 but not as symmetrical as for northings or depth (Fig. 4.6f).

Discussion

The importance of spatial and temporal dependency in species distribution modeling

Spatio-temporal models are increasingly used in ecology, and many software packages have been developed over the past decades to facilitate its implementation (Dormann et al. 2007, Beale et al. 2010, Saas and Gosselin 2014). However, many ecological studies still ignore spatial and/or temporal dependence (Dormann 2007). This is the case for many marine ecosystem studies where spatio-temporal data are commonly used to create an index of population biomass but the models seldom consider the spatial or spatio-temporal correlation structure (Maunder and Punt 2004, Robinson et al. 2011, Thorson and Ward 2013). In this study, we have shown that spatio-temporal modeling is a versatile method that could easily be applied in fishery ecology to answer practical problems such as (i) examining the change in the spatial distribution of a species within or between years, (ii) looking at the impact of exploitation to the local population structure, (iii) detecting patterns of population change and its relation to biological phenomena. Its use is not only elegant but important for the analysis of spatial data to reduce the risk of producing unreliable and inaccurate parameter estimates (Dormann 2007, Beale et al. 2010, Saas and Gosselin 2014). While data are becoming easier and cheaper to acquire, we rarely have data on all 'influential' environmental variables. The inclusion of spatial (or temporal) autocorrelation in the model provides a flexible way to account for factors not explicitly included in the model (Dormann 2007, Beale et al. 2010, Saas and Gosselin 2014, Shelton et al. in review).

Pattern in Dover sole biomass change along the U.S. West coast: potential causes and consequences

Despite its economic importance, exploitation rates for Dover sole have been quite low in recent years (Hicks and Wetzel 2011). As a consequence, most of the observed change in biomass for this species was due to factors other than fishing such as growth, death, movement or recruitment. We detected three main factors influencing the seasonal change in Dover sole biomass: depth, latitude, and the presence of rock outcrops.

Between summer and fall, Dover sole biomass decreased at intermediate depth ([100; 400m]) to increase in shallow (<100m) and deeper waters (>400m), in a consistent manner across years. There are at least two possible explanations for these observations. First, Toole et al. (2011) noted that juvenile Dover sole (10-22cm) tended to move inshore (<150m) during summer. Summer coastal upwelling brings nutrient-rich water from the deep to the shallow waters off the west coast of the U.S., increasing its primary productivity, and creating a favorable conditions for juvenile Dover sole (Landry et al. 1989). The positive change in biomass observed in shallow waters in late summer/early fall might therefore reflect movement of juvenile Dover sole into these nursery grounds. As for the flux of biomass in deeper water, this could be related to the ontogenetic movement of Dover sole as they grow and mature (Jacobson et al. 2001). While we hypothesized that seasonal movement might be responsible for these patterns in population change, we cannot exclude the possibility of differential growth or recruitment. However, the comparison of NCB_1 and NCB_2 with respect to depth confirmed that movement was likely the main reason behind these seasonal changes in biomass.

Dover sole biomass also changed in a complex manner between summer and fall as a function of latitude. NCB_1 indicated that Dover sole congregated in the late summer along the Washington coast (>1500km north), north of Cape Blanco and west of San Francisco and left regions southwest of Eureka and southwest of San Francisco. Although the origin of these fish could not be determined using the current methodology, a parsimonious explanation is that fish moved from nearby areas (as suggested by comparing NCB_1 and NCB_2), but they could have also moved to or from deeper waters not covered by the survey.

Finally, Dover sole biomass was estimated to be slightly higher near rocky habitat. This is a surprising result, given previous studies that have suggested that Dover sole prefer sandy/muddy bottom. However, some flatfish species such as Petrale sole could be found in high concentration in sandy bottom close to rocky habitats (Allan Hicks, pers. comm.). In this study, distance to rock outcrops was only calculated on a coarser 2x2km grid, and it is possible that many of these areas had sand and mud habitat within. Putting this aside, Dover sole biomass then increased with distance to rocks which is in line with the habitat preference of this flatfish species. Places further distant from rocks were mostly located in deeper waters and as a result, its effects was harder to separate from the effect of depth which was more influential in general.

Conclusion and future work

The use of habitat variables in species distribution modeling and biomass estimation has a long history in terrestrial ecosystems, but basic habitat information has been lacking in marine ecosystems until the past decades or so. While these data have been used to inform the location of marine reserves (Ward and Vanderklift 1999, Sunblad et al. 2011) or for the identification of vulnerable and critical habitat (Krigsman et al. 2012), they have rarely been integrated into a

models of fish distribution (Robinson et al. 2011, Sunblad et al. 2011). In this study, we took advantage of newly available benthic habitat data and incorporated it into a spatio-temporal model to study the seasonal dynamics of Dover sole across the U.S. West coast. Dover sole appeared to move seasonally along the coast during late summer/early fall. The species moved to shallow and deeper water during that time following their ontogeny. They also appeared to move north in late summer and aggregate north of Cape Blanco and west of San Francisco while leaving regions southwest of Eureka and southwest of San Francisco. Furthermore, our results seemed to be quire robust to the assumptions made in this study. A sensitivity test on the choice of q value (the catchability coefficient), and the choice of covariates (Fig. 4.A1-4) showed that the main results did not change qualitatively; the same regions along the coast showed the consistent loss or gain in population and the three habitat covariates (depth, northings and distance to nearest rock outcrops) affected the net change in biomass in a similar pattern.

In summary, spatially-referenced catch and survey data indicated considerable year-to-year and season to season variability in the spatial distribution of Dover sole. These changes were mostly attributed to individual movement but growth and recruitment could be factors that can also shape the population. Separating the role of growth, recruitment, and movement on spatial patterns in production (i.e., NCB) remains an important topic for future research. As more and more data and spatio-temporal modeling software become available, we hope there will be interest in extending this work to many other species – particularly those in marine ecosystems. Additionally, it might also be worth investigating if individual fish are moving beyond the lower depth limit of the bottom trawl survey used by NMFS to assess this population. No physical barrier exists to stop Dover sole from moving deeper into the continental slope and this study showed there is a chance that Dover might be doing that. Finally, while Dover sole was a lightly

exploited species, it would be interesting to expand the study to other species with stronger fishing pressure to examine the potential effect of fishing on the population dynamics.

Table

Table 4.1: Parameter definition and prior specifications in INLA

Parameter	Symbol	Prior (non informative)
Fixed effects	β	N(0, 1000)
Log precision for the measurement error	$\log(1/\sigma_p^2)$	Loggamma(1;5e-05)
Log precision for the spatial variance	$\log(1/\tau_p^2)$	Loggamma(1;5e-05)
Log of spatial range	$\log(2/\kappa)$	Loggamma(1;5e-05)

Table 4.2: Covariates selection results for the spatio-temporal GLMM models. Model selection was performed for the Dover sole presence/absence at survey pass 1 (1-) and survey pass 2 (2-); and for Dover sole density at each survey pass (1+ and 2+). Deviance information criterion (DIC) and the mean logarithmic score are used jointly to determine the best model (highlighted in **bold**). In case of conflicting result between DIC and the mean logarithmic score, the best model was chosen based on DIC as the difference in mean logscore was rarely significantly different.

Model	Variables	Delta DIC	Mean(LS)	p-value
1+	D+D2+T+T2+S+S2+R	0.00	1.683	ref
	D+D2+T+T2+S+R	3.83	1.683	0.986
	D+D2+T+T2+S	0.69	1.683	0.998
	D+D2+T+T2+R	3.14	1.683	0.982
	D+D2+T+S+S2+R	8.97	1.693	0.784
	D+D2+T+S+S2	4.86	1.693	0.795
	D+D2+T+S+R	12.70	1.694	0.761
	D+D2+T+R	9.96	1.694	0.767
	D+D2+T+S	9.59	1.693	0.776
	D+D2+T	9.54	1.694	0.778
	D+D2+T+T2	3.06	1.683	0.987
	D+D2+R+S+S2	25.10	1.696	0.722
	D+D2+R+S	29.26	1.696	0.709
	D+D2+R	26.36	1.696	0.727
	D+D2+S+S2	23.08	1.696	0.730
	D+D2+S	28.19	1.696	0.728
	D+D2	28.72	1.696	0.731
2+	D+D2+T+T2+S+S2+R	23.69	1.695	0.952
	D+D2+T+T2+S+R	26.99	1.694	0.968
	D+D2+T+T2+S	24.72	1.692	ref
	D+D2+T+T2+R	24.66	1.694	0.975
	D+D2+T+S+S2+R	82.87	1.711	0.619
	D+D2+T+S+S2	86.91	1.712	0.610
	D+D2+T+S+R	92.49	1.713	0.578
	D+D2+T+R	91.54	1.713	0.586

	D+D2+T+S	98.16	1.714	0.581
	D+D2+T	96.40	1.713	0.876
	D+D2+T+T2	38.14	1.695	0.951
	D+D2+R+S+S2	0.00	1.697	0.908
	D+D2+R+S	7.45	1.698	0.891
	D+D2+R	7.85	1.697	0.905
	D+D2+S+S2	4.62	1.697	0.899
	D+D2+S	13.23	1.698	0.870
	D+D2	11.36	1.698	0.892
1-	D+D2+T+T2+S+S2+R	8.25	0.279	0.915
	D+D2+T+T2+S+R	16.24	0.280	0.869
	D+D2+T+T2+S	24.60	0.282	0.828
	D+D2+T+T2+R	13.90	0.280	0.885
	D+D2+T+S+S2+R	8.58	0.278	0.931
	D+D2+T+S+S2	16.16	0.280	0.879
	D+D2+T+S+R	13.92	0.279	0.896
	D+D2+T+R	11.53	0.279	0.916
	D+D2+T+S	22.16	0.281	0.844
	D+D2+T	22.65	0.281	0.843
	D+D2+T+T2	24.58	0.282	0.820
	D+D2+R+S+S2	0.00	0.276	ref
	D+D2+R+S	5.00	0.277	0.974
	D+D2+R	1.39	0.276	0.998
	D+D2+S+S2	9.96	0.278	0.937
	D+D2+S	15.67	0.279	0.901
	D+D2	16.33	0.279	0.898
2-	D+D2+T+T2+S+S2+R	0.00	0.277	ref
	D+D2+T+T2+S+R	3.46	0.278	0.986
	D+D2+T+T2+S	4.09	0.278	0.983
	D+D2+T+T2+R	3.32	0.278	0.989

D+D2+T+S+S2+R	13.18	0.280	0.917
D+D2+T+S+S2	13.48	0.280	0.907
D+D2+T+S+R	16.84	0.280	0.900
D+D2+T+R	16.21	0.280	0.902
D+D2+T+S	16.83	0.280	0.896
D+D2+T	16.35	0.280	0.908
D+D2+T+T2	3.45	0.278	0.987
D+D2+R+S+S2	16.78	0.280	0.910
D+D2+R+S	19.8	0.281	0.888
D+D2+R	17.29	0.280	0.902
D+D2+S+S2	16.86	0.280	0.899
D+D2+S	19.49	0.281	0.891
D+D2	17.41	0.279	0.905

Annotation: D (log of depth), T (temperature), S (sediment size) and R (distance to closest rocks). D2 and T2 are for squared covariate effect

Figure

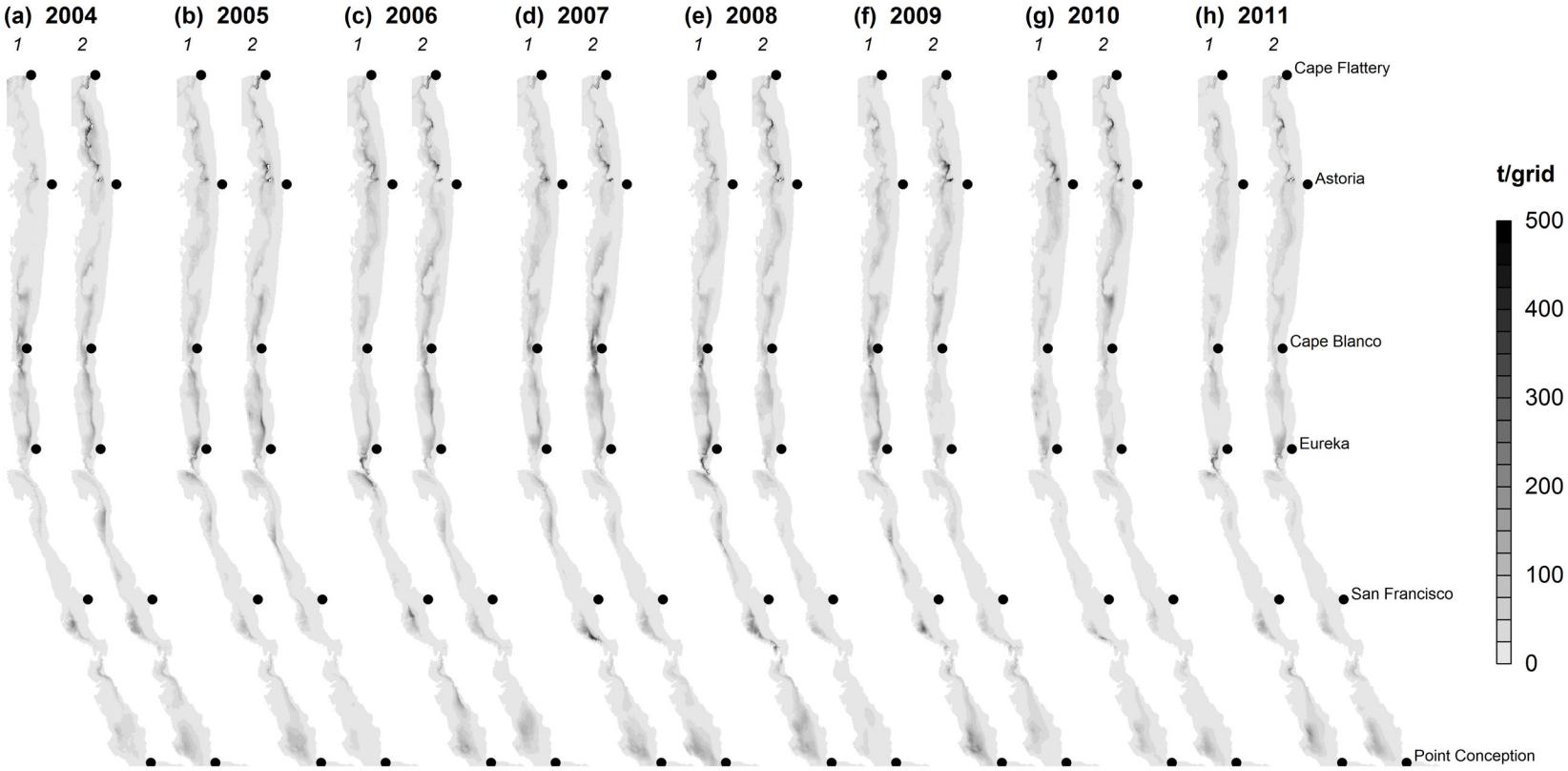

Figure 4.1: (a)-(h) Biomass maps of Dover sole along the U.S. West coast between 2004 and 2011. For each year, the biomass distribution estimated at the first survey pass ("*1*") and at the second survey pass ("*2*") are put side by side.

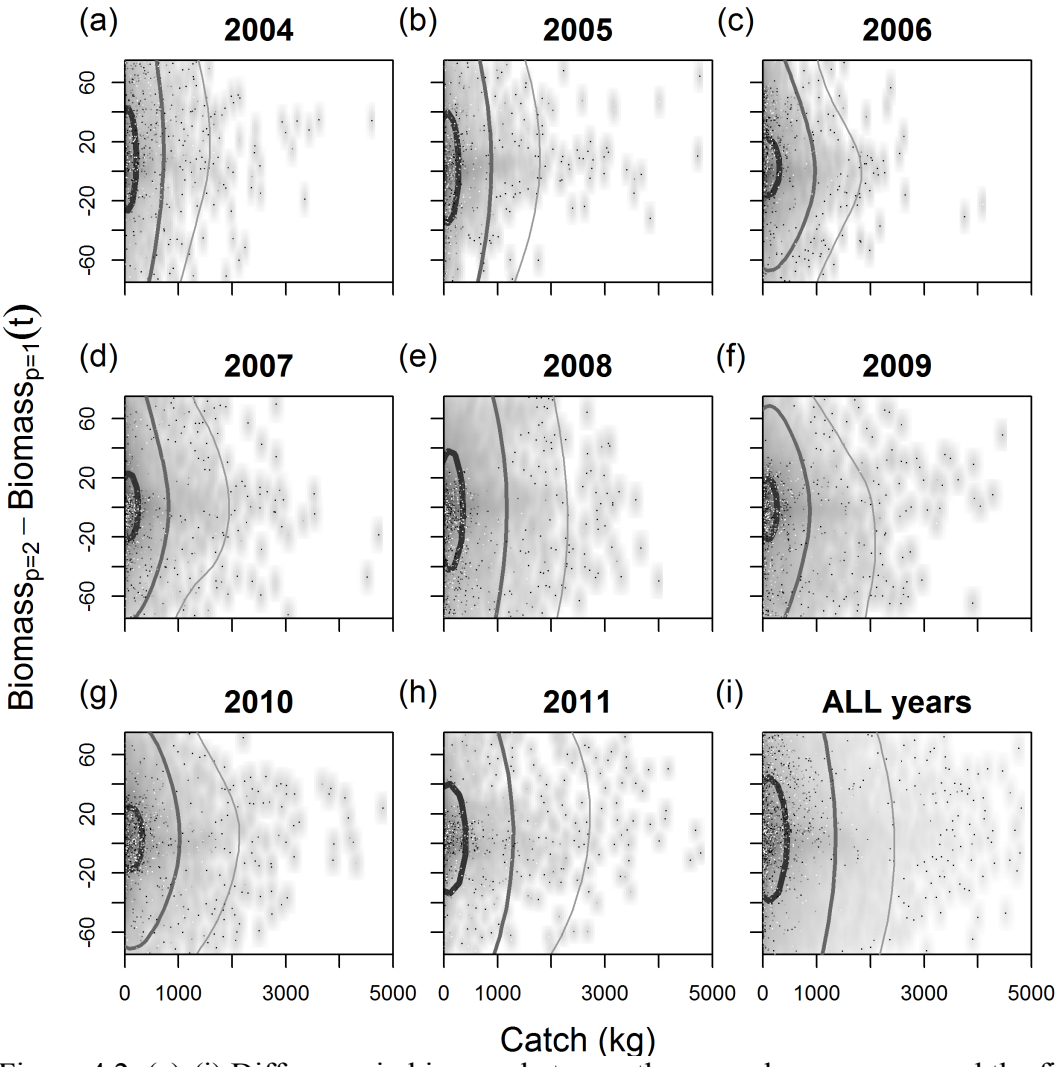

Figure 4.2: (a)-(i) Difference in biomass between the second survey pass and the first survey pass for the whole U.S. West coast and for each year, plotted against catch. The darker the shading or the lines, the more data points are concentrated in the area. The lines corresponds to the kernel density estimates

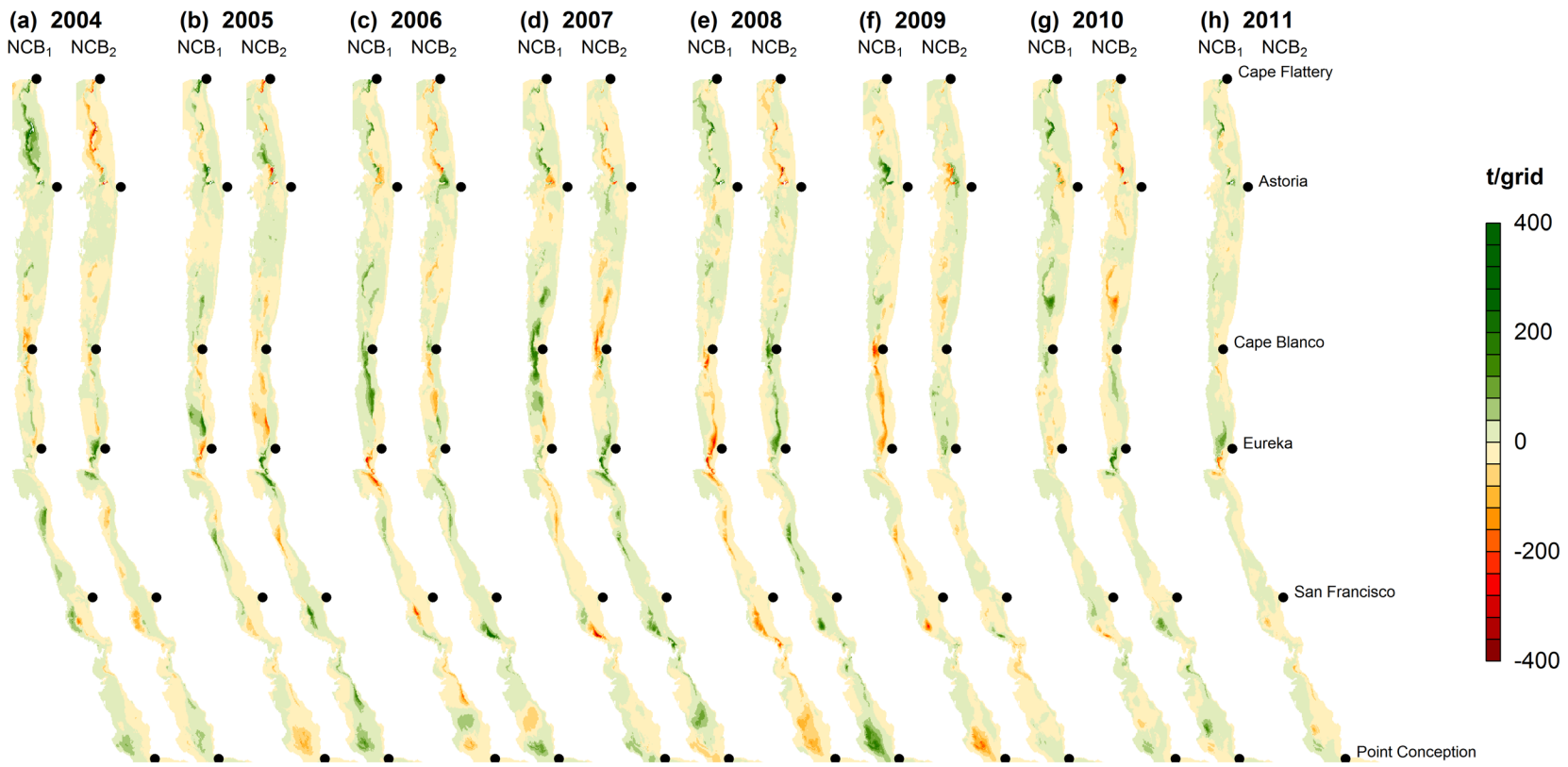

Figure 4.3: (a)-(h) 2004-2011 posterior mean estimate of net change in biomass between pass 1 and pass 2 within the same year (NCB_1), and between pass 2 of year *t* i and pass 1 of year *t+1* (NCB_2), for each 2x2km spatial grid along the U.S. West coast.

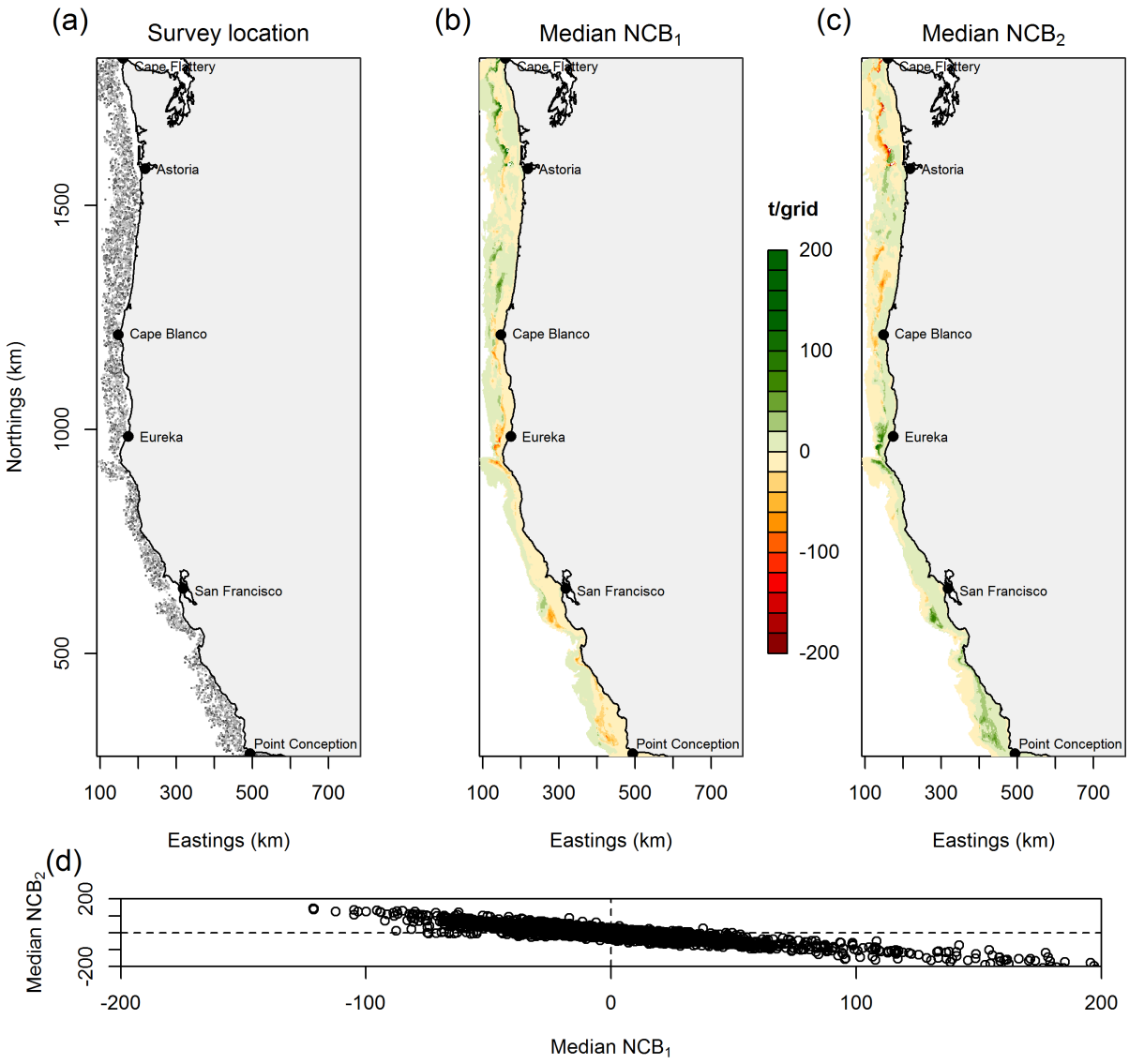

Figure 4.4: (a) Annual survey locations between 2004 and 2011. (b) Median across the 2004-2011 posterior mean estimate of net change in biomass between pass 1 and pass 2 within the same year (NCB_1), for each 2x2km spatial grid along the U.S. West coast. (c) Median across the 2004-2010 posterior mean estimate of net change in biomass between pass 2 of year *t* and pass 1 of year *t+1* (NCB_2), for each 2x2km spatial grid along the U.S. West coast. (d) Plot of median NCB_1 versus median NCB_2

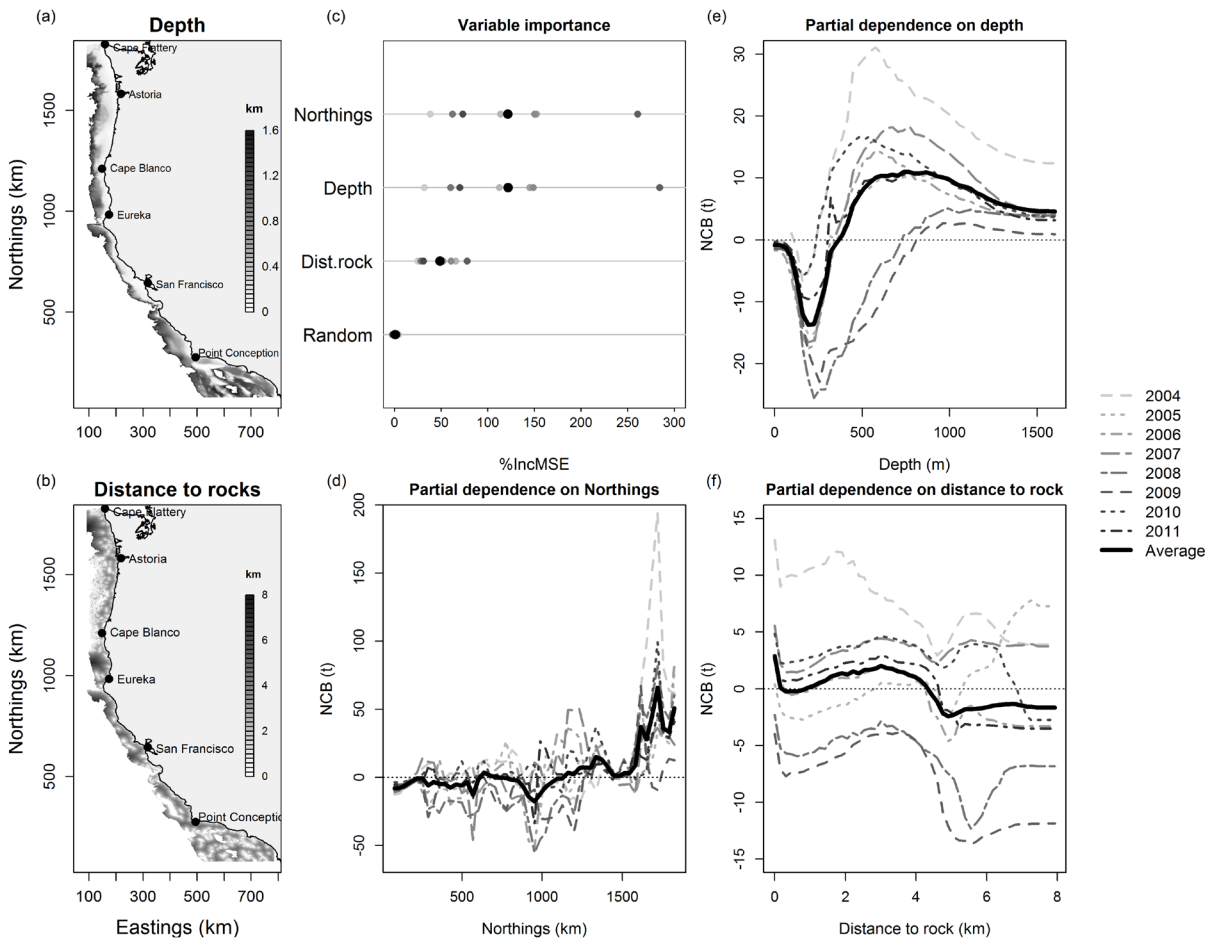

Figure 4.5: (a) Depth distribution along the West coast. (b) Distance to nearest rock outcrops along the West coast. (c) Variable importance plot for the predictor variables from the random forest (RF) used for predicting the net change in biomass (NCB_1) between pass 2 and pass 1 within the same year. (d)-(f) Partial dependence plots for RF for NCB and three predictor variables. Partial dependence is the dependence of NCB on one predictor variable after averaging out the effects of the other predictor variables in the model. RF is run independently on the estimate of NCB by year and results are color coded in grey intensity.

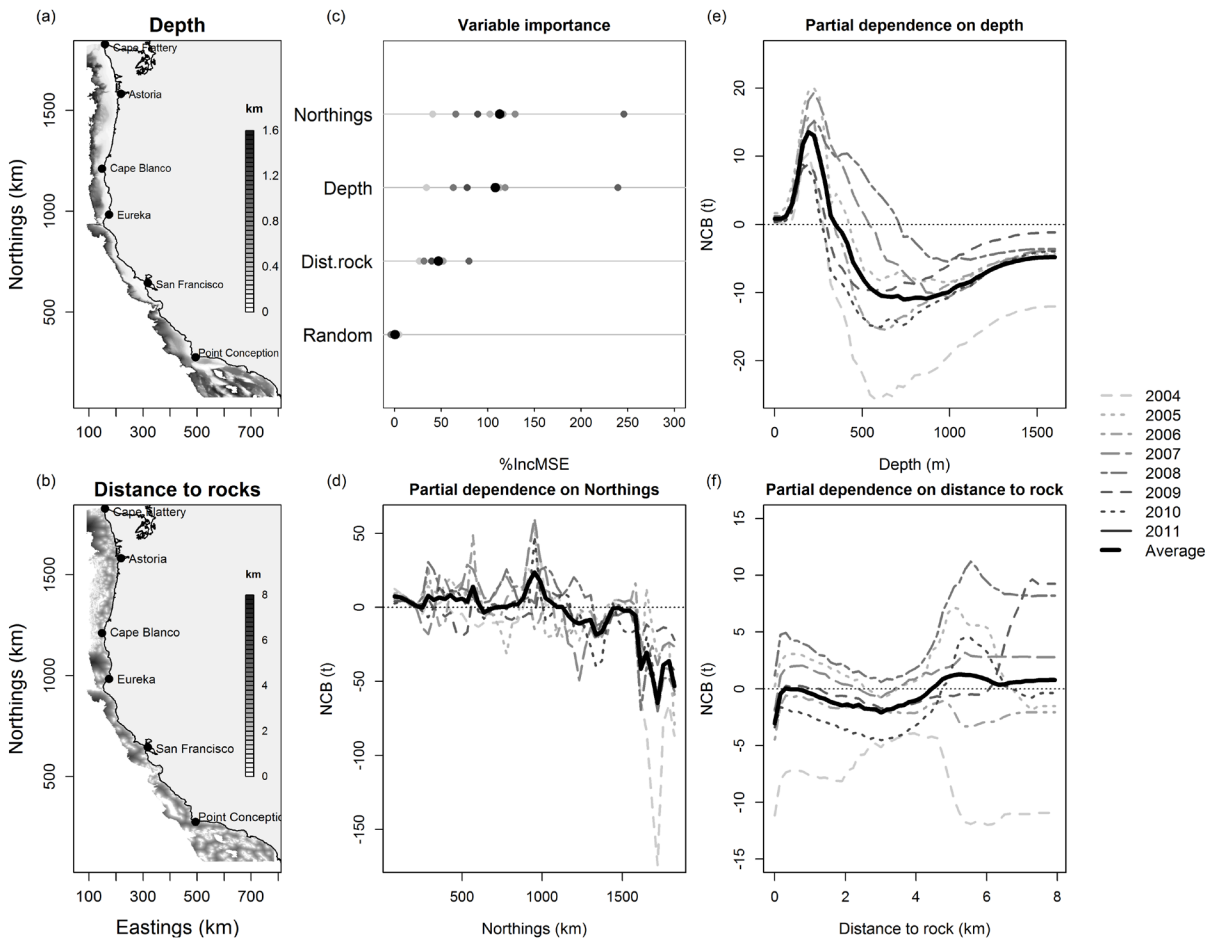

Figure 4.6: (a) Depth distribution along the West coast. (b) Distance to nearest rock outcrops along the West coast. (c) Variable importance plot for the predictor variables from the random forest (RF) used for predicting the net change in biomass between pass 1 and pass 2 of different years (NCB_2). (d)–(f) Partial dependence plots for RF for NCB and three predictor variables.

Appendix

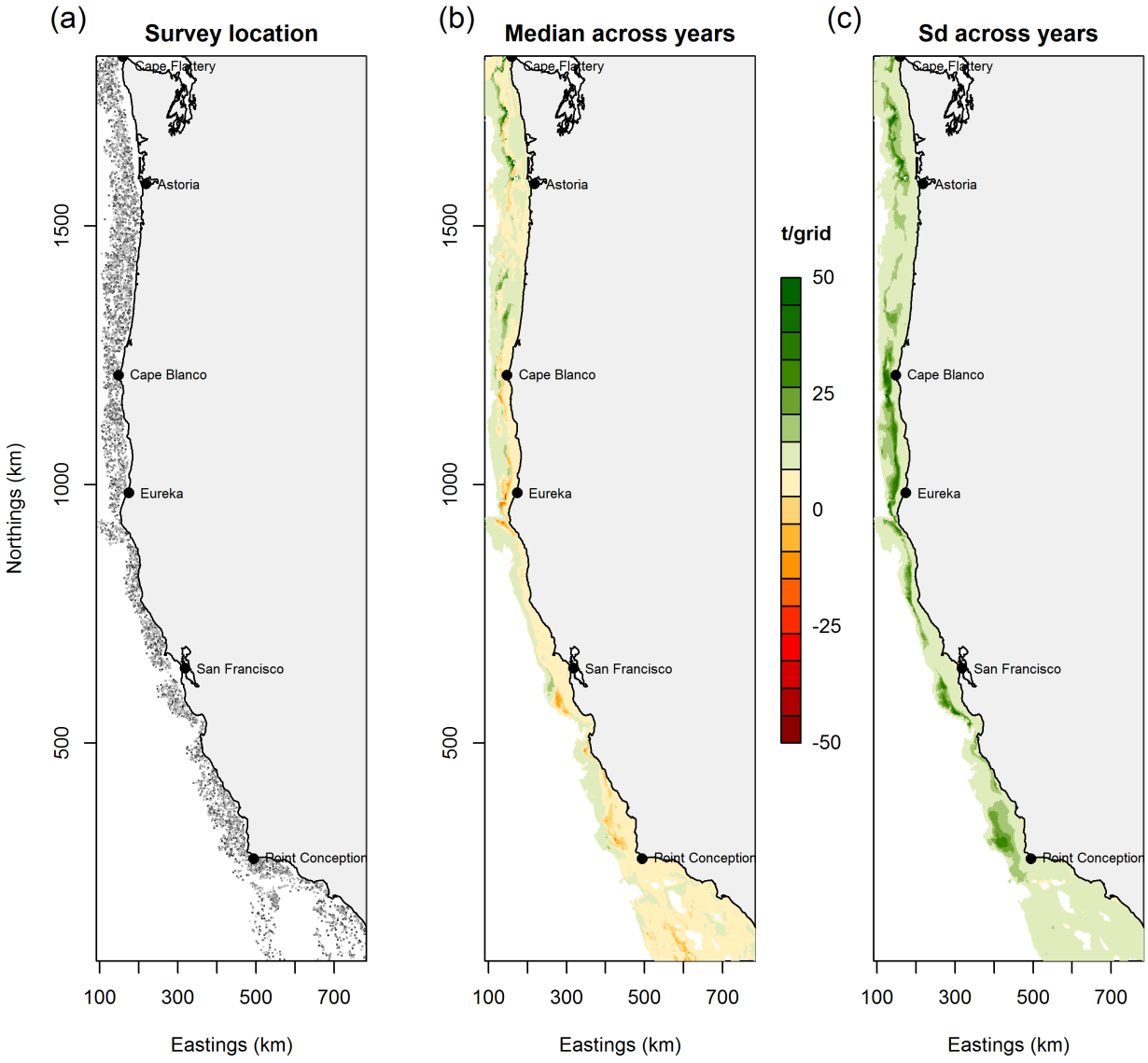

Figure A4.1: Sensitivity of the model result to the choice of q (catchability coefficient) q=1. (a) Annual survey locations between 2004 and 2011. (b) Median across the 2004-2011 posterior mean estimate of net change in biomass between pass 1 and pass 2 within the same year (NCB_1), for each 2x2km spatial grid along the U.S. West coast. (c) Standard deviation across the 2004-2011 posterior mean estimate of net change in biomass between pass 1 and pass 2 within the same year (NCB_1), for each 2x2km spatial grid along the U.S. West coast.

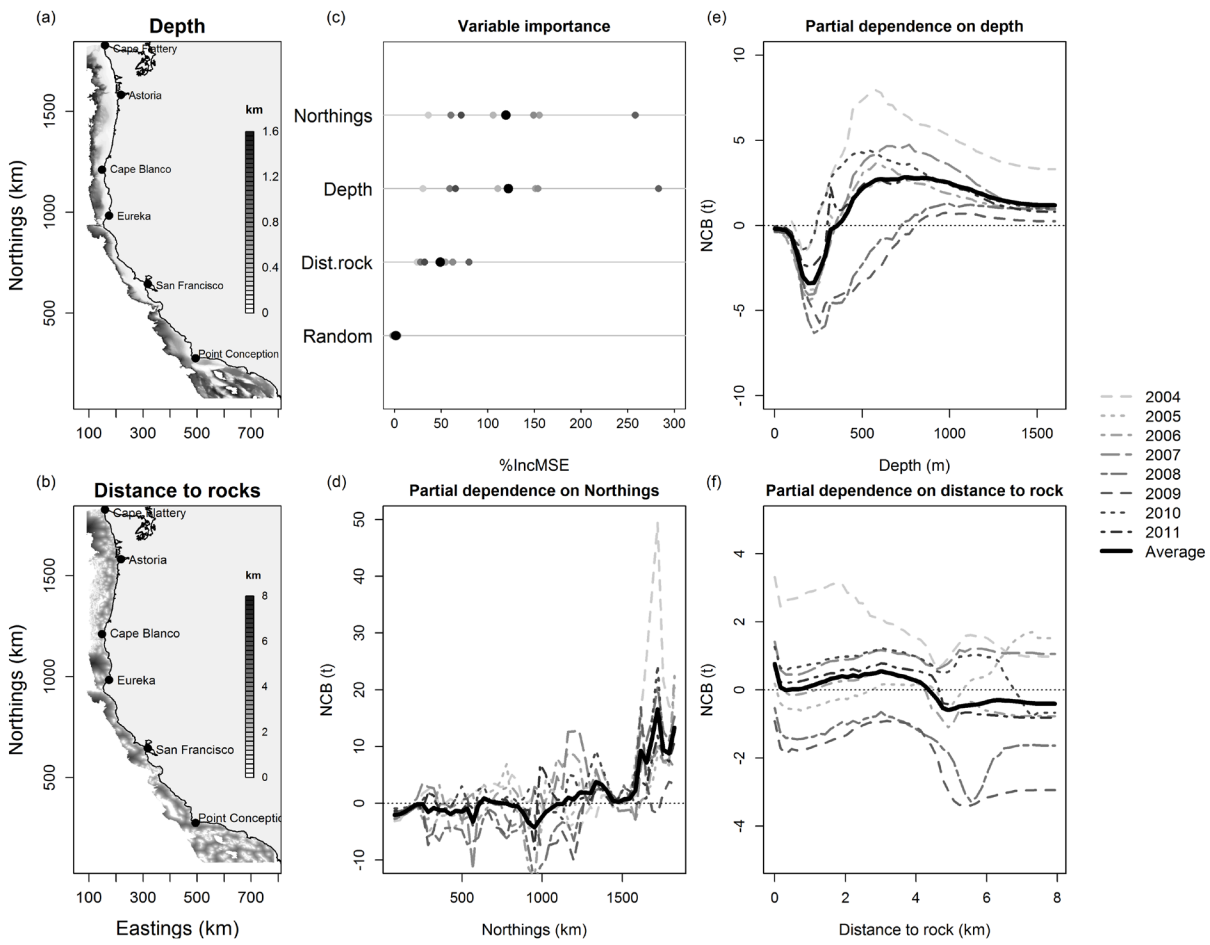

Figure A4.2: Sensitivity of the model result to the choice of q (catchability coefficient). q=1. (a) Depth distribution along the West coast. (b) Distance to nearest rock outcrops along the West coast. (c) Variable importance plot for the predictor variables from the random forest (RF) used for predicting the net change in biomass (NCB_1) between pass 2 and pass 1 within the same year. (d)-(f) Partial dependence plots for RF for NCB and three predictor variables. Partial dependence is the dependence of NCB on one predictor variable after averaging out the effects of the other predictor variables in the model. RF is run independently on the estimate of NCB by year and results are color coded in grey intensity.

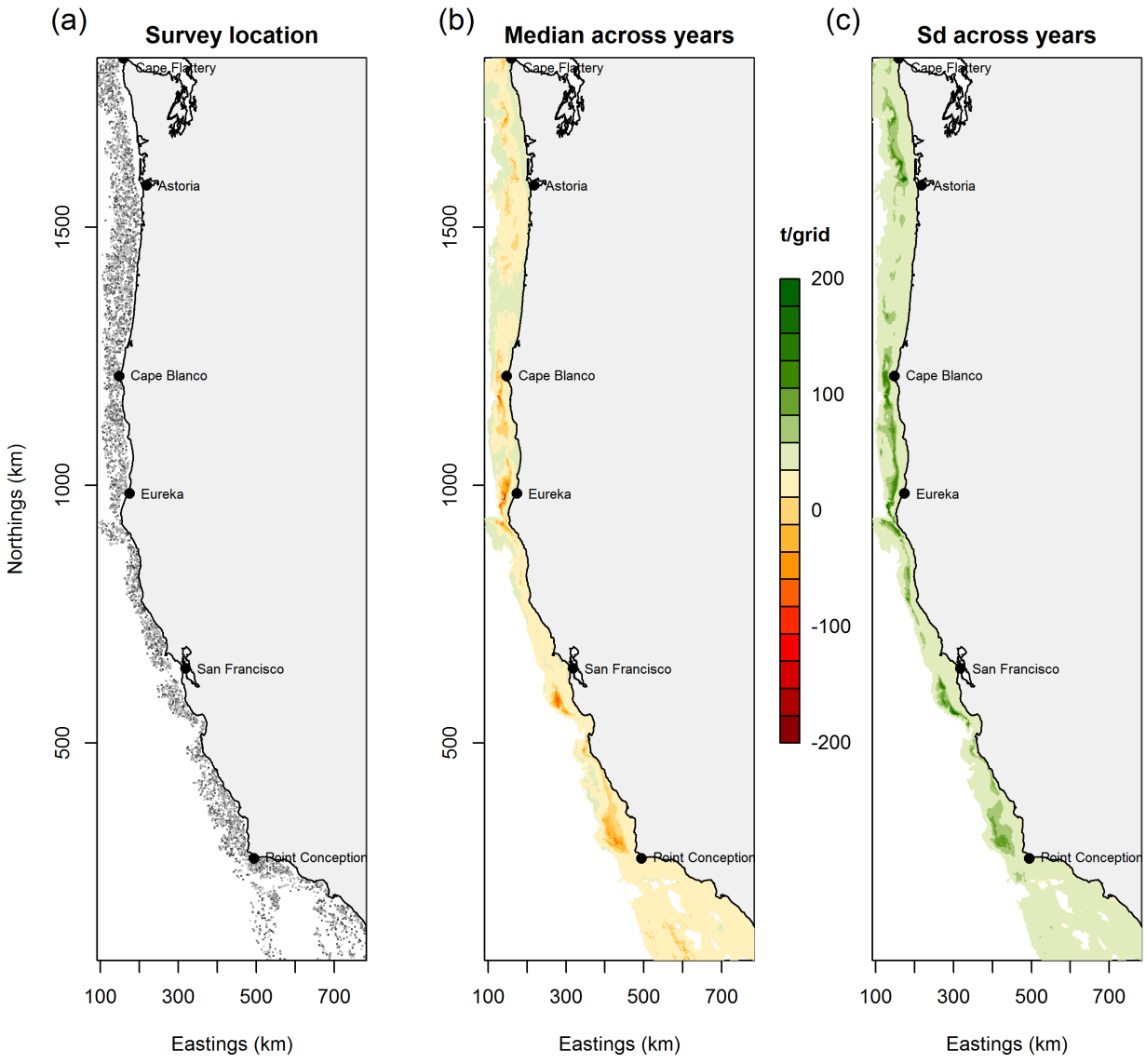

Figure A4.3: Sensitivity of the model result to the choice of covariates (full model results). (a) Annual survey locations between 2004 and 2011. (b) Median across the 2004-2011 posterior mean estimate of net change in biomass between pass 1 and pass 2 within the same year (NCB_1), for each 2x2km spatial grid along the U.S. West coast. (c) Standard deviation across the 2004-

2011 posterior mean estimate of net change in biomass between pass 1 and pass 2 within the same year (NCB_1), for each 2x2km spatial grid along the U.S. West coast.

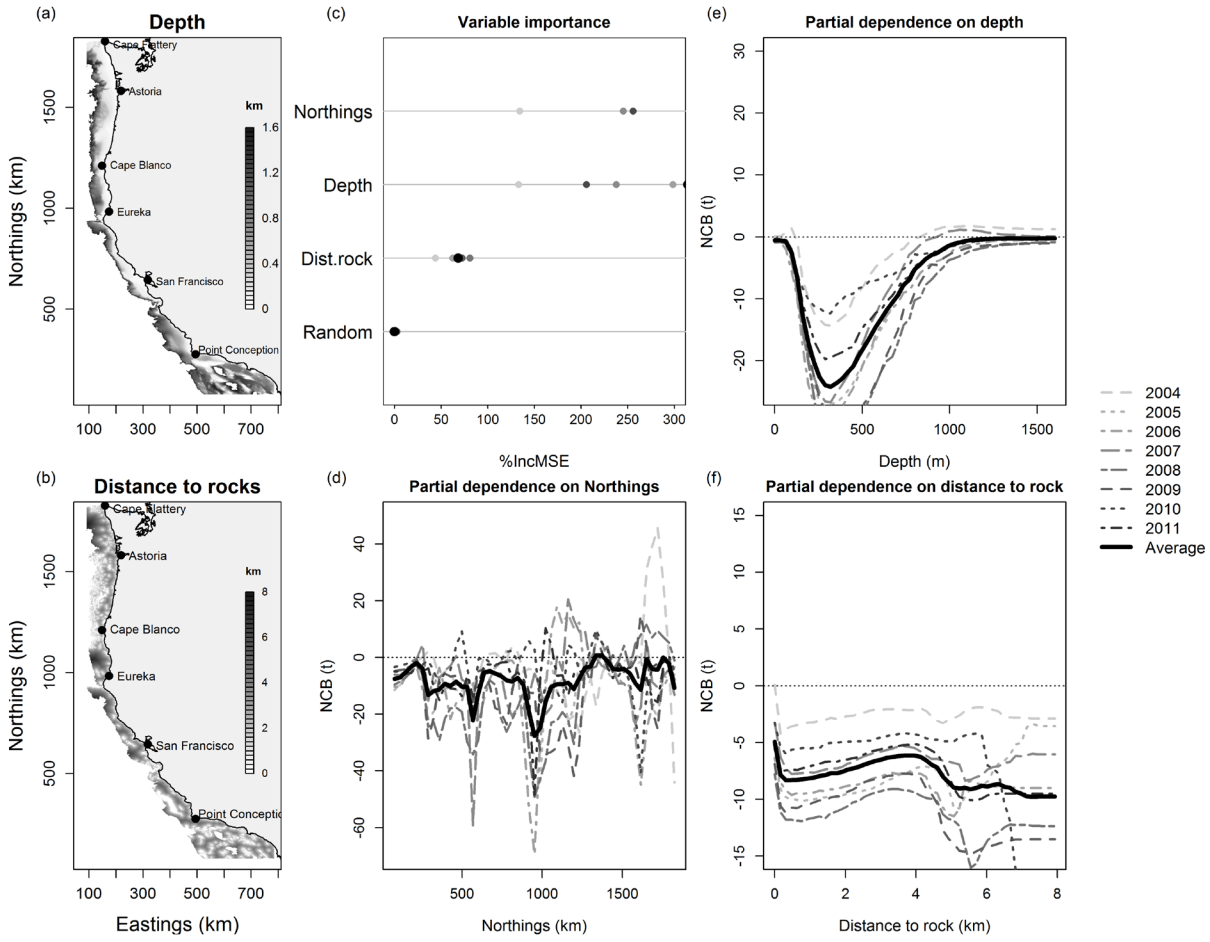

Figure A4.4: Sensitivity of the model result to the choice of covariates (full model results). (a) Depth distribution along the West coast. (b) Distance to nearest rock outcrops along the West coast. (c) Variable importance plot for the predictor variables from the random forest (RF) used for predicting the net change in biomass (NCB_1) between pass 2 and pass 1 within the same year. (d)-(f) Partial dependence plots for RF for NCB and three predictor variables. Partial dependence is the dependence of NCB on one predictor variable after averaging out the effects of the other predictor variables in the model. RF is run independently on the estimate of NCB by year and results are color coded in grey intensity.

Conclusion

Overview

In this study, I developed and tested novel fishery analysis methods which better integrate the spatial structure of the fish and fishery to help improve information for fisheries management in three ways:

1. An exploration of how the performance of different management measures can change depending on the spatial structure of the targeted marine resources;
2. A method to create a more accurate index of population abundance that could be used to infer the status of population; and
3. A spatio-temporal model to improve the quality of species distribution predictions and potentially detect areas of management interest along the coast, e.g. areas with higher abundance of certain overfished species.

The effect of population structure to the fishery management performance

Many studies in the literature have identified the importance of socio-economic factors affecting the efficiency of management regimes and the sustainable use of resources (e.g., Gutierrez et al. 2011). The first chapter of this thesis shows that the biological and economic efficiency of management regimes is quite sensitive to the level of species overlap on the fishing grounds (population structure). The results of this study can therefore provide insight to managers regarding what to expect in terms of population preservation and fishery profitability by switching management methods, given what they know about the population distribution in their fishery.

Improved indices of abundance

Observational data are used in fishery and wildlife studies to estimate indices of abundance which are then included in stock assessment models which provide advice regarding likely outcomes from alternative management measures or actions. The novel methods presented in this dissertation help improve the accuracy of the resulting indices of abundance and increase the biological interpretability of those indices. For example, the use of objective area stratification created strata that more closely followed the actual population structure while reducing bias in the derived indices of abundance. In another example, the novel CPUE standardization approach reduced the bias in estimated abundance indices when area closures existed in the fishery. Marine closures and MPAs are now being implemented worldwide and becoming a common tool for management. It is therefore important to develop utilize methods that deal with area closures in assessment models, as marine reserves continue expanding around the globe.

Better understand the species distribution

Species distribution models are vital tools for expanding our understanding of species habitat associations, and for conservation planning and resource management. However, to date many of these models fail to consider space and time dependence (Dormann 2007). Being able to explicitly account for spatio-temporal changes is crucial for understanding current and future threats from anthropogenic forces, and for reducing the risks of erroneous results, given that many exogenous (e.g. climate and habitat) and endogenous (e.g. dispersal, predation, and breeding) drivers of species distributions are likely to vary through time and space. In Chapter 4, I showed how spatio-temporal models could easily be applied to marine species to study the temporal dynamics of a species and examine the effects of fishing at the local population level. It

is crucial to keep developing such modeling tools to help guide conservation and management actions to reduce the likelihood of major threats to or the decline of aquatic living resources in the context of climate change and increasing human population.

Conclusion and future work

In conclusion, this dissertation demonstrates that the consideration of spatial structure within model-based inference can often be expected to yield benefits, both in terms of interpretable biological outputs and improved accuracy in the resulting population indices. Together these improvements increase the quality and quantity of information for fishery managers.

Future work should continue expanding and developing methods that incorporate spatial information for species assessments. In particular, separating the role of growth, recruitment, fishing and movement on spatial patterns in productivity might yield useful information for fisheries managers. Such analyses will be increasingly feasible with advances in data acquisition technology and computer software for species distribution modeling. Non-parametric techniques, such as machine learning algorithms, are also increasingly used in the field of ecology, and future studies could examine their performance compared to traditional parametric or semi-parametric models in the context of CPUE standardization and species distribution modeling.

Bibliography

Babcock, E. A., and A. D. MacCall. 2011. How useful is the ratio of fish density outside versus inside no-take marine reserves as a metric for fishery management control rules? Canadian Journal of Fisheries and Aquatic Sciences 68:343–359.

Banerjee, S., A. E. Gelfand, A. O. Finley, and H. Sang. 2008. Gaussian predictive process models for large spatial data sets. Journal of the Royal Statistical Society: Series B (Statistical Methodology) 70:825–848.

Beale, C. M., J. J. Lennon, J. M. Yearsley, M. J. Brewer, and D. A. Elston. 2010. Regression analysis of spatial data. Ecology letters 13:246–64.

Berkeley, S. A. 2006. Pacific rockfish management: are we circling the wagons around the wrong paradigm? Bulletin of Marine Science 78:655–667.

Beverton, R. J. H., and S. J. Holt. 1957. On the dynamics of exploited fish populations. Page 533. Ministry of Agriculture, Fisheries and Food, London.

Bishop, J. 2006. Standardizing fishery-dependent catch and effort data in complex fisheries with technology change. Reviews in Fish Biology and Fisheries 16:21–38.

Bordalo-Machado, P. 2006. Fishing effort analysis and its potential to evaluate stock size. Reviews in Fisheries Science 14:369–393.

Botsford, L. W., F. Micheli, and A. Hastings. 2003. Principles for the design of marine reserves. Ecological Applications 13:25–31.

Bradburn, M. J., A. A. Keller, and B. H. Horness. 2011. The 2003 to 2008 U.S. West Coast bottom trawl surveys of groundfish resources off Washington, Oregon, and California: estimates of distribution, abundance, length, and age composition. Page 323.

Branch, T. A. 2006. Discards and revenues in multispecies groundfish trawl fisheries managed by trip limits on the U.S. West coast and by ITQs in British Columbia. Bulletin of Marine Science 78:669–689.

Branch, T. A. 2009. How do individual transferable quotas affect marine ecosystems? Fish and Fisheries 10:39–57.

Branch, T. A., and R. Hilborn. 2008. Matching catches to quotas in a multispecies trawl fishery: targeting and avoidance behavior under individual transferable quotas. Canadian Journal of Fisheries and Aquatic Sciences 65:1435–1446.

Branch, T. A., R. Hilborn, A. C. Haynie, G. Fay, L. FLynn, J. Griffiths, K. N. Marshall, J. K. Randall, M. Scheuerell, E. J. Ward, and M. Young. 2006a. Fleet dynamics and fishermen behavior: lessons for fisheries managers. Canadian Journal of Fisheries and Aquatic Sciences 1668:1647–1668.

Branch, T., K. Rutherford, and R. Hilborn. 2006b. Replacing trip limits with individual transferable quotas: implications for discarding. Marine Policy 30:281–292.

Breiman, L. 2001. Random forests. Machine Learning 45:5–32.

Burnham, K. P., and D. R. Anderson. 2002. Model selection and multimodel inference: a practical information-theoretic approach. Page 488.

Caddy, J. F. 1975. Spatial model for an exploited shellfish population, and its application to the Georges Bank scallop fishery. Journal of the Fisheries Research Board of Canada 32:1305–1328.

Cameletti, M., F. Lindgren, D. Simpson, and H. Rue. 2013. Spatio-temporal modeling of particulate matter concentration through the SPDE approach. AStA Advances in Statistical Analysis 97:109–131.

Campbell, R. A. 2004. CPUE standardisation and the construction of indices of stock abundance in a spatially varying fishery using general linear models. Fisheries Research 70:209–227.

Candy, S., P. Ziegler, and D. Welsford. 2014. A nonparametric model of empirical length distributions to inform stratification of fishing effort for integrated assessments. Fisheries Research 159:34–44.

Carruthers, T. R., R. N. M. Ahrens, M. K. McAllister, and C. J. Walters. 2011a. Integrating imputation and standardization of catch rate data in the calculation of relative abundance indices. Fisheries Research 109:157–167.

Carruthers, T. R., M. K. McAllister, and N. G. Taylor. 2011b. Spatial surplus production modeling of Atlantic tunas and billfish. Ecological applications 21:2734–55.

Chouakria, A. D., and P. N. Nagabhushan. 2007. Adaptive dissimilarity index for measuring time series proximity. Advances in Data Analysis and Classification 1:5–21.

Clark, C. W. 1990. Mathematical bioeconomics: the optimal management of renewable resources. Page 368. 2nd editio.

Clarke, M. E., N. Tolimieri, and H. Singh. 2009. Using the seabed AUV to assess populations of groundfish in untrawlable areas. Pages 357–372 *in* R. Beamish and B. Rothschild, editors. The future of fisheries science in North America. Springer. The Netherlands.

Clements, C., V. Bonito, R. Grober-Dunsmore, and M. Sobey. 2012. Effects of small, Fijian community-based marine protected areas on exploited reef fishes. Marine Ecology Progress Series 449:233–243.

Cope, J. M., and A. E. Punt. 2009. Drawing the lines: resolving fishery management units with simple fisheries data. Canadian Journal of Fisheries and Aquatic Sciences 66:1256–1273.

Costello, C., and R. Deacon. 2007. The efficiency gains from fully delineating rights in an ITQ fishery. Marine Resource Economics 22:347–361.

Cowen, R. K., G. Gawarkiewicz, J. Pineda, S. R. Thorrold, and F. E. Werner. 2007. Population connectivity in marine systems: an overview. Oceanography 20:14–21.

Cutler, D. R., T. C. Edwards, K. H. Beard, A. Cutler, K. T. Hess, J. Gibson, and J. J. Lawler. 2007. Random forests for classification in ecology. Ecology 88:2783–92.

Dormann, C. F. 2007. Effects of incorporating spatial autocorrelation into the analysis of species distribution data. Global Ecology and Biogeography 16:129–138.

Dormann, C. F., J. M. McPherson, M. B. Araújo, R. Bivand, J. Bolliger, G. Carl, R. G. Davies, A. Hirzel, W. Jetz, W. D. Kissling, I. Kühn, R. Ohlemüller, P. R. Peres-Neto, B. Reineking, B.

Schröder, F. M. Schurr, and R. Wilson. 2007. Methods to account for spatial autocorrelation in the analysis of species distributional data: a review. Ecography 30:609–628.

Edgar, G., and R. Stuart-Smith. 2009. Ecological effects of marine protected areas on rocky reef communities—a continental-scale analysis. Marine Ecology Progress Series 388:51–62.

Elith, J., and J. R. Leathwick. 2009. Species distribution models: ecological explanation and prediction across space and time. Annual Review of Ecology, Evolution, and Systematics 40:677–697.

Elith, J., J. R. Leathwick, and T. Hastie. 2008. A working guide to boosted regression trees. The Journal of Animal Ecology 77:802–13.

Essington, T. E. 2010. Ecological indicators display reduced variation in North American catch share fisheries. Proceedings of the National Academy of Sciences 107:754–9.

Field, J. C., A. E. Punt, R. D. Methot, and C. J. Thomson. 2006. Does MPA mean "Major Problem for Assessments"? Considering the consequences of place-based management systems. Fish and Fisheries 7:284–302.

Finley, A. O., S. Banerjee, and A. E. Gelfand. 2012. Bayesian dynamic modeling for large space-time datasets using Gaussian predictive processes. Journal of Geographical Systems 14:29–47.

Finley, A. O., H. Sang, S. Banerjee, and A. E. Gelfand. 2009. Improving the performance of predictive process modeling for large datasets. Computational Statistics & Data Analysis 53:2873–2884.

Fournier, D. A., J. Hampton, and R. Sibert, John. 1998. Multifan_CL: a length-based, age structured model fo fisheries stock assessment, with application to South Pacific albacore *Thunnus alalunga*. Canadian Journal of Fisheries and Aquatic Sciences 55:2105–2116.

Fox, H. E., M. B. Mascia, X. Basurto, A. Costa, L. Glew, D. Heinemann, L. B. Karrer, S. E. Lester, A. V. Lombana, R. S. Pomeroy, C. A. Recchia, C. M. Roberts, J. N. Sanchirico, L. Pet-Soede, and A. T. White. 2012. Reexamining the science of marine protected areas: linking knowledge to action. Conservation Letters 5:1–10.

Francis, R. I. C. C. 1999. The impact of correlations in standardized CPUE indices. NZ Fisheries Association Research Document No. 99/42.

Francis, R. I. C. C. 2011. Data weighting in statistical fisheries stock assessment models. Canadian Journal of Fisheries and Aquatic Sciences 68:1124–1138.

Fuentes, M. 2007. Approximate likelihood for large irregularly spaced spatial data. Journal of the American Statistical Association 102:321–331.

Fulton, E. A., A. D. M. Smith, D. C. Smith, and I. E. van Putten. 2011. Human behaviour: the key source of uncertainty in fisheries management. Fish and Fisheries 12:2–17.

Furrer, R., M. G. Genton, and D. Nychka. 2006. Covariance tapering for interpolation of large spatial datasets. Journal of Computational and Graphical Statistics 15:502–523.

Gaines, S. D., C. White, M. H. Carr, and S. R. Palumbi. 2010. Designing marine reserve networks for both conservation and fisheries management. Proceedings of the National Academy of Sciences 107:18286–93.

Gneiting, T., and A. E. Raftery. 2007. Strictly proper scoring rules, prediction, and estimation. Journal of the American Statistical Association 102:359–378.

Gordon, H. S. 1953. An economic approach to the optimum utilization of fisher resources. Journal of the Fisheries Research Board of Canada 10.

Grüss, A., D. M. Kaplan, S. Guénette, C. M. Roberts, and L. W. Botsford. 2011. Consequences of adult and juvenile movement for marine protected areas. Biological Conservation 144:692–702.

Guay, J., and D. Boisclair. 2000. Development and validation of numerical habitat models for juveniles of Atlantic salmon (Salmo salar). Canadian Journal of Fisheries and Aquatic Sciences 57:2065–2075.

Guisan, A., and W. Thuiller. 2005. Predicting species distribution: offering more than simple habitat models. Ecology Letters 8:993–1009.

Gulland, J. A. 1965. Estimation of mortality rates. Page 9. Annex to Arctic Fisheries Working Group report. (ICES Council Meeting papers), ICES Gadoid Fish.Comm., CM 3.

Hagerman, F. B. 1952. The biology of the Dover sole, *Microstomus pacificus* (Lockington). Page 48. Fish Bulletin.

Halpern, B. S., and R. R. Warner. 2002. Marine reserves have rapid and lasting effects. Ecology Letters 5:361–366.

Haltuch, M. A., K. Ono, and J. L. Valero. 2013. Status of the U.S. petrale sole resource in 2012. Page 480.

Harley, S. J., R. A. Myers, and A. Dunn. 2001. Is catch-per-unit-effort proportional to abundance? Canadian Journal of Fisheries and Aquatic Sciences 58:1760–1772.

Herrmann, M. 1996. Estimating the induced price increase for Canadian Pacific halibut with the introduction of the individual vessel quota program. Canadian Journal of Agricultural Economics 44:151–164.

Herrmann, M., and K. Criddle. 2006. An econometric market model for the Pacific halibut fishery. Marine Resource Economics 21:129–158.

Hicks, A. C., and C. Wetzel. 2011. The Status of Dover Sole (*Microstomus pacificus*) along the U.S. West Coast in 2011. Page 321.

Hicks, C. C., and T. R. McClanahan. 2012. Assessing gear modifications needed to optimize yields in a heavily exploited, multi-species, seagrass and coral reef fishery. PloS One 7:e36022.

Hilborn, R., and R. Kennedy. 1992. Spatial pattern in catch rates: A test of economic theory. Bulletin of Mathematical Biology 54:263–273.

Hilborn, R., A. E. Punt, and J. Orensanz. 2004. Beyond band-aids in fisheries management: Fixing world fisheries. Bulletin of Marine Science 74:493–507.

Hilborn, R., I. J. Stewart, T. A Branch, and O. P. Jensen. 2012. Defining trade-offs among conservation, profitability, and food security in the California current bottom-trawl fishery. Conservation Biology 26:257–66.

Hilborn, R., and C. J. Walters. 1992. Quantitative fisheries stock assessment: Choice, dynamics and uncertainty. Page 570. Chapman and Hall, New York.

Holand, A. M., I. Steinsland, S. Martino, and H. Jensen. 2013. Animal models and integrated nested Laplace approximations. G3 (Bethesda, Md.) 3:1241–51.

Holland, D. S. 2000. A bioeconomic model of marine sanctuaries on Georges Bank. Canadian Journal of Fisheries and Aquatic Sciences 57:1307–1319.

Holland, D. S. 2003. Integrating spatial management measures into traditional fishery management systems : the case of the Georges Bank multispecies groundfish fishery 3139:915–929.

Holland, D. S. 2008. Are fishermen rational? A fishing expedition. Marine Resource Economics 23:325–344.

Holland, D. S., and G. E. Herrera. 2006. Flexible catch-balancing policies for multispecies individual fishery quotas. Canadian Journal of Fisheries and Aquatic Sciences 63:1669–1685.

Holland, D. S., and J. E. Jannot. 2012. Bycatch risk pools for the U.S. West Coast Groundfish Fishery. Ecological Economics 78:132–147.

Holland, D. S., and J. G. Sutinen. 2000. Location choice in New England trawl fisheries: Old habits die hard. Land Economics 76:133.

Holland, D., and K. Schnier. 2006. Individual habitat quotas for fisheries. Journal of Environmental Economics and Management 51:72–92.

Ichinokawa, M., and J. Brodziak. 2010. Using adaptive area stratification to standardize catch rates with application to North Pacific swordfish (*Xiphias gladius*). Fisheries Research 106:249–260.

Irigoyen, A. J., D. E. Galván, L. A. Venerus, and A. M. Parma. 2013. Variability in abundance of temperate reef fishes estimated by visual census. PloS One 8:e61072.

Jacobson, L., J. Brodziak, and J. Rogers. 2001. Depth distributions and time-varying bottom trawl selectivities for Dover sole (*Microstomus pacificus*), sablefish (*Anoplopoma fimbria*), and thornyheads (*Sebastolobus alascanus* and *S. altivelis*) in a commercial fishery. Fishery Bulletin 99:309–327.

Kaplan, I., P. Levin, M. Burden, and E. A. Fulton. 2010. Fishing catch shares in the face of global change: a framework for integrating cumulative impacts and single species management. Canadian Journal of Fisheries and Aquatic Sciences 67:1968–1982.

Kareiva, P., A. Chang, and M. Marvier. 2014. Development in world goals and conservation. Science 321:1638–1639.

Kaufman, L., and P. J. Rousseeuw. 1990. Finding groups in data: an introduction to cluster analysis. Page 368.

Keller, A. A., J. R. Wallace, B. H. Horness, O. S. Hamel, and I. J. Stewart. 2012. Variations in eastern North Pacific demersal fish biomass based on the U.S. west coast groundfish bottom trawl survey (2003-2010). Fish Bulletin 110:205–222.

Kellner, J. B., I. Tetreault, S. D. Gaines, and R. M. Nisbet. 2007. Fishing the line near marine reserves in single and multispecies fisheries. Ecological Applications 17:1039–54.

Krigsman, L. M., M. M. Yoklavich, E. J. Dick, and G. R. Cochrane. 2012. Models and maps: predicting the distribution of corals and other benthic macro-invertebrates in shelf habitats. Ecosphere 3:1–16.

Krnjajić, M., A. Kottas, and D. Draper. 2008. Parametric and nonparametric Bayesian model specification: A case study involving models for count data. Computational Statistics & Data Analysis 52:2110–2128.

Landry, M. R., J. R. Postel, W. K. Peterson, and J. Newman. 1989. Broad-Scale Distributional Patterns of Hydrographic Variables on the Washington/Oregon Shelf. Pages 1–40 *in* M. R. Landry and B. M. Hickey, editors. Coastal Oceanography of Washington and Oregon. Elsevier, Armsterdam.

Latimer, A. M., S. Banerjee, H. Sang, E. S. Mosher, and J. A. Silander. 2009. Hierarchical models facilitate spatial analysis of large data sets: a case study on invasive plant species in the northeastern United States. Ecology letters 12:144–54.

Lauck, T., and C. Clark. 1998. Implementing the precautionary principle in fisheries management through marine reserves. Ecological applications 8:72–78.

Legendre, P. 1993. Spatial autocorrelation: trouble or new paradigm? Ecology 74:1659–1673.

Lester, S., B. Halpern, K. Grorud-Colvert, J. Lubchenco, B. Ruttenberg, S. Gaines, S. Airamé, and R. Warner. 2009. Biological effects within no-take marine reserves: a global synthesis. Marine Ecology Progress Series 384:33–46.

Liaw, A., and M. Wiener. 2002. Classification and regression by randomForest. R News.

Lindgren, F., H. Rue, and J. Lindström. 2011. An explicit link between Gaussian fields and Gaussian Markov random fields: the stochastic partial differential equation approach. Journal of the Royal Statistical Society: Series B (Statistical Methodology) 73:423–498.

Lomeli, M., and W. Wakefield. 2013. A flexible sorting grid to reduce Pacific halibut (*Hippoglossus stenolepis*) bycatch in the U.S. west coast groundfish bottom trawl fishery. Fisheries Research 143:102–108.

Maunder, M. N. 2001. A general framework for integrating the standardization of catch per unit of effort into stock assessment models. Canadian Journal of Fisheries and Aquatic Sciences 58:795–803.

Maunder, M. N., and A. E. Punt. 2004. Standardizing catch and effort data: a review of recent approaches. Fisheries Research 70:141–159.

Maunder, M. N., and A. E. Punt. 2013. A review of integrated analysis in fisheries stock assessment. Fisheries Research 142:61–74.

Maunder, M. N., J. R. Sibert, A. Fonteneau, J. Hampton, P. Kleiber, and S. J. Harley. 2006. Interpreting catch per unit effort data to assess the status of individual stocks and communities. ICES Journal of Marine Science 63:1373–1385.

McGilliard, C. R., R. Hilborn, A. MacCall, A. E. Punt, and J. C. Field. 2010. Can information from marine protected areas be used to inform control-rule-based management of small-scale, data-poor stocks? ICES Journal of Marine Science 68:201–211.

Methot, R. D. J., and C. R. Wetzel. 2013. Stock synthesis: A biological and statistical framework for fish stock assessment and fishery management. Fisheries Research 142:86–99.

Moilanen, A., and M. Nieminen. 2002. Simple connectivity measures in spatial ecology. Ecology 83:1131–1145.

Myers, R. A., and B. Worm. 2003. Rapid worldwide depletion of predatory fish communities. Nature 423:280–3.

Nakano, H. 1998. Stock status of Pacific swordfish, *Xiphias gladius*, inferred from CPUE of the Japanese longline fleet standardized using general linear model. Pages 195–209.

National Marine Fisheries Service (NMFS). 2013. Groundfish essential fish habitat synthesis: a report to the pacific fishery management council. Page 107.

National Oceanic and Atmospheric Administration, (NOAA). 2001. U.S. Vector Shoreline Derived from NOAA Nautical Charts. Silver Spring, MD: NOAA's Ocean Service, Office of Coast Survey (OCS).

National Oceanic and Atmospheric Administration, (NOAA). 2003. U.S. Coastal Relief Model - Northwest Pacific. Boulder, CO: National Geophysical Data Center, NESDIS.

National Oceanic and Atmospheric Administration, (NOAA). 2013. Status of stocks 2012. Annual report to congress on the status of U.S. fisheries.

Ono, K., D. S. Holland, and R. Hilborn. 2013. How does species association affect mixed stock fisheries management? A comparative analysis of the effect of marine protected areas, discard bans, and individual fishing quotas. Canadian Journal of Fisheries and Aquatic Sciences 70:1792–1804.

Pelletier, D., and S. Mahevas. 2005. Spatially explicit fisheries simulation models for policy evaluation. Fish and Fisheries 6:307–349.

PFMC (Pacific Fishery Management Council), and NMFS (National Marine Fisheries Service). 2010. Rationalization of the Pacific Coast Groundfish Limited Entry Trawl Fishery; Final Environmental Impact Statement Including Regulatory Impact Review and Initial Regulatory Flexibility Analysis.

Pinsky, M. L., B. Worm, M. J. Fogarty, J. L. Sarmiento, and S. A. Levin. 2013. Marine taxa track local climate velocities. Science 341:1239–42.

Polacheck, T. 2006. Tuna longline catch rates in the Indian Ocean: Did industrial fishing result in a 90% rapid decline in the abundance of large predatory species? Marine Policy 30:470–482.

Polacheck, T., R. Hilborn, and A. E. Punt. 1993. Fitting surplus production models: Comparing methods and measuring uncertainty. Canadian Journal of Fisheries and Aquatic Sciences 50:2597–2607.

Poos, J. J., J. A. Bogaards, F. J. Quirijns, D. M. Gillis, and A. D. Rijnsdorp. 2009. Individual quotas, fishing effort allocation, and over-quota discarding in mixed fisheries. ICES Journal of Marine Science 67:323–333.

Prasad, A. M., L. R. Iverson, and A. Liaw. 2006. Newer classification and regression tree techniques: Bagging and random forests for ecological prediction. Ecosystems 9:181–199.

Punt, A., T. Walker, B. Taylor, and F. Pribac. 2000. Standardization of catch and effort data in a spatially-structured shark fishery. Fisheries Research 45:129–145.

R Core Team. 2013. R: A language and environment for statistical computing. R Foundation for Statistical Computing, Vienna, Austria.

Robinson, L. M., J. Elith, A. J. Hobday, R. G. Pearson, B. E. Kendall, H. P. Possingham, and A. J. Richardson. 2011. Pushing the limits in marine species distribution modelling: lessons from the land present challenges and opportunities. Global Ecology and Biogeography 20:789–802.

Rodwell, L., and E. Barbier. 2003. The importance of habitat quality for marine reserve fishery linkages. Canadian Journal of Fisheries and Aquatic Sciences 181:171–181.

Rosenberg, A. A., J. J. H. Swasey, and M. Bowman. 2006. Rebuilding U.S. fisheries: progress and problems. Frontiers in Ecology and the Environment 4:303–308.

Rue, H., S. Martino, and N. Chopin. 2009. Approximate Bayesian inference for latent Gaussian models by using integrated nested Laplace approximations. Journal of the Royal Statistical Society: Series B (Statistical Methodology) 71:319–392.

Rue, H., S. Martino, F. Lindgren, D. Simpson, and A. Riebler. 2013. INLA: Functions which allow to perform full Bayesian analysis of latent Gaussian models using Integrated Nested Laplace Approximations.

Saas, Y., and F. Gosselin. 2014. Comparison of regression methods for spatially-autocorrelated count data on regularly- and irregularly-spaced locations. Ecography 37:001–014.

Salas, S., and D. Gaertner. 2004. The behavioural dynamics of fishers: management implications. Fish and Fisheries 5:153–167.

Sale, P. F., R. K. Cowen, B. S. Danilowicz, G. P. Jones, J. P. Kritzer, K. C. Lindeman, S. Planes, N. V. C. Polunin, G. R. Russ, Y. J. Sadovy, and R. S. Steneck. 2005. Critical science gaps impede use of no-take fishery reserves. Trends in Ecology & Evolution 20:74–80.

Sanchirico, J. N., and J. E. Wilen. 1999. Bioeconomics of spatial exploitation in a patchy environment. Journal of Environmental Economics and Management 37:129–150.

Schaefer, M. B. 1954. Some aspects of the dynamics of populations important to the management of the commercial marine fisheries. Bulletin Inter-American Tropical Tuna Commission 1:27–56.

Scheld, A. M., C. M. Anderson, and H. Uchida. 2012. The economic effects of catch share management: the Rhode Island fluke sector pilot program. Marine Resource Economics 27:203–228.

Schlather, M. 2012. RandomFields: Simulation and analysis of random fields. R package version 2.0.59.

Schnute, J. 1985. A general theory for analysis of catch and effort data. Canadian Journal of Fisheries and Aquatic Sciences 42:414–429.

Schrödle, B., and L. Held. 2011. Spatio-temporal disease mapping using INLA. Environmetrics 22:725–734.

Shono, H. 2005. Is model selection using Akaike's information criterion appropriate for catch per unit effort standardization in large samples? Fisheries Science:978–986.

Simpson, E. H. 1951. The interpretation of interaction in contingency tables. Journal of the Royal Statistical Society: Series B (Statistical Methodology) 13:238–241.

Smith, M. D., and J. E. Wilen. 2003. Economic impacts of marine reserves: the importance of spatial behavior. Journal of Environmental Economics and Management 46:183–206.

Spiegelhalter, D. J., N. G. Best, B. P. Carlin, and A. van der Linde. 2002. Bayesian measures of model complexity and fit. Journal of the Royal Statistical Society: Series B (Statistical Methodology) 64:583–639.

Sundblad, G., U. Bergström, and A. Sandström. 2011. Ecological coherence of marine protected area networks: a spatial assessment using species distribution models. Journal of Applied Ecology 48:112–120.

Thorson, J. T., I. J. Stewart, and A. E. Punt. 2012. Development and application of an agent-based model to evaluate methods for estimating relative abundance indices for shoaling fish such as Pacific rockfish (*Sebastes spp*.). ICES Journal of Marine Science 69:635–647.

Thorson, J. T., and E. J. Ward. 2013. Accounting for space–time interactions in index standardization models. Fisheries Research 147:426–433.

Toft, J. E., A. E. Punt, and L. R. Little. 2011. Modelling the economic and ecological impacts of the transition to individual transferable quotas in the multispecies U.S. west coast groundfish trawl fleet. ICES Journal of Marine Science 68:1566–1579.

Toole, C., R. Brodeur, C. Donohoe, and D. Markle. 2011. Seasonal and interannual variability in the community structure of small demersal fishes off the central Oregon coast. Marine Ecology Progress Series 428:201–217.

van Putten, I. E., S. Kulmala, O. Thébaud, N. Dowling, K. G. Hamon, T. Hutton, and S. Pascoe. 2012. Theories and behavioural drivers underlying fleet dynamics models. Fish and Fisheries 13:216–235.

Walters, C. J. 2003. Folly and fantasy in the analysis of spatial catch rate data. Canadian Journal of Fisheries and Aquatic Sciences 60:1433–1436.

Walters, C. J., R. Hilborn, and R. Parrish. 2007. An equilibrium model for predicting the efficacy of marine protected areas in coastal environments 1018:1009–1018.

Ward, T., and M. Vanderklift. 1999. Selecting marine reserves using habitats and species assemblages as surrogates for biological diversity. Ecological Applications 9:691–698.

Whittaker, R., S. Levin, and R. Root. 1973. Niche, habitat, and ecotope. American Naturalist 107:321–338.

Williams, E. H., and S. Ralston. 2002. Distribution and co-occurrence of rockfishes (family : *Sebastidae*) over trawlable shelf and slope habitats of California and southern Oregon. Fishery Bulletin 100:836–855.

Wilson, J. R., J. D. Prince, and H. S. Lenihan. 2010. A management strategy for sedentary nearshore species that uses marine protected areas as a reference. Marine and Coastal Fisheries 2:14–27.

Worm, B., R. Hilborn, J. K. Baum, T. A. Branch, J. S. Collie, C. Costello, M. J. Fogarty, E. A. Fulton, J. A. Hutchings, S. Jennings, O. P. Jensen, H. K. Lotze, P. M. Mace, T. R. McClanahan, C. Minto, S. R. Palumbi, A. M. Parma, D. Ricard, A. A. Rosenberg, R. Watson, and D. Zeller. 2009. Rebuilding global fisheries. Science 325:578–85.

Zuur, A. F., E. N. Ieno, N. J. Walker, A. A. Saveliev, and G. M. Smith. 2009. Mixed effects models and extensions in ecology with R. Page 549.

Vita

Kotaro Ono was born in Aichi-ken, Japan. He spent many years in western Africa growing up following his father who was a working as a consultant for fishery managers. Naturally, he became interested in fisheries issues and pursued his education in an agronomic school in France, Ecole Nationale Superieure Agronomique de Rennes (France), where he received an engineering degree with a minor in aquatic and fishery sciences and a focus on quantitative methodologies in fisheries in 2007. He later worked with Si Simenstad at the University of Washington, where he received a Master of Science degree in Fisheries in 2010. He received a Doctor of Philosophy degree in Aquatic and Fisheries Science from the University of Washington in 2014 while working with Dr. Ray Hilborn.